UNIVERSITY OF ALBERTA

PARAMETERS AFFECTING WATER PERMEABILITY ACROSS BIOLOGICAL CELL MEMBRANES

by

HEIDI YAKOUT ELMOAZZEN

A thesis submitted to the Faculty of Graduate Studies and Research in partial fulfillment of the requirements for the degree of Master of Science

in

Chemical Engineering and Experimental Pathology

Departments of Chemical and Materials Engineering

and

Laboratory Medicine and Pathology

Edmonton, Alberta

Spring 2000

National Library of Canada
Acquisitions and Bibliographic Services
395 Wellington Street
Ottawa ON K1A 0N4
Canada

Bibliothèque nationale du Canada
Acquisitions et services bibliographiques
395, rue Wellington
Ottawa ON K1A 0N4
Canada

Your file Votre référence

Our file Notre référence

The author has granted a non-exclusive licence allowing the National Library of Canada to reproduce, loan, distribute or sell copies of this thesis in microform, paper or electronic formats.

L'auteur a accordé une licence non exclusive permettant à la Bibliothèque nationale du Canada de reproduire, prêter, distribuer ou vendre des copies de cette thèse sous la forme de microfiche/film, de reproduction sur papier ou sur format électronique.

The author retains ownership of the copyright in this thesis. Neither the thesis nor substantial extracts from it may be printed or otherwise reproduced without the author's permission.

L'auteur conserve la propriété du droit d'auteur qui protège cette thèse. Ni la thèse ni des extraits substantiels de celle-ci ne doivent être imprimés ou autrement reproduits sans son autorisation.

0-612-60118-8

Canada

UNIVERSITY OF ALBERTA

LIBRARY RELEASE FORM

Name of author: Heidi Yakout Elmoazzen

Title of Thesis: Parameters Affecting Water Permeability Across Biological Cell Membranes

Degree: Master of Science

Year this Degree Granted: 2000

Permission is hereby granted to the University of Alberta Library to reproduce single copes of this thesis and to lend or sell such copies for private, scholarly or scientific research purposes only.

The author reserves all other publication and other rights in association with the copyright thesis, and except as herein before provided, neither the thesis nor any substantial portion thereof may be printed or otherwise reproduced in any material form whatever without the author's prior written permission.

Heidi Y. Elmoazzen
302 Ferris Way
Edmonton, Alberta
T6R 2C8

March 31, 2000
Date

UNIVERSITY OF ALBERTA

FACULTY OF GRADUATE STUDIES AND RESEARCH

The undersigned certify that they have read, and recommend to the Faculty of Graduate Studies and Research for acceptance, a thesis entitled **Parameters Affecting Water Permeability Across Cell Membranes** submitted by **Heidi Yakout Elmoazzen** in partial fulfillment of the requirements for the degree of **Master of Science** in **Chemical Engineering and Experimental Pathology.**

Dr. J. A. W. Elliott (Co-Supervisor)

Dr. L. E. McGann (Co-Supervisor)

Dr. S. M. Kresta

Dr. H. Uludag

March 31, 2000

Date

Abstract

Parameters Affecting Water Permeability Across Biological Cell Membranes

In order to optimize the viability of cryopreserved cells and tissues, a better understanding of osmotic transport across cell membranes is required. The objective of this thesis was to examine the parameters effecting water permeability across biological cell membranes.

First, Statistical Rate Theory was applied to develop new osmotic transport equations in terms of measurable parameters including temperature and concentration. This approach led to linearity conditions and a theoretical verification of Onsager's reciprocity relation for a particular case.

Next, the change in cell size distribution with time was experimentally measured. It was shown that the single-cell mass transport equation fit to the mean cell volume as a function of time did not accurately model the osmotic response of size distributions.

Finally, the experimental temperature dependence of membrane hydraulic conductivity was examined using two different membrane models to gain insight into the mechanisms of water transport and the presence of aqueous pores.

This thesis is dedicated to my parents,

Afaf and Yakout. Thank you for all of your

love and support throughout my life.

Acknowledgments

I wish to express my sincere appreciation and gratitude to the following people without whom this work would not have been possible.

To Dr. Janet A. W. Elliott, my co-supervisor. Her enthusiasm for this project has been contagious and her encouragement has been greatly appreciated.

To Dr. Locksley E. McGann, my co-supervisor. His dedication and enthusiasm for science has been inspirational and his guidance has helped me develop as a researcher and as a person.

To Dr. Murray R. Gray, for serving as my examination committee chairman.

To Dr. Suzanne M. Kresta and Dr. Hasan Uludag, for serving as committee members and for their insightful comments.

To the members of my lab, for all the enlightening science and cryobiology conversations, for helping me solve my computer problems and for the many needed coffee breaks.

To all of my friends who have provided me with support and encouragement during this part of my life. You all know who you are.

Finally to my family - my parents Afaf and Yakout and my sister Randa, for their continued love, patience and support during all my scholastic endeavors. I love you all.

Thank you.

Table of Contents

		PAGE
Chapter 1-	**Introduction**	1
1.1	Introduction to Cryobiology	1
1.2	Cellular Cryobiology	4
	1.2a Slow Cool Injury	6
	1.2b Rapid Cool Injury	8
	1.2c Warming Rates	8
1.3	Traditional Cryopreservation of Cells	9
	1.3a Permeating Cryoprotectants	10
	1.3b Non-Permeating Cryoprotectants	11
1.4	Cell Membrane Permeability	12
1.5	Objectives and Scope of this Thesis	15
1.6	References	19
Chapter 2-	**Theoretical Modeling of Water Transport across Cell Membranes**	28
2.1	Introduction	28
	2.1a Theories of Osmotic Transport	28
	2.1b Statistical Rate Theory	31
2.2	Mass Transport across Cell Membranes: Case 1	34
	2.2a The Onsager Approach	35
	2.2b The Statistical Rate Theory Approach	39
2.3	Discussion of Case 1	44
2.4	Mass Transport across Cell Membranes: Case 2	45

2.5 Discussion of Case 2 51

2.6 Mass Transport across Cell Membranes: Case 3 52

2.7 Discussion of Case 3 56

2.8 Conclusions 57

2.9 References 60

Chapter 3- The Effect of Cell Size Distribution on Predicted Osmotic Responses of Cells 67

3.1 Introduction 67

3.2 Theory 70

3.2a Osmotic Response of Cells of a Single Size 70
3.2b Osmotic Response of Cells with Size Distributions 73

3.3 Materials and Methods 74

3.3a Cell Culture 74
3.3b Electronic Particle Counter 75
3.3c Coulter Principle 76
3.3d Osmotic Experiments 76
3.3e Obtaining Size Distributions from Electronic Particle Counter Data 77

3.4 Results 77

3.4a Experimental Cell Size Distributions as a Function of Time 77
3.4b Theoretical Cell Size Distributions as a Function of Time 78

3.5 Discussion 79

3.6 Conclusions 81

3.7 References 83

Chapter 4- The Effect of Temperature on Membrane Hydraulic Conductivity 97

4.1 Introduction 97

4.1a Water Transport across Cell Membranes 97
4.1b The Discovery of Aquaporins 98
4.1c Biophysical Properties Used to Characterize Aquaporins 99

4.2 Objective 104

4.3 Theory 105

4.3a Diffusion through Aqueous Pores 105
4.3b Solubility-Diffusion through a Lipid Bilayer Modeled as Liquid Hexadecane 108

4.4 Methods and Materials 111

4.4a Cell Culture 111
4.4b Osmotic Experiments 111
4.4c Calculation of Osmotic Parameters 111

4.5 Results 113

4.6 Discussion 118

4.7 Conclusions 121

4.8 References 123

Chapter 5- Overall Discussion and Conclusions 138

List of Tables

		PAGE
Table 4-1.	L_p's for V79W Hamster Fibroblast Cells at Various Temperatures (calculated using the mean cell volume, E_a = 4.7 kcal/mol)	113
Table 4-2.	L_p's for V-79W Hamster Fibroblast Cells at Various Temperatures (calculated using the mode cell volume, E_a = 5.1 kcal/mol)	114
Table 4-3.	L_p's for Human Bone Marrow Stem Cells at Various Temperatures (calculated using the mean cell volumes, E_a = 6.4 kcal/mol, McGann et al., (1987))	115
Table 4-4.	L_p's for Hamster Pancreatic Islet Cells at Various Temperatures (calculated using the mean cell volume, E_a = 11.4 kcal/mol, Liu et al., (1995))	116
Table 4-5.	L_p's for Articular Cartilage Chondrocytes at Various Temperatures (calculated using the mean cell volume, E_a = 15.4 kcal/mol, McGann et al., (1988))	117

List of Figures

		PAGE
Figure 1-1.	Osmotic Response during the Addition and Dilution of Cryoprotectants: Permeating Solutes	25
Figure 1-2.	Osmotic Response during the Addition and Dilution of Cryoprotectants: Non-Permeating Solutes	26
Figure 1-3.	Water and Solute Movement Across a Homogeneous Membrane	27
Figure 2-1.	Case 1: A Two-component System of Water and Solute where Both May Permeate the Cell Membrane and where there is Tension in the Membrane	64
Figure 2-2.	Case 2: A Two-component System of Water and Solute where Both May Permeate the Cell Membrane but where there is no Tension in the Membrane	65
Figure 2-3.	Case 3: A Two-component System of Water and Solute where only the Water May Permeate the Cell Membrane and where there is no Tension in the Membrane	66
Figure 3-1.	Coulter Counter and Computer Set Up	86
Figure 3-2.	Coulter Counter Aperture and Electrode Set Up	87
Figure 3-3.	Experimental MDCK Cell Size Distribution as a Function of Time (L_{po} = 1.48 $\mu m^3/\mu m^2/atm/min$, solution concentration = 1533 mOsmol/kg)	88
Figure 3-4.	Experimental V-79W Cell Size Distribution as a Function of Time (L_{po} = 1.19 $\mu m^3/\mu m^2/atm/min$, solution concentration = 1732 mOsmol/kg)	89
Figure 3-5.	Normalized Cell Volume vs Time Showing the Kinetics of Cell Shrinkage for V-79W cells with an Lp_o of 1.19 $\mu m^3/\mu m^2/atm/min$ (solution concentration = 1732 mOsmol/kg)	90
Figure 3-6.	Theoretical MDCK Cell Size Distribution as a Function of Time Using an L_p of 1.48 $\mu m^3/\mu m^2/atm/min$ (solution concentration = 1533 mOsmol/kg)	91

Figure 3-7.	Theoretical V-79W Cell Size Distribution as a Function of Time Using an L_p of 1.19 $\mu m^3/\mu m^2/atm/min$ (solution concentration = 1732 mOsmol/kg)	92
Figure 3-8.	Theoretical MDCK Cell Size Distribution as a Function of Time Using an L_p of 0.10 $\mu m^3/\mu m^2/atm/min$ (solution concentration = 1533 mOsmol/kg)	93
Figure 3-9.	Theoretical MDCK Cell Size Distribution as a Function of Time Using an L_p of 0.30 $\mu m^3/\mu m^2/atm/min$ (solution concentration = 1533 mOsmol/kg)	94
Figure 3-10.	Theoretical V-79W Cell Size Distribution as a Function of Time Using an L_p of 0.45 $\mu m^3/\mu m^2/atm/min$ (solution concentration = 1732 mOsmol/kg)	95
Figure 3-11.	Theoretical V-79W Cell Size Distribution as a Function of Time Using an L_p of 0.75 $\mu m^3/\mu m^2/atm/min$ (solution concentration = 1732 mOsmol/kg)	96
Figure 4-1.	Diffusion through Aqueous Pores	131
Figure 4-2.	Solubility-Diffusion through a Lipid Bilayer Membrane	132
Figure 4-3.	Temperature Vs L_p for V-79W Hamster Fibroblasts (using mean cell volumes)	133
Figure 4-4.	Temperature Vs L_p for V-79W Hamster Fibroblasts (using mode cell volumes)	134
Figure 4-5.	Temperature Vs L_p for Human Bone Marrow Stem Cells	135
Figure 4-6.	Temperature Vs L_p for Hamster Pancreatic Islets	136
Figure 4-7.	Temperature Vs L_p for Articular Cartilage Chondrocytes:	137

List of Symbols

Å	Angstrom
A	cell surface area
A_p	cell surface area of pores
B_α	represents a constant in Eq. 4-13
B_{ms}	represents a constant for the membrane-solution interface in Eqs. 4-19, 4-20 and 4-21
B_{sm}	represents a constant for the solution-membrane interface in Eqs. 4-19, 4-20, and 4-21
c	concentration
c^*	concentration of a pure substance
$\tilde{c}_s$	a value for the concentration defined by Eqs. 2-29 and 2-30
D	diffusion coefficient
D_o	represents a constant in Eqs. 4-19, 4-20, and 4-21
E_a	activation energy
E_{am}	activation energy for the diffusion process across the membrane
E_{ams}	activation energy for the diffusion process across the membrane-solution interface
E_{asm}	activation energy for the diffusion process across the solution-membrane interface
f	friction factor
G	represents a constant in Eqs. 4-21, 4-22, and 4-23
J	flux
J_s	flux of solute molecules across a cell membrane

J_w	flux of water molecules across a cell membrane
k	Boltzmann's constant
k_α	in chapter 4, Eq. 4-13, k_α represents a rate of diffusion
k_m	rate of diffusion across the membrane
k_{ms}	rate of diffusion across the membrane-solution interface
k_{sm}	rate of diffusion across the solution-membrane interface
K	degrees Kelvin
K_e	equilibrium exchange rate
L	phenomenological coefficient
L_p	membrane hydraulic conductivity
L_{po}	in chapter 3 L_{po} represents the membrane hydraulic conductivity found by fitting the mean of the experimental volume distribution to the single-cell equation
L_p^o	a constant in chapter 4, Eq. 4-4
m	the number of jumps required for a molecule to move across the membrane
M	osmolality
M_m	molar mass
N	number of molecules
$\dot{N}$	rate of change in the number of molecules
P	pressure
P_d	membrane diffusional permeability
P_f	membrane osmotic water permeability
P_s	membrane solute permeability
r	radius of a cell

R	universal gas constant
s	solute
S	entropy
t	time
T	temperature
U	internal energy
$\bar{v}$	partial molar volume
$\bar{v}_w^*$	specific volume of water
$\bar{V}$	partial molecular volume
$\bar{V}_s$	partial molecular volume of solute
$\bar{V}_W$	partial molecular volume of water
v_b	osmotically inactive fraction
v_{bo}	in chapter 3 v_{bo} represents the osmotically inactive fraction found by fitting the mean of the experimental volume distribution to the single-cell equation
V	volume
V_W	water volume
V_{W+S}	volume of water plus solute
x	mole fraction
X	a thermodynamic force
y	a variable
σ	reflection coefficient in the Kedem-Katchalsky equations
δ	membrane thickness
μ	chemical potential

λ	the length of a molecular jump
γ	surface tension
η	viscosity
η_T	the viscosity at temperature T
Δ	an operator used to indicate a difference
ΔC	difference in osmotic pressure
ΔP	difference in hydrostatic pressure
ΔS_b	the change in the entropy of an isolated system as a result of a molecule moving in the "backward" direction
ΔS_f	the change in the entropy of an isolated system as a result of a molecule moving in the "forward" direction

Subscripts

b	backward direction
f	forward direction
iso	refers to isotonic conditions
k	in sec 2.2, Eqs. 2-15, 2-20, 2-39, and 2-46, k indicates the k^{th} molecular species in the membrane
n	non-permeating solutes
ps	permeating solutes
s	solute
sys	isolated system
w	water

Superscripts

i	internal cell solution
m	membrane
o	external cell solution
R	reservoir

Glossary

Chondrocytes: cartilage cells that are produced during the growth of bone

Ciliary Body: the portion of the eye that produces aqueous humor (the watery fluid in the eye) and contains ciliary muscle.

Colligative Properties: properties such as vapor pressure, boiling point, freezing point, and osmotic pressure that depend only on the concentration of solute in the solution

Cytosol: the semi-liquid portion of the cytoplasm not occupied by organelles

Endothelial cells: a single sheet of highly flattened cells that forms the lining of all blood vessels

Ependymal cells: cells that line the internal cavities of the central nervous system; contribute to the formation of cerebrospinal fluid

Epidermis: the outermost layer of the skin

Epithelial Cells: cells specialized in the exchange of materials between the cell and it's environment; lines and covers various body surfaces and cavities and forms the secretory glands

Fibroblasts: a common cell type found in connective tissue

Hemolysis: rupture of red blood cells

Hypertonic: describes any medium with a higher osmolality than a normal cell. Placing a cell in a hypertonic solution will cause water to move out of a cell due to osmosis

Hypotonic: describes any medium with a lower osmolality than a normal cell. Placing a cell in a hypotonic solution will cause water to move into a cell due to osmosis

Keratinocytes: cells whose differentiated activity is the synthesis of intermediate filament proteins (keratin) mainly in the epithelium. Some specialized keratin is found in hair, nails and feathers.

Keratocytes: a fibroblastic cell type resident in the collagen matrix of corneal stroma

Lipoproteins: a lipid-protein complex

Lumen: a cavity enclosed by an epithelial sheet (in a tissue) or by a membrane (in a cell)

Lymphocytes: white blood cells that make an immune response when activated by a foreign molecule (an antigen)

Organ: a distinct structural unit composed of two or more types of primary tissue organized to perform a particular function or functions

Organelles: highly organized membrane-bound structures located in the cytoplasm of cells. Each type of organelle contains a specific set of chemicals for carrying out a particular cellular function

Parietal cells: the stomach cells that secrete hydrochloric acid and intrinsic factor

Pia Matter: the highly fragile, innermost meningeal layer that adheres to the surface of the brain and spinal cord

Quasi-statically: when processes proceed in a manner such that the system remains infinitesimally close to an equilibrium state at all times. A system that changes "quasi-statically" does so at a sufficiently slow rate which allows the system to adjust itself internally so that properties in one part of the system do not change faster than those at other parts

Renal Proximal Tubule: a highly convoluted tube that extends between Bowman's capsule and the loop of Henle in the kidney's nephron

Stem Cell: a relatively undifferentiated cell that can continue dividing indefinitely, throwing off daughter cells that can undergo terminal differentiation into particular cell types

Tissue: a functional aggregation of cells of a single specialized type

Chapter 1: Introduction

1.1 Introduction to Cryobiology

Water has been called the fundamental molecule of life. It posses unique and rare qualities that makes our day to day lives possible. No living system can exist without the presence of liquid water. It is essential in the maintenance of cellular structure and function. Hence, when water solidifies and freezes, it is hardly surprising that it is usually lethal. However, paradoxically, temperatures below freezing can also be used to preserve cells and tissues for long-term storage. The phase transition between water and ice is of critical importance and it is during this transition that injury and death often occur.

Cryobiology is the field in which the effects of low temperatures on biological systems are studied. In cryobiology, when we refer to low temperatures, we are usually referring to temperatures below that at which water freezes. The word *cryobiology* was first used in the 1950's to describe the newly developing field of low temperature biology. Low-temperature biology has many practical applications and incorporates many other disciplines. In the area of agriculture, cryobiology has had various applications. For example, a better understanding of how plants and seeds behave when frozen has led to improvements in seed preservation techniques. Also, the cryopreservation of bovine sperm (Polge & Lovelock, 1952) and embryos (Wilmut & Rowson, 1973; Leibo, 1983) has revolutionized the cattle breeding industry. In the area of food science, freezing has had many practical applications such as the preservation of frozen food

(Fennema, 1966). One of the most beneficial areas of freezing has been seen in the medical application of cryobiology. Cryosurgery is the process in which freezing is used to destroy cells in a diseased target area. Understanding the low temperature response of cells and tissues allows for the development of strategies to maximize cryoinjury in localized areas while minimizing injury to surrounding tissue. Cryosurgery is used to treat dermatological malignancies as well as for treating cancer of the liver, prostate and breast. The other major medical application of cryobiology has been in the area of cryopreserving cells and tissues for transplantation. Cryopreservation is the technique used to store and preserve cells at low temperatures. Often cryopreservation takes place in liquid nitrogen at -196°C. At temperatures this low, cells can often be stored for many years in a biologically stable state since practically no chemical reactions can take place. At such low temperatures of storage, bacterial growth is prevented. The only limitation to the length of storage in liquid nitrogen is the accumulation of damage caused by background ionizing radiation (Ashwood-Smith & Friedmann, 1979; Mazur, 1984). Transplantation of cryopreserved cells and tissues has been used to replace cells and tissues that are no longer functional due to disease or injury.

With the advances that have taken place in cryobiology over the last 50 years, improved cryopreservation techniques for the preservation of cellular and tissue systems have been developed. There are many advantages to being able to bank cryopreserved cells and tissues for long periods of time. Cryopreservation

allows time for donor screening and testing. This has recently become more important because of increased transmission of infectious diseases, so a full social, behavioral and medical history of the donor is desired before transplantation. This storage allows for more effective donor-recipient matching, tissue typing, infectious disease testing and national sharing. The cryopreservation of cells and tissues also makes it easier to coordinate donor availability and recipient need. One of the main challenges has been to take the cells and tissues through the temperature range which damage occurs and bring them back without irreparable damage.

The cryopreservation of most cells in suspension is now a routine procedure. Bone marrow cells are routinely stored for transplantation after ablative therapy in the treatment of leukemia and other malignancies (Pegg, 1964; Buckner et al., 1981). Sperm cells and embryo tissues for many different species including plants, insects, mammals and other animals have been stored for several reasons including the preservation of biological diversity in rare and endangered species. The transplantation of human tissue is becoming more routine and tissue banks around the world are being developed where tissues such as skin, blood, heart valves and articular cartilage are being cryopreserved. The islets of Langerhans are the structures in the pancreas that produce insulin in response to blood glucose levels. These are being banked and cryopreserved for the treatment of diabetic patients. The cryopreservation of other tissue types and organs is still a complex task that requires an accumulation of understanding of

the many different biophysical processes that are taking place. Because tissues and organs are made up of many different cell types, cryopreservation is not a trivial task. The intrinsic response of cells depends on whether the cells are isolated or part of a tissue system and each cell type has it's own ideal cryopreservation conditions.

1.2 Cellular Cryobiology

As a biological sample is cooled to temperatures below its equilibrium freezing point, ice forms in the extracellular liquid either spontaneously or by induced freezing. The deliberate "seeding" of ice occurs by the introduction of an ice crystal to the external solution, by touching the surface of the media with a cold probe, by mechanical vibration or by rapidly lowering the temperature until ice nucleation occurs. As ice forms in the extracellular media, free water becomes bound in the ice. Ice does not immediately form intracellularly because the cell membrane acts as a barrier for the growth of ice crystals into the cell through the membrane (Mazur, 1965) and the cytoplasm contains few effective nucleators (Mazur, 1970; Rasmussen et al., 1975; Franks et al., 1983). The cells become exposed to an increasingly hypertonic solution due to the progressive increase in the external solute concentration that occurs as more extracellular ice forms and the cell contents remain unfrozen or super-cooled. The water in the unfrozen cell then has, by definition, a higher chemical potential than that of water in the partially frozen solution. In response to this difference in chemical potential, an

osmotic pressure gradient is created. This gradient provides the driving force for the efflux of water out of the cell that results in cell shrinkage.

The survival of cryopreserved cells is strongly dependent on the rate at which cells are cooled and warmed. In cryopreservation protocols, the sample is cooled at a finite rate that is optimized for each cell type. This is one of the reasons why it is difficult to cryopreserve organs. Organs are large, multi-compartment structures that have a high degree of structural organization. Since organs are composed of many different cell types, finding an optimal cooling rate is difficult.

Cell injury is related to the nature and kinetics of the cell response to temperature-induced conditions. If cells are cooled at rates higher or lower than the optimal cooling rate, damage will occur to the cells. If the cooling rate is rapid, the formation of ice in the extracellular solution is much faster than the efflux of water from the cells. Because water efflux from the cell is too slow to maintain osmotic equilibrium, the cytoplasm becomes increasingly supercooled until it eventually freezes. Cells that are cooled too quickly do not shrink appreciably and equilibrate by forming intracellular ice. The presence of intracellular ice has been found to be lethal for cells in suspension. In contrast, if cells are cooled too slowly, damage can also occur. At slow cooling rates, the cell is able to lose water rapidly enough by exosmosis to concentrate the intracellular solutes sufficiently to eliminate super-cooling and maintain the

chemical potential of intracellular water in equilibrium with that of extracellular water. As a result, the cell dehydrates and does not form intracellular ice. Lower than optimal cooling rates result in damage to the cells caused by prolonged exposure at relatively high sub-zero temperatures to the increased concentration of electrolytes in the intracellular solution. The ability of a cell to react osmotically to the changing environment is therefore a fundamental element in its response to low temperatures.

In 1963, Mazur (1963) suggested a quantitative approach to describing a cell's response during freezing. He proposed that the rate of efflux of water from a cell during exposure to low temperature could be predicted if the water permeability of the cell, the initial osmolality of the cells and the surface area to volume ratio were known. The expressions he developed allow one to calculate the extent of supercooling in cells as a function of the cooling rate and to estimate the probability of intracellular ice formation as a function of cooling rate. As a result, cryopreservation protocols could be designed that avoided cellular injury. Mazur et al., (1972) proposed a 'two-factor hypothesis' of freezing damage, according to which there are two independent mechanisms of damage during freezing, one active at slow cooling rates and the other at rapid cooling rates.

1.2a Slow Cool Injury

Mazur et al., (1972) proposed that during slow cooling, cellular injury was due to the relatively long exposure to the altered properties of the intracellular and

extracellular solutions as a result of ice formation. These 'solution effects' included dehydration, concentration of solutes, changes in pH and the precipitation of solutes. Despite the fact that the cell can maintain osmotic equilibrium with the extracellular space through dehydration so that no ice forms inside the cytoplasm, cellular damage can still occur. Damage during slow cooling is thought to occur as a result of solute toxicity (Lovelock, 1953a; Mazur et al., 1972, Meryman, 1974) and physical damage caused during cell shrinkage (Meryman, 1974; Steponkus & Weist, 1978). The high concentration of electrolytes and other solutes in the extracellular medium and the resulting cell dehydration during slow cooling has been proposed as a source of damage. Lovelock (1957) showed that hemolysis in red blood cells could be induced by denaturation of lipoproteins caused by a hypertonic salt solution. It was also proposed that damage during freezing is the result of water loss and volume reduction. Meryman (1974) proposed the existence of a critical volume of tolerance that cells could withstand during shrinkage and that injury occurred when cells reached a 'minimum critical volume'. It has also been suggested that during slow cool injury, the cell surface area is reduced as a result of a loss in membrane material (Steponkus & Weist, 1978). It has been found that plasma lipids can be deleted from the membrane during osmotic dehydration and that damage can occur during rehydration if there is insufficient membrane material for the cell to return to its isotonic volume. The specifics of the molecular mechanisms involved in slow cool injury are still relatively unknown and work is currently being undertaken in this area of cryobiology.

1.2b Rapid Cool Injury

During rapid cooling, the formation of extracellular ice and the concentration of the extracellular solutes both occur too quickly for the cells to respond by osmotic shrinkage. As a result, the cytoplasm becomes increasingly supercooled and ice forms intracellularly (Mazur et al., 1972). There has been significant evidence for the correlation between cell injury and intracellular ice formation during rapid cooling (Mazur, 1984). It has been proposed that injury results from intracellular ice and the possible sites of damage may include intracellular organelles (Mazur, 1966) and the plasma membrane (Fijikawa, 1980). It has also been proposed that the damage mechanism during fast cooling rates may be the result of membrane rupture due to osmotic fluxes (Muldrew & McGann, 1990; Muldrew & McGann, 1994). Many non-mechanical theories of injury have also been suggested (Karlsson et al., 1993). For example, the osmotic effects due to the melting of intracellular ice during warming (Farrant, 1977) or the induction of gas bubble formation by intracellular ice (Morris & McGrath, 1981; Ashwood-Smith et al., 1988)

1.2c Warming Rates

The recovery of cells after freezing and thawing is not only dependent on the cooling rate but also on the rate of warming (Miller & Mazur, 1976; Akhtar et al., 1979; Pegg et al., 1984). It has been found experimentally that cells that are cooled more slowly than the optimal rate survive better when the warming rate is low than when it is high. Because cells that are cooled slowly do not form

intracellular ice but are severely dehydrated, if warmed rapidly, these cells may become osmotically stressed as the result of the rapid water influx. As a result, slowly cooled cells give higher recovery when warmed slowly. Conversely, cells that are cooled more rapidly than the optimum rate of cooling survive better when the warming rate is high because the small intracellular ice crystals formed during rapid cooling coalesce into larger damaging crystals during warming by the process of recrystallization (Forsyth & MacFarlane, 1986). To minimize the effects of recrystallization, rapid warming rates must be used for rapidly cooled cells.

1.3 Traditional Cryopreservation of Cells

Damage to cells during freezing is caused by both intracellular freezing during rapid cooling and exposure to high concentrations of solutes during slow cooling. Successful cryopreservation protocols have been dependent on the development of novel techniques to minimize both types of damage. Many types of cells do not survive freezing and thawing unless a cryoprotectant is present. Cryoprotectants are chemical compounds that are added to the biological sample to minimize the deleterious effects of freezing. In 1949, Polge, Smith and Parkes were the first to use chemical compounds to enhance the survival of frozen biological material, when they discovered the cryoprotective action of glycerol. They found an increased viability in fowl sperm after freezing when the samples were suspended in a medium containing glycerol (Polge et al., 1949). There are

two main groups of cryoprotective agents: permeating cryoprotectants and non-permeating cryoprotectants.

1.3a Permeating Cryoprotectants

The permeating cryoprotectants are those that act by crossing the cell membrane. Examples of permeating cryoprotectants include glycerol and dimethyl sulfoxide (DMSO). These two cryoprotectants are the most commonly used for cryopreserving cells. Dimethyl sulfoxide and glycerol have very different cell permeabilities with that of glycerol being much lower than that of DMSO. The permeating cryoprotectants act by reducing colligatively both the amount of ice formed and the rise in electrolyte concentration inside and outside the cell (since less ice is formed both intracellularly and extracellularly and less osmotic shrinkage occurs), at any given temperature (Lovelock, 1953b). The permeating cryoprotectants are primarily effective in protecting the cells against slow cool injury. In general, as the concentration of cryoprotectant increases, cell survival improves and the optimum-cooling rate is reduced (Mazur et al., 1970). However, the cryoprotective chemicals themselves can be damaging. High concentrations of cryoprotectants have detrimental toxic and osmotic effects on cells, the latter of which are a consequence of the cell membrane being more permeable to the water than to the cryoprotectant.

In work done by McGann in 1984, the osmotic responses of bovine chondrocytes were modeled during the addition and dilution of various concentrations of the

permeating cryoprotectant, DMSO, at different temperatures, shown in Figure 1-1. When exposed to the permeating cryoprotectant, the cell initially shrinks as water moves out of the cell to restore osmotic equilibrium. As the cryoprotectant enters the cell, it is accompanied by water and the cell returns to its normal volume. During dilution, the cell swells as water enters to restore osmotic equilibrium. The cell then returns to its normal volume as the cryoprotectant and water both leave the cell simultaneously (Davson and Danielli, 1952). From Figure 1-1, we see that the rate of cell shrinkage depends on both the concentration of the cryoprotectant and the temperature at which it was added. This is important because the rate of cell shrinkage affects whether slow cool injury or rapid cool injury takes place.

1.3b Non-Permeating Cryoprotectants

The non-permeating cryoprotectants are those that cannot cross the cell membrane. Examples of non-permeating cryoprotectants include hydroxyethyl starch, dextran and sucrose. As water is removed from the solution as ice at high sub-zero temperatures, the non-permeating cryoprotectant is concentrated in the extracellular region only, while the other solutes become concentrated both inside and outside the cell. The non-permeating cryoprotectant is then responsible for an additional osmotic stress on the cell that results in an increased loss of water at these high subzero temperatures. Water loss from the cell occurs at a lower concentration of other solutes than if the non-permeating cryoprotectant was absent. Protection against further cooling is obtained by

osmotic shrinkage due to the increased concentration of the non-permeating cryoprotectant in the extracellular region (McGann, 1978).

In work done by McGann in 1984, the osmotic responses of bovine chondrocytes were modeled during the addition and dilution of various concentrations of a non-permeating cryoprotectant at different temperatures, shown in Figure 1-2. When exposed to the non-permeating cryoprotectant, since the cryoprotectant does not move across the membrane, the cell shrinks to maintain osmotic equilibrium. Also, during the dilution stage, the cell swells to maintain osmotic equilibrium. Once again as with the permeating cryoprotectants, the osmotic response of the cell depends on both the concentration of the cryoprotectant and the temperature at which the cryoprotectant is added. This is again important in determining the rate of cell shrinkage to avoid cellular injury.

Innovative cryopreservation protocols for the addition and dilution of permeating and non-permeating cryoprotectants that decrease the time of exposure and the concentration of the cryoprotectants continue to be developed in efforts to avoid their toxic effects when used in high concentrations.

1.4 Cell Membrane Permeability

As seen from the previous sections, an understanding of cell membrane permeability is very important in predicting a successful outcome from a

cryopreservation protocol. The survival of the cell during cryopreservation depends on a complex interaction between the cooling rate, the warming rate and the type and concentration of cryoprotectant used. The optimal cooling rate that avoids slow cool and rapid cool injury depends on the ratio of the volume of a cell to its surface area and on its permeability to water (Mazur, 1963; Mazur, 1965; Mazur 1970). Using these permeability parameters, it is possible to model both the optimal conditions for the addition and removal of cryoprotectants that maintain cell volume changes within the limits of non-detrimental and non-toxic effects, and the optimal cooling rate for cell cryopreservation (Mazur, 1963; Arnaud & Pegg, 1990; Gao et al., 1995). The membrane permeability is concentration-dependant and strongly temperature-dependant. Therefore, a better understanding of this dependence is necessary to improve cryopreservation protocols.

In Figure 1-3, water and solute movement across a homogeneous cell membrane is illustrated. The flux of water (w) across the cell membrane is denoted by J_W and the flux of solute (s) across the membrane is denoted by J_S. There is a concentration (c) and/or pressure (P) difference between the outside (o) and the inside (i) of the cell membrane and it is this difference in concentration (Δc) and/or hydrostatic pressure (ΔP), which leads to transport across the cell membrane.

A number of formalisms have been developed to determine the permeability characteristics. The one that is most commonly used in cryobiology today is that which was developed by Kedem and Katchalsky in 1958 (Kedem & Katchalsky, 1958). Their formalism was developed specifically to handle situations for which water and solute transport across a cell membrane was physically coupled but can also be used to describe situations where the solute and solvent fluxes do not interact. The equation they developed to describe the change in water and solute volume (V_{W+S}) with time (t) resulting from water and solute fluxes is given by:

$$\frac{dV_{W+S}}{dt} = -L_p ART\left\{\left(M_n^o - M_n^i\right) + \sigma\left(M_{ps}^o - M_{ps}^i\right)\right\} \qquad (1\text{-}1)$$

where L_p is the membrane hydraulic conductivity, A is the area of the cell, R is the universal gas constant, and T is absolute temperature. M is the osmolality with the superscripts denoting the internal cell solution (i) and the solution external to the cell (o) and the subscripts denoting the non-permeating solutes (n) and the permeating solutes (ps). Sigma (σ) is the reflection coefficient which characterizes the degree of interaction between the water and solute and is constrained by the following condition:

$$0 \le \sigma \le 1 - \frac{P_S \bar{\upsilon}_S}{RTL_p} \qquad (1\text{-}2)$$

where P_S is the membrane solute permeability coefficient and $\bar{\upsilon}_s$ is the partial molar volume of the solute.

The equation for water flux alone across the cell membrane was used by Jacobs and Stewart in 1932 (Jacobs & Stewart, 1932) and then was reviewed again by Kedem and Katchalsky in their 1958 paper (Kedem and Katchalsky, 1958). The rate of change of cell volume with time, can be given by the following membrane mass transport model:

$$\frac{dV_W}{dt} = L_p ART(M^i - M^o) \qquad (1\text{-}3)$$

where V_W is the water volume of the cell.

The magnitude and speed of the volume change that takes place in the cell is dependent on the size of the concentration gradient across the membrane, the membrane hydraulic conductivity, the solute permeability coefficient, and the reflection coefficient (House, 1974).

1.5 Objectives and Scope of this Thesis

In order to optimize the viability of cryopreserved cells and tissues, a better understanding of osmotic transport is required. The main objective of this thesis is to gain insight into the movement of water across cell membranes and two parameters that effect cell permeability, cell size distribution and temperature.

In the second chapter of this thesis the theoretical descriptions for osmotic transport across cell membranes are examined. The traditional theoretical descriptions of osmotic transport across cell membranes are based on the work

of Kedem and Katchalsky, which was based on Onsager's linear theory of non-equilibrium thermodynamics, published in 1931 (Onsager, 1931a; Onsager, 1931b). This theory is written in terms of coefficients that do not have an explicit physical meaning. The coefficients cannot be derived from within the theory and must be evaluated empirically. The theoretical validity of Onsager's reciprocity assumption that two of these coefficients (the cross coefficients) are equal has been discussed at various levels and often has been proven often to be the case experimentally.

Statistical Rate Theory is a relatively new complete theory of non-equilibrium thermodynamics (Ward, 1977) that has recently been shown to lead to improvements over traditional theories for chemical kinetics, ion transport across cell membranes, evaporation, crystal growth from solution, adsorption and absorption. One of the main advantages of Statistical Rate Theory is that it may be written entirely in terms of physical, experimental parameters that may be measured or controlled.

Statistical Rate Theory is used to develop new osmotic transport equations that can be written in terms of measurable parameters such as concentration, pressure, temperature and physical membrane properties. Also, for a particular situation, the Onsager reciprocity relation is examined.

In the third chapter of this thesis, the effect of cell size distribution on the osmotic response of cells is examined. Traditionally, a mathematical model of cell osmotic response is obtained by applying mass transport and Boyle-van't Hoff equations using numerical methods. In the usual application of these equations, it is assumed that all cells are the same size. However, real biological cells have variations in size, and a population of cells may exhibit a different osmotic response than that of a single cell. In this study, cell shrinkage kinetics of Chinese hamster fibroblast cells (V-79W) and Madin-Darby Canine Kidney cells (MDCK) placed in solutions of different concentrations are reported. A mathematical model of cell osmotic response (found by solving mass transport and Boyle-van't Hoff equations analytically and then applying this analytical solution to a measured size distribution of cells) is evaluated.

In the fourth chapter of this thesis, the temperature dependence of water movement across cell membranes is examined. Two models are examined to analyze the temperature dependence of water movement across cell membranes. The first model involves using Fick's Law of Diffusion and assuming water diffuses through aqueous pores and the second model is based on solubility-diffusion through a lipid bilayer. These two models of osmotic transport across cell membranes are compared to experimental data along with the traditional Arrhenius equation. The two models are Arrhenius behaving but only have one free parameter compared with the traditional Arrhenius equation that has two free parameters. The models are applied to four cell types.

Experimental data for one cell type (V-79W hamster fibroblast cells) are obtained in this thesis while data for the other three cell types are obtained from the literature.

1.6 References

1. Akhtar, T., Pegg, D. E., and Foreman, L. 1979. The effect of cooling and warming rates on the survival of cryopreserved L-cells. *Cryobiology*, **16**, 424-429.
2. Arnaud, F. G., & Pegg, D. E. 1990. Permeation of glycerol and propane-1,2-diol into human platelets. *Cryobiology*, **27**, 107-118.
3. Ashwood-Smith, M. J. & Friedmann, G. B. 1979. Lethal and chromosomal effects of freezing, thawing, storage time, and x-irradiation on mammalian cells preserved at -196°C in dimethyl sulfoxide. *Cryobiology*, **16**, 132-140.
4. Ashwood-Smith, M. J., Morris, G. W., Fowler, R., Appleton, T. C. and Ashorn, R. 1988. Physical factors are involved in the destruction of embryos and oocytes during freezing and thawing procedures. *Human Reprod.*, **3**, 795-802.
5. Buncker, C. D., Appelbaum, F. R., and Thomas, E. D. 1981. Bone marrow and fetal liver. In *Organ Preservation for Transplantation* (ed. A. M. Karow and D. E. Pegg), 355-357. New York: Dekker
6. Davson, H., & Danielli, J. F. 1952. *The permeability of Natural Membranes*. Cambridge: Cambridge University Press.
7. Diller, K. R. 1979. Intracellular freezing of glycerolized red cells. *Cryobiology*, **16**, 125-131.

8. Farrant, J. 1977. Water transport and cell survival in cryobiological procedures. *Phil Trans Royal Soc London B*, **278**, 191-205.

9. Fennema, O. 1966. An over-all view of low temperature food preservation. *Cryobiology*, **3**, 197-213.

10. Forsyth, M., & McFarlane, D. R. Recrystallization revisited. *Cryo. Lett.*, **7**, 367-378.

11. Franks, F., Mathias, S. F., Glafre, P., Webster, S. D and Brown, D. 1983. Ice nucleation and freezing in undercooled cells. *Cryobiology*, **20**, 298-309.

12. Fujikawa, S. 1980. Freeze-fracture and etching studies on membrane damage on human erythrocytes caused by formation of intracellular ice. *Cryobiology*, **17**, 351-362.

13. Gao, D. Y., Liu, J., Liu, C., McGann, L. E., Watson, P. F., Kleinhans, F. W., Mazur, P., Critser, E. S., and Critser, J. K. 1995. Prevention of osmotic injury to human spermatozoa during addition and removal of glycerol. *Hum. Reprod.* **10**, 1109-1122.

14. House, C. R. 1974. *Water transport in cells and tissues*. London: Arnold.

15. Jacobs, M. H., & Stewart, D. R. 1932. A Simple Method for the Quantitative Measurement of Cell Permeability. *J. Cell. Comp. Physiol.* **1**, 71-82.

16. Karlsson, J. O. M., Cravalho, E. G., Toner, M. 1993. Intracellular ice formation: causes and consequences. *Cryo. Lett.*, **14**, 323-336.

17. Kedem, O., & Katchalsky, A. 1958. Thermodynamic analysis of the permeability of biological membranes to non-electrolytes. *Biochim. Biophys. Acta.* **27**, 229-246.

18. Leibo, S. P. 1983. Field trails of one-step diluted frozen-thawed bovine embryos. *Cryobiology*, **20**, 742.

19. Liu, C., Benson, C. T., Gao, D., Haag, B. W., McGann, L. E., Critser, J. K. 1995. Water permeability and its activation energy for individual hamster pancreatic islet cells. *Cryobiology*, **32**, 493-502.

20. Lovelock, J. E. 1953a. The haemolysis of human red blood cells by freezing and thawing. *Biochim. Biophys. Acta*, **10**, 414-426.

21. Lovelock, J. E. 1953b. The mechanism of the protective action of glycerol against haemolysis by freezing and thawing. *Biochim. Biophys. Acta*, **11**, 28-36.

22. Lovelock, J. E. 1957. The denaturation of lipid-protein complexes as a cause of damage by freezing. *Proc. Royal Soc. London Ser. B*, **147**, 427-433.

23. Mazur, P. 1963. Kinetics of water loss from cells at subzero temperatures and the likelihood of intracellular freezing. *J. Gen Physiol*, **47**, 347-369.

24. Mazur, P. 1965. The role of cell membranes in the freezing of yeast and other single cells. *Ann NY. Acad. Sci.*, **125**, 658-676.

25. Mazur, P. 1966. Physical and chemical basis of injury of single-celled microorganisms subjected to freezing and thawing. In: Meryman HT, ed. *Cryobiology*, New York: Academic Press, 214-315.

26. Mazur, P. 1970. Cryobiology: The freezing of biological systems. *Science*, **168**, 939-949.

27. Mazur, P. 1977. The role of intracellular freezing in the death of cells cooled at supraoptimal rates. *Cryobiology*, **14**, 251-272.

28. Mazur, P. 1984. Freezing of living cells: Mechanisms and implications. *Am. J. Physiol.*, **247** (Cell Physiol. 16) C125-C142.

29. Mazur, P., Leibo, S. P., Farrarnt, J., Chu, E. H. Y., Hanna, M. G. and Smith, L. H. 1970. Interactions of cooling rate, warming rate and protective additives on the survival of frozen mammalian cells. In *Ciba Foundation Symposium on the Frozen Cell* (ed. G. E. W. Wolstenholme & M. O'Connor), 69-88. London, Churchill.

30. Mazur, P., Leibo, S. P., and Chu, E. H. Y. 1972. A two-factor hypothesis of freezing injury: Evidence from Chinese hamster tissue-culture cells. *Exper. Cell Res.*, **71**, 345-355.

31. McGann, L. E. 1978. Differing Actions of Penetrating and Nonpenetrating Cryoprotective Agents. *Cryobiology*, **15**, 382-390.

32. McGann, L. E. 1984. Unpublished data.

33. McGann, L. E., Janowska-Wieczorek, A., Turner, A. R., Hogg, L., Muldrew, K. B., Turc, J. M. 1987. Water permeability of human hematopoetic stem cells. *Cryobiology*, **24**, 112-119.

34. McGann, L. E., Stevenson, M., Schachar, N. 1988. Kinetics of osmotic water movement in chondrocytes isolated from articular cartilage and applications to cryopreservation. *J. Orthop. Res.*, **6**, 109-115.

35. Meryman, H. T. 1974. Freezing injury and its prevention in living cells. *Annu. Rev. Biophys*, **3**, 341-363.

36. Miller, R. H., & Mazur, P. 1976. Survival of human red cells as a function of cooling and warming velocities. *Cryobiology*, **13**, 404-414.

37. Morris, G. J. & McGrath, J. J. 1981. Intracellular ice nucleation and gas bubble formation in spirogyra. *Cryo. Lett.*, **2**, 341-352.

38. Muldrew, K. & McGann, L. E. 1990. Mechanisms of intracellular ice formation. *Biophys. J.*, **57**, 525-532.

39. Muldrew, K. & McGann, L. E. 1994. The osmotic rupture hypothesis of intracellular freezing injury. *Biophys. J.*, **66**, 532-541.

40. Onsager, L. 1931a. Reciprocal relations in irreversible processes. I. *Phys. Rev.*, **37**, 405-426.

41. Onsager, L. 1931b. Reciprocal relations in irreversible processes. II. *Phys. Rev.*, **38**, 2265-2279.

42. Pegg, D. E. 1964. Freezing of bone marrow for clinical use. *Cryobiology*, **1**, 64-71.

43. Pegg, D. E., Diaper, M. P., Skaer, H., LeB. And Hunt, C. J. 1984. The effect of cooling rate on the packing effect in human erythrocytes frozen and thawed in the presence of 2M glycerol. *Cryobiology*, **21**, 491-502.

44. Polge, C. & Lovelock, J. E. 1952. Preservation of bull semen at -79°C. *Vet. Rec.*, **64**, 396-397.

45. Polge, C., Smith, A. U., and Parkes, A. S. 1949. Revival of spermatozoa after vitrification and dehydration at low temperatures. *Nature, Lond.* **164**, 666.

46. Rasmussen, D. H., MacAulay, M. N and MacKenzie, A. P. 1975. Supercooling and nucleation of ice in single cells. *Cryobiology*, **12**, 328-339.

47. Steponkus, P. L & Weist, S. C. 1978. Plasma membrane alterations following cold acclimation and freezing. In *Plant Cold Hardiness and Freezing Stress-Mechanisms and Crop Implications* (P. H. Li and A. Sakai, Eds.), 75-91, Academic Press, New York

48. Ward, C. A. 1977. The rate of gas adsorption at a liquid interface. *J. Chem. Phys.* **67(1)**, 229-235.

49. Wilmut, I. & Rowson, L. E. 1973. Experiments on the low temperature preservation of cow embryos. *Vet. Rec.*, **92**, 686-690.

Figure 1-1 Osmotic Response During the Addition and Dilution of Cryoprotectants: Permeating Solutes

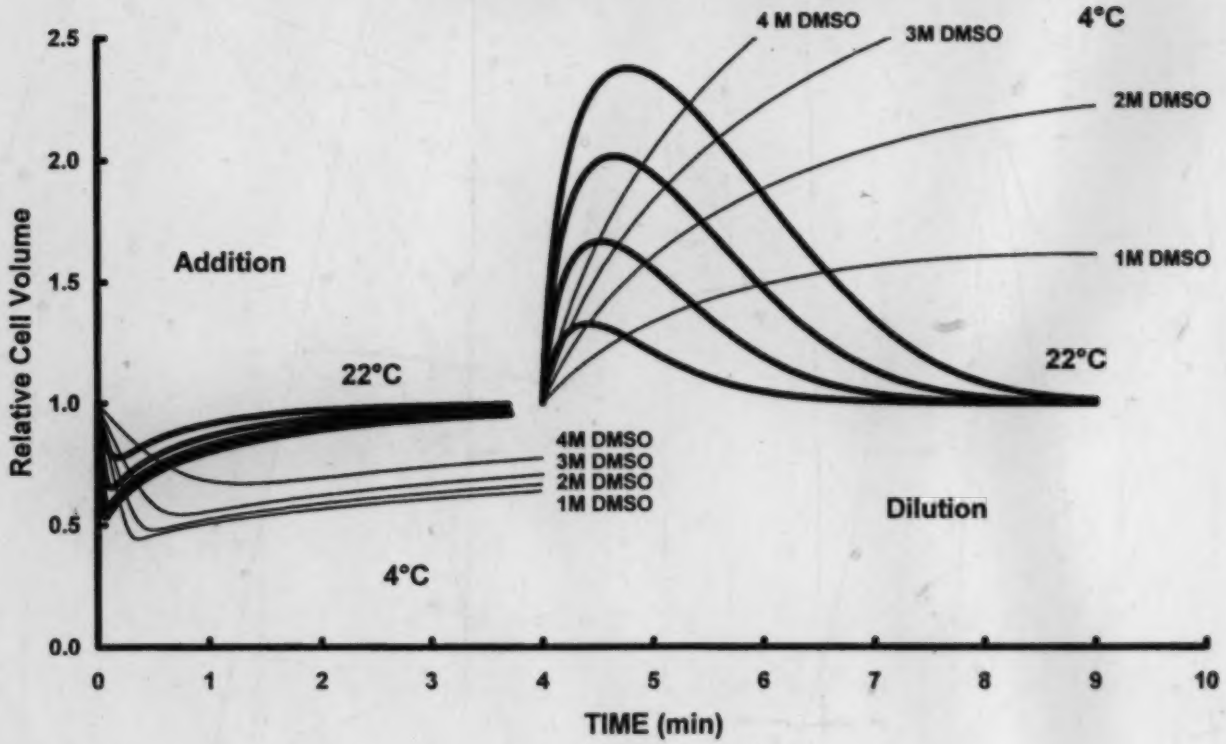

Figure 1-2 Osmotic Response During the Addition and Dilution of Cryoprotectants: Non-Permeating Solutes

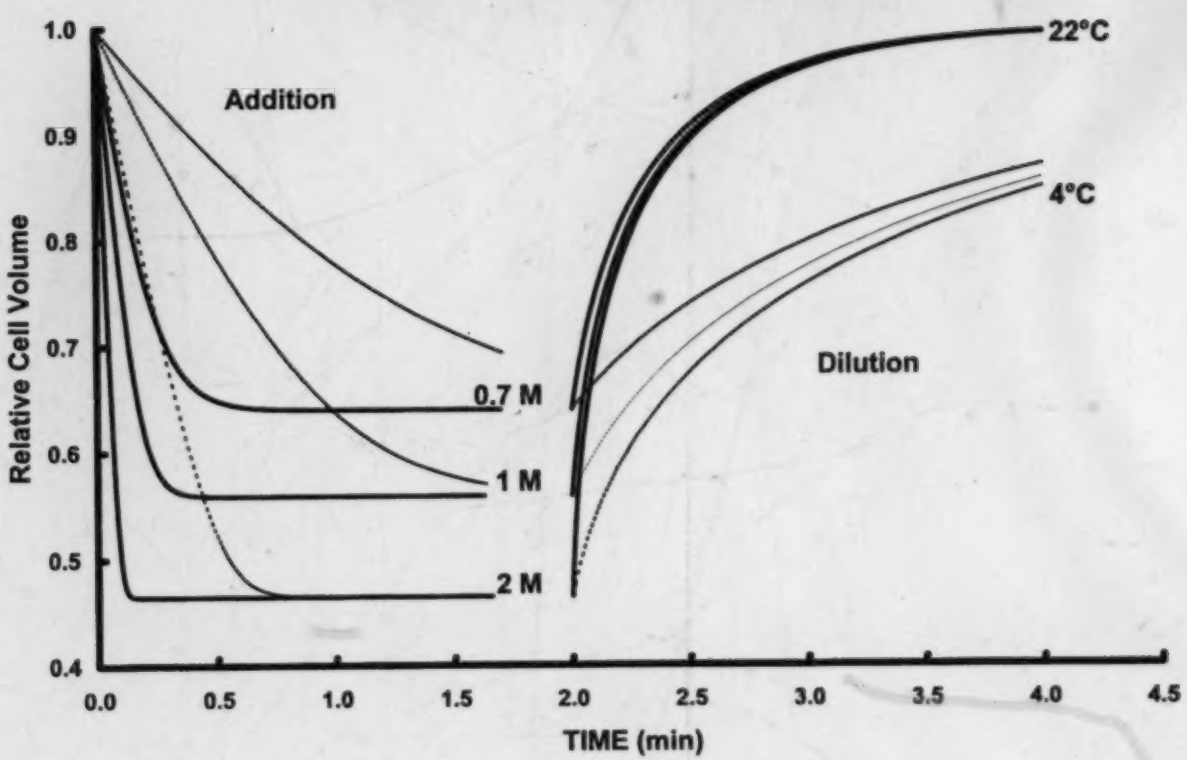

Figure 1-3 Water and Solute Movement Across a Homogeneous Membrane

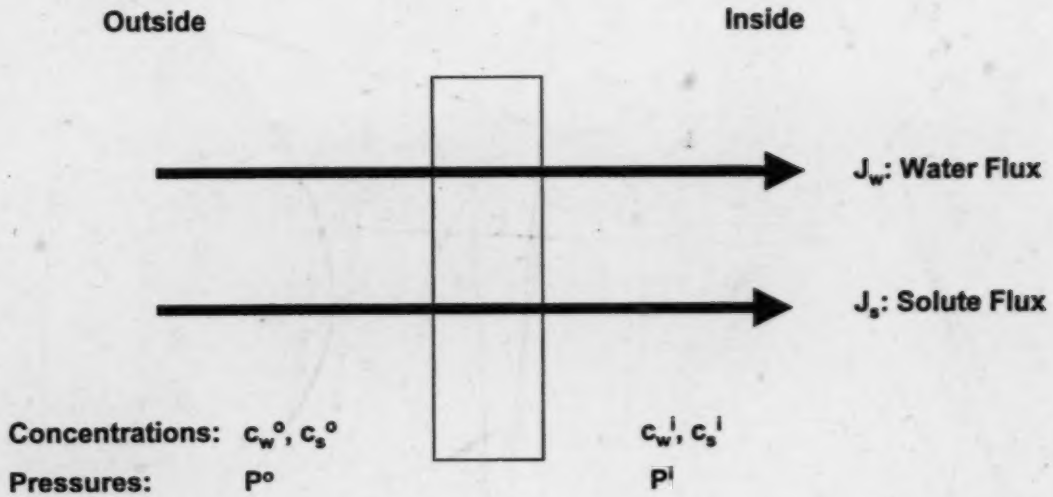

$\Delta c = c^o - c^i$

$\Delta P = P^o - P^i$

Chapter 2: Theoretical Modeling of Water Transport across Cell Membranes*

2.1 Introduction

An understanding of cell membrane permeability is very important in predicting a successful outcome from a cryopreservation protocol. Since the 1930's, formalisms have been developed to describe the efflux of water and solutes across cell membranes (Jacobs & Stewart, 1932; Kedem & Katchalsky, 1958).

2.1a Theories of Osmotic Transport

Much of our understanding of transport phenomena is based on linear irreversible thermodynamics, and cell volume change due to solute and solvent flow across cell membranes is an example of such a phenomenon. In 1952, Staverman approached the problem of osmotic transport across cell membranes and measuring osmotic pressures by employing the theory of irreversible thermodynamics, formalized most notably by Onsager in 1931 (Onsager, 1931a; Onsager, 1931b). In 1958, Kedem and Katchalsky modified and extended the work of previous authors again using irreversible thermodynamics. The theory is based on the premise that for a system sufficiently close to equilibrium, any flux, J, (such as a heat flux or a mass flux) is linearly proportional to a driving force, X, (or a gradient in an intensive property such as pressure or concentration). To identify the fluxes and forces in a system, the entropy production is written in a

* Portions of this chapter have been submitted to the Journal of Chemical Physics as: J. A. W. Elliott, H. Y. Elmoazzen, and L. E. McGann, "A method whereby Onsager's reciprocity hypothesis may be examined"

form whereby fluxes are multiplied by forces. For a system with a single flux as a result of a single thermodynamic force driving the system towards equilibrium, the entropy production has the following form:

$$\frac{dS}{dt} = JX \qquad (2\text{-}1)$$

where S is the entropy. An equation for the flux can then be written in the following form:

$$J = LX \qquad (2\text{-}2)$$

where L is a phenomenological coefficient also known as an Onsager coefficient. Many transport processes such as diffusion, heat conduction, and electrical conduction, are given in the above form. In Fick's Law of Diffusion, the flux, J, is that of a diffusing solute and the driving force, X, is the concentration gradient. The phenomenological coefficient in this case is the diffusion coefficient. In Fourier's Law of Heat Transfer, the flux is the heat flux and the driving force is the gradient in temperature. The phenomenological coefficient is the thermal conductivity. In Ohm's Law, the flux is current density and the driving force is a voltage gradient. The phenomenological coefficient is conductivity.

In the case of a system with two fluxes, J_1 and J_2, that are linearly dependent on two forces, X_1 and X_2, the entropy production has the following form:

$$\frac{dS}{dt} = J_1X_1 + J_2X_2 \qquad (2\text{-}3)$$

The flux equations may then be written as follows:

$$J_1 = L_{11}X_1 + L_{12}X_2 \qquad (2-4)$$
$$J_2 = L_{21}X_1 + L_{22}X_2 \qquad (2-5)$$

where once again the L's are phenomenological coefficients. A reciprocity relation known as Onsager's reciprocity relation exists between the phenomenological cross coefficients, L_{12} and L_{21}:

$$L_{12} = L_{21} \qquad (2-6)$$

In the case of more than two thermodynamic forces and fluxes, there will be multiple reciprocal relations. For example, in a system with three forces, X_1, X_2 and X_3, the flux equations may be written as follows:

$$J_1 = L_{11}X_1 + L_{12}X_2 + L_{13}X_3 \qquad (2-7)$$
$$J_2 = L_{21}X_1 + L_{22}X_2 + L_{23}X_3 \qquad (2-8)$$
$$J_3 = L_{31}X_1 + L_{32}X_2 + L_{33}X_3 \qquad (2-9)$$

and the phenomenological coefficients are related by:

$$L_{12} = L_{21},\ L_{23} = L_{32},\ L_{31} = L_{13} \qquad (2-10)$$

Since the 1850's, work has been done to prove the validity of the reciprocity relation (Onsager, 1931a). In his papers, Onsager makes the assumption of "microscopic reversibility" and that the cross coefficients are equal at equilibrium since for each reaction at equilibrium, the forward rate of reaction will balance the backward rate. Despite the fact that the Onsager reciprocity relationship has been experimentally demonstrated to be true for many situations (Nerst, 1888, Miller, 1960), and certain statistical mechanical arguments exist for it's validity (Kirkwood & Fitts, 1960), it has not been theoretically proven by linearizing a general far-from-equilibrium theory. One advantage to finding Onsager

coefficients by linearizing a general theory is that rather than being phenomenological, such coefficients would be expressed in terms of physical experimental variables. Another advantage of linearizing a general theory is that explicit conditions under which the linearity assumption holds may be derived whereas there is no way from within the Onsager approach to determine whether a system is close enough to equilibrium for the Onsager equations to apply.

2.1b Statistical Rate Theory

Statistical Rate Theory is a fairly new, complete theory of non-equilibrium thermodynamics that was developed in 1977 (Ward, 1977) and has been published in a more current form in 1982 (Ward et al., 1982a) and 1983 (Ward, 1983). The theory is derived from a mathematical model that uses entropy and is based on a quantum mechanical description of a multi-particle system (Ward et al., 1982a; Ward, 1983; Elliott & Ward, 1997a). Statistical Rate Theory provides an expression for the instantaneous net molecular transport rate across the interface of two similar or different phases.

Statistical Rate Theory can be considered a 'complete' theory in the sense that no near-equilibrium assumptions are made in its development and it can be used to derive rate equations that can be written entirely in terms of experimental and thermodynamic variables that may be tabulated, measured or controlled. The theory has led to improvements over traditional theories for many rate processes including: electron exchange between isotopes in solution (Ward, 1983; Elliott &

Ward, 1997a), gas-solid adsorption (Findlay & Ward, 1982; Ward & Findlay, 1982; Ward & Elmoselhi, 1986; Elliott & Ward, 1997a; Elliott & Ward, 1997b; Elliott & Ward, 1997c), gas absorption at a liquid interface (Ward et al., 1982b; Ward et al., 1986a; Tikuisis & Ward, 1992), hydrogen absorption by metals (Ward et al., 1986b), permeation in ionic channels in biological membranes (Skinner et al., 1993), crystal growth from solution (Dejmek & Ward, 1998), evaporation (Ward & Fang, 1998; Fang & Ward, 1998) and diffusion of adsorbates on stepped surfaces (Torri & Elliott, 1999).

From Statistical Rate Theory, the expression for the instantaneous net rate of molecular transport (flux), J, across the interface between two phases (Ward et al., 1982a; Ward, 1983; Elliott & Ward, 1997a) is:

$$J = K_e\left[\exp\frac{(\Delta S_f)}{k} - \exp\frac{(\Delta S_b)}{k}\right] \qquad (2\text{-}11)$$

where K_e is the equilibrium exchange rate of molecules across the interface, ΔS_f and ΔS_b are the entropy changes as a result of a molecule moving in the "forward" direction and in the reverse "backward" direction, respectively and k is the Boltzmann constant.

In this Statistical Rate Theory approach, the local thermodynamic equilibrium assumption was made that assumes that there exists a surrounding of some dimension small enough that the thermodynamic properties within the surroundings are constant but large enough that there are enough molecules that thermodynamic relations apply. This same assumption was made in Onsager's

approach. However, with the Statistical Rate Theory approach, in Eq. 2-11, there are no linearity or near-equilibrium assumptions made.

If the transport of a molecule across an interface results in the entropy change in Eq. 2-11 being large, then the exponentials in the equation cannot be linearized (Torri & Elliott, 1999). Note that when treating chemical reactions, the exponentials appearing in Eq. 2-11 cannot be linearized (Elliott & Ward, 1997b). If the transport of a molecule across an interface results in a small enough entropy change, then the Statistical Rate Theory equation can be linearized. For the cases in which the Statistical Rate Theory equation can be linearized, the equations can be directly compared to the Onsager approach. The Onsager approach assumes linearity and results in the expressions with phenomenological coefficients; however, with the Statistical Rate Theory approach, there is no *a priori* assumption of linearity. Linearizing the Statistical Rate Theory equation will result in well-defined coefficients in terms of parameters that may be measured or controlled rather than phenomenological coefficients that cannot be derived from theory and must be evaluated empirically. It will also allow us to validate the Onsager reciprocity relation.

Several different cases of osmotic transport across cell membranes will be examined using both the Onsager approach and the Statistical Rate Theory approach and the results will be discussed.

2.2 Mass Transport Across Cell Membranes: Case 1

The first example that is examined is a well-known example that was treated using the Onsager approach by Kedem and Katchalsky (Kedem & Katchalsky, 1958). In this example mass transport across a cell membrane with both an osmotic and a pressure gradient is considered.

We assume that we have a biological cell that can be treated as a two-component composite system as illustrated in Figure 2-1. The cell is immersed in a hypertonic or hypotonic solution and undergoes osmotic shrinkage or swelling, respectively. We assume the cell contains a thermodynamically dilute solution of water (w) and solute (s) and is immersed in a dilute solution of water and the same solute and that the cell is permeable to both the water and the solute. There is a tension in the membrane that results in a pressure difference between the inside (i) and the outside (o) of the cell. We assume that the inside and outside of the cell are not at equilibrium with respect to water concentration, solute concentration or pressure but that the cell membrane is in mechanical equilibrium at all times so that the pressure difference is balanced by the membrane tension. We also assume that our entire system is surrounded by a thermal reservoir that keeps the cell and the surroundings at a constant temperature, T.

2.2a The Onsager Approach

The first step in the Onsager approach is to write the entropy production for the entire process. For the system shown in Figure 2-1, the differential change in entropy for the isolated system, dS_{sys} may be written as:

$$dS_{sys} = dS^{o} + dS^{i} + dS^{m} + dS^{R} \qquad (2\text{-}12)$$

where S^{o}, S^{i}, S^{m} and S^{R} are the entropies of the fluid outside the cell, the fluid inside the cell, the cell membrane and the reservoir, respectively. The differential entropies of each of the subsystems may be written in terms of the independent extensive variables of each of the subsystems by using the fundamental thermodynamic equation in the entropy form (Callen, 1985). For the fluid outside the cell:

$$dS^{o} = \frac{1}{T}dU^{o} + \frac{P^{o}}{T}dV^{o} - \frac{\mu_{w}^{o}}{T}dN_{w}^{o} - \frac{\mu_{s}^{o}}{T}dN_{s}^{o} \qquad (2\text{-}13)$$

where U^{o}, P^{o} and V^{o} are the internal energy, the pressure and the volume, respectively, of the fluid outside the cell; μ_{w}^{o} and N_{w}^{o} are the chemical potential of the water outside the cell and the number of molecules of water outside the cell, respectively and μ_{s}^{o} and N_{s}^{o} are the chemical potential of the solute outside the cell and the number of molecules of solute outside the cell, respectively.

Similarly, for the fluid inside the cell, the differential entropy may be written as:

$$dS^{i} = \frac{1}{T}dU^{i} + \frac{P^{i}}{T}dV^{i} - \frac{\mu_{w}^{i}}{T}dN_{w}^{i} - \frac{\mu_{s}^{i}}{T}dN_{s}^{i} \qquad (2\text{-}14)$$

where the subscript i indicates that properties refer to the fluid inside the cell.

For the cell membrane, the differential entropy may be written as:

$$dS^m = \frac{1}{T} dU^m - \frac{\gamma^m}{T} dA^m - \sum_k \frac{\mu_k^m}{T} dN_k^m \qquad (2\text{-}15)$$

where the superscript, m, denotes the properties for the cell membrane. U^m, γ^m, and A^m are the internal energy, the tension and the surface area of the cell membrane, respectively. In using Eq. 2-15, it is assumed that the cell membrane is two-dimensional and thus any effects due to the three-dimensional nature of a real cell membrane are neglected. μ_k^m is the chemical potential of the k^{th} molecular species in the membrane and N_k^m is the number of molecules of the k^{th} species in the membrane.

If we assume that the reservoir is heated quasi-statically and that the internal energy of the isolated system is constant, then the differential entropy of the reservoir may be written as:

$$dS^R = -\frac{1}{T} dU^o - \frac{1}{T} dU^i - \frac{1}{T} dU^m \qquad (2\text{-}16)$$

If we assume that the total volume remains constant, that mass is conserved for the water and solute and that the total number of molecules in the membrane is constant, then we can apply the following constraints:

$$V^o + V^i = \text{constant} \qquad \text{thus} \qquad dV^o = -dV^i \qquad (2\text{-}17)$$

$$N_s^o + N_s^i = \text{constant} \qquad \text{thus} \qquad dN_s^o = -dN_s^i \qquad (2\text{-}18)$$

$$N_w^o + N_w^i = \text{constant} \qquad \text{thus} \qquad dN_w^o = -dN_w^i \qquad (2\text{-}19)$$

$$N_k^m = \text{constant} \qquad \text{thus} \qquad dN_k^m = 0 \qquad (2\text{-}20)$$

Substituting Eqs. 2-13 through 2-16 into Eq. 2-12 and applying constraints 2-17 through 2-20, we get:

$$dS_{sys} = \frac{(P^i - P^o)}{T} dV^i - \frac{\gamma^m}{T} dA^m + \frac{(\mu_w^o - \mu_w^i)}{T} dN_w^i + \frac{(\mu_s^o - \mu_s^i)}{T} dN_s^i \qquad (2-21)$$

If we assume that the cell is spherical and that mechanical equilibrium holds for the membrane, then the Laplace equation may be used which is given by the following expression:

$$(P^i - P^o) = \frac{2\gamma^m}{r} \qquad (2-22)$$

where r is the radius of the cell. If we substitute the Laplace equation into Eq. 2-21, it yields the following:

$$dS_{sys} = \frac{(\mu_w^o - \mu_w^i)}{T} dN_w^i + \frac{(\mu_s^o - \mu_s^i)}{T} dN_s^i \qquad (2-23)$$

The rate of entropy production can be written in terms of the rate of change of the number of water and solute molecules inside the cell, $\dot{N}_w^i$ and $\dot{N}_s^i$, respectively. Thus, Eq. 2-23 may be re-written as:

$$\frac{dS_{sys}}{dt} = \frac{(\mu_w^o - \mu_w^i)}{T} \dot{N}_w^i + \frac{(\mu_s^o - \mu_s^i)}{T} \dot{N}_s^i \qquad (2-24)$$

Kedem and Katchalsky (1958) obtained the rate of entropy production given in Eq. 2-24. In order to arrive at this equation, they neglected the pressure difference between the inside and the outside of the membrane; however, this pressure difference showed up in the chemical potential equations that were used later.

For a thermodynamically dilute solution the difference in the chemical potential for the water may be written as:

$$\mu_w^o - \mu_w^i = \bar{v}_w(P^o - P^i) - kT(x_s^o - x_s^i) \qquad (2\text{-}25)$$

where $\bar{v}_w$ is the partial molecular volume of water, and x_s is the mole fraction of solute which may approximately be written as:

$$x_s = \frac{c_s}{c_w^*} \qquad (2\text{-}26)$$

where c_s is the concentration of solute and c_w^* is the concentration of pure water. The difference in the chemical potential for the solute may be written as:

$$\mu_s^o - \mu_s^i = \bar{v}_s(P^o - P^i) + kT[\ln(x_s^o) - \ln(x_s^i)] \qquad (2\text{-}27)$$

where $\bar{v}_s$, is the partial molecular volume of the solute. We may re-write the term in the square brackets in Eq. 2-27 as:

$$\ln(x_s^o) - \ln(x_s^i) = \frac{c_s^o - c_s^i}{\tilde{c}_s} \qquad (2\text{-}28)$$

where

$$\tilde{c}_s \equiv \frac{c_s^o - c_s^i}{\ln\left(\frac{x_s^o}{x_s^i}\right)} = \frac{c_s^o - c_s^i}{\ln\left(\frac{c_s^o}{c_s^i}\right)} = \frac{c_s^o - c_s^i}{\ln\left(\frac{c_s^i + (c_s^o - c_s^i)}{c_s^i}\right)} = \frac{c_s^o - c_s^i}{\ln\left(1 + \frac{c_s^o - c_s^i}{c_s^i}\right)} \qquad (2\text{-}29)$$

If $c_s^o - c_s^i \ll c_s^i$, then Eq. 2-29 can be expanded and reduces to:

$$\tilde{c}_s \approx \frac{c_s^o - c_s^i}{2} \qquad (2\text{-}30)$$

Since the condition given in Eq. 2-30 is more stringent than the dilute solution assumption, Eq. 2-29 will be taken as a definition and $\tilde{c}_s$ will be left in the equations.

Substituting Eqs. 2-25 through 2-28 into Eq. 2-24 yields the following expression:

$$\frac{dS_{sys}}{dt} = \left[\bar{v}_s \dot{N}_s^i + \bar{v}_w \dot{N}_w^i\right]\left(P^o - P^i\right) + \left[\frac{\dot{N}_s^i}{\tilde{c}_s} - \frac{\dot{N}_w^i}{c_w^*}\right] kT\left(c_s^o - c_s^i\right) \qquad (2-31)$$

The term in the first set of square brackets is the total volume flux across the cell membrane; the driving force for which is a pressure gradient. The term in the second set of square brackets is the differential volume flux between solute and water molecules. The driving force for this term is $kT\left(c_s^o - c_s^i\right)$, which is related to the concentration gradient. By using the linearity assumptions of the Onsager approach and by identifying the terms in the square brackets as fluxes and the factors multiplying them as thermodynamic forces, the following relations are obtained:

$$\left[\bar{v}_s \dot{N}_s^i + \bar{v}_w \dot{N}_w^i\right] = L_{11}\left(P^o - P^i\right) + L_{12} kT\left(c_s^o - c_s^i\right) \qquad (2-32)$$

$$\left[\frac{\dot{N}_s^i}{\tilde{c}_s} - \frac{\dot{N}_w^i}{c_w^*}\right] = L_{21}\left(P^o - P^i\right) + L_{22} kT\left(c_s^o - c_s^i\right) \qquad (2-33)$$

where the L's are phenomenological coefficients that do not have an explicit physical meaning in that they cannot be derived from linear nonequilibrium thermodynamics and must be evaluated empirically. Also, as stated earlier, according to the Onsager approach, the cross coefficients, L_{12} and L_{21} are equal.

2.2b The Statistical Rate Theory Approach

Using the Statistical Rate Theory approach, the net rate of change of solute molecules inside the cell may be written as:

$$\frac{dN_s^i}{dt} = K_o^s\left[\exp\frac{(\Delta S_f)}{k} - \exp\frac{(\Delta S_b)}{k}\right] \qquad (2\text{-}34)$$

where K_o^s is the equilibrium exchange rate for the solute molecules crossing the membrane, ΔS_f is the entropy change of the isolated system as a result of a single solute molecule being transferred from the outside of the cell to the inside of the cell and ΔS_b is the entropy change of the isolated system as a result of a single solute molecule being transferred from the inside of the cell to the outside of the cell.

The forward and backward entropy changes may be written as follows:

$$\Delta S_f = \Delta S^o + \Delta S^i + \Delta S^m + \Delta S^R \qquad (2\text{-}35)$$

$$\Delta S_b = -\left(\Delta S^o + \Delta S^i + \Delta S^m + \Delta S^R\right) \qquad (2\text{-}36)$$

where ΔS^o, ΔS^i, ΔS^m and ΔS^R are the entropy change of the solution outside the cell, the solution inside the cell, the cell membrane and the reservoir, respectively, as a result of the movement of one solute molecule from the outside of the cell to the inside of the cell. Using the appropriate Euler relations (Callen, 1985) and again assuming that internal energy is constant and that the reservoir is heated quasi-statically, the change in entropy for each phase may be written as follows:

$$\Delta S^o = \frac{1}{T}\Delta U^o + \frac{P}{T}\Delta V^o - \frac{\mu_w^o}{T}\Delta N_w^o - \frac{\mu_s^o}{T}\Delta N_s^o \qquad (2\text{-}37)$$

$$\Delta S^i = \frac{1}{T}\Delta U^i + \frac{P}{T}\Delta V^i - \frac{\mu_w^i}{T}\Delta N_w^i - \frac{\mu_s^i}{T}\Delta N_s^i \qquad (2\text{-}38)$$

$$\Delta S^m = \frac{1}{T}\Delta U^m - \frac{\gamma^m}{T}\Delta A^m - \sum_k \frac{\mu_k^m}{T}\Delta N_k^m \qquad (2\text{-}39)$$

$$\Delta S^R = -\frac{1}{T}\Delta U^o - \frac{1}{T}\Delta U^i - \frac{1}{T}\Delta U^m \qquad (2\text{-}40)$$

If it is assumed that the total volume of the system remains constant, that none of the water molecules cross the membrane, that there is no change in the number of molecules in the membrane and that only one solute molecule moves from the outside of the cell to the inside of the cell, then the following constraints may be applied:

$$\Delta V^o = -\Delta V^i \qquad (2\text{-}41)$$

$$\Delta N_w^o = 0 \qquad (2\text{-}42)$$

$$\Delta N_w^i = 0 \qquad (2\text{-}43)$$

$$\Delta N_s^i = 1 \qquad (2\text{-}44)$$

$$\Delta N_s^o = -1 \qquad (2\text{-}45)$$

$$\Delta N_k^m = 0 \qquad (2\text{-}46)$$

Next, substituting Eqs. 2-35 through 2-40 into Eq. 2-34 as well as using constraints 2-41 through 2-46 and again making the assumption of mechanical equilibrium from Eq. 2-22, the following expression is obtained:

$$\frac{dN_s^i}{dt} = K_e^s\left[\exp\left(\frac{\mu_s^o - \mu_s^i}{kT}\right) - \exp\left(\frac{\mu_s^i - \mu_s^o}{kT}\right)\right] \qquad (2\text{-}47)$$

Again, using the Statistical Rate Theory approach, the net rate of change of water molecules inside the cell may be written as:

$$\frac{dN_w^i}{dt} = K_e^w\left[\exp\frac{(\Delta S_f)}{k} - \exp\frac{(\Delta S_b)}{k}\right] \qquad (2\text{-}48)$$

where K_e^w is the equilibrium exchange rate for the water molecules crossing the membrane, ΔS_f is the entropy change of the isolated system as a result of a single water molecule being transferred from the outside of the cell to the inside of the cell and ΔS_b is the entropy change of the isolated system as a result of a single water molecule being transferred from the inside of the cell to the outside of the cell. The forward and backward entropy changes are again given by Eqs. 2-35 and 2-36 and the change in entropy for each phase are given by Eqs. 2-37 through 2-40.

If it is once again assumed that the total volume of the system remains constant (Eq. 2-41), that none of the solute molecules cross the membrane, that there is no change in the number of molecules in the membrane (Eq. 2-46) and that only one water molecule moves from the outside of the cell to the inside of the cell, then the following constraints may be applied:

$$\Delta N_s^o = 0 \qquad (2-49)$$

$$\Delta N_s^i = 0 \qquad (2-50)$$

$$\Delta N_w^i = 1 \qquad (2-51)$$

$$\Delta N_w^o = -1 \qquad (2-52)$$

Again substituting Eqs. 2-35 through 2-40 into Eq. 2-48 and using constraints 2-41, 2-46 and 2-49 through 2-52 and again making the assumption of mechanical equilibrium (Eq. 2-22), the following expression is obtained:

$$\frac{dN_w^i}{dt} = K_o^w\left[\exp\left(\frac{\mu_w^o - \mu_w^i}{kT}\right) - \exp\left(\frac{\mu_w^i - \mu_w^o}{kT}\right)\right] \qquad (2-53)$$

Equations 2-47 and 2-53 are complete nonequilibrium thermodynamic equations that describe the osmotic transport of solute and water across the membrane without any near-equilibrium assumptions being made. In order to be able to compare these two equations to Onsager's linear near-equilibrium equations, we can linearize the exponentials*. Thus for small chemical potential differences:

$$\frac{dN_s^i}{dt} = \frac{2K_o^s}{kT}\left(\mu_s^o - \mu_s^i\right) \qquad (2-54)$$

$$\frac{dN_w^i}{dt} = \frac{2K_o^w}{kT}\left(\mu_w^o - \mu_w^i\right) \qquad (2-55)$$

Adding and subtracting Eqs. 2-54 and 2-55 as required and making use of Eqs. 2-25 through 2-28 for the chemical potential differences for the solute and solvent, equivalent equations to Eqs. 2-32 and 2-33 from the Onsager approach can be derived:

---

* For small values of y, the linearization of the exp (y) = 1 + y + ½ y^2 + ...

$$\bar{v}_s \dot{N}_s^i + \bar{v}_w \dot{N}_w^i = \frac{2}{kT}\left(K_o^s \bar{v}_s^2 + K_o^w \bar{v}_w^2\right)\left(P^o - P^i\right) + \frac{2}{kT}\left(K_o^s \frac{\bar{v}_s}{\bar{c}_s} - K_o^w \frac{\bar{v}_w}{c_w^*}\right) kT\left(c_s^o - c_s^i\right) \quad (2\text{-}56)$$

$$\frac{\dot{N}_s^i}{\bar{c}_s} - \frac{\dot{N}_w^i}{c_w^*} = \frac{2}{kT}\left(K_o^s \frac{\bar{v}_s}{\bar{c}_s} - K_o^w \frac{\bar{v}_w}{c_w^*}\right)\left(P^o - P^i\right) + \frac{2}{kT}\left(\frac{K_o^s}{\bar{c}_s^2} + \frac{K_o^w}{c_w^{*2}}\right) kT\left(c_s^o - c_s^i\right) \quad (2\text{-}57)$$

2.3 Discussion of Case 1

By comparing Eqs. 2-32 and 2-33 obtained using the Onsager approach with Eqs. 2-56 and 2-57 from the Statistical Rate Theory approach, the following equations are obtained for the phenomenological coefficients:

$$L_{11} = \frac{2}{kT}\left(K_o^s \bar{v}_s^2 + K_o^w \bar{v}_w^2\right) \quad (2\text{-}58)$$

$$L_{12} = \frac{2}{kT}\left(K_o^s \frac{\bar{v}_s}{\bar{c}_s} - K_o^w \frac{\bar{v}_w}{c_w^*}\right) \quad (2\text{-}59)$$

$$L_{21} = \frac{2}{kT}\left(K_o^s \frac{\bar{v}_s}{\bar{c}_s} - K_o^w \frac{\bar{v}_w}{c_w^*}\right) \quad (2\text{-}60)$$

$$L_{22} = \frac{2}{kT}\left(\frac{K_o^s}{\bar{c}_s^2} + \frac{K_o^w}{c_w^{*2}}\right) \quad (2\text{-}61)$$

There are two main results that are immediately evident when comparing the Onsager approach with the Statistical Rate Theory approach. The first result is that for this particular example Onsager's reciprocity relation was shown to be true. The second result is that by using Statistical Rate Theory, equations for the phenomenological coefficients are obtained in terms of measurable parameters such as temperature, concentration and the equilibrium exchange rates. Once

again the equilibrium exchange rate, K_e, is the number of molecules crossing the membrane per unit time at equilibrium. The equilibrium exchange rate has been expressed in terms of measurable macroscopic thermodynamic properties such as temperature, pressure and tabulated molecular properties, for various problems (Ward, 1977; Ward & Elmoselhi, 1986; Elliott & Ward, 1997a; Elliott & Ward, 1997b; Elliott & Ward, 1997c; Dejmek & Ward, 1998; Fang & Ward, 1998; Ward & Fang, 1998; Torri & Elliott, 1999).

In addition, Statistical Rate Theory is a complete nonlinear theory of nonequilibrium thermodynamics, and the circumstance under which it may be linearized depends on the particular problem. By expanding the exponentials in Eqs. 2-47 and 2-53 at room temperature and making use of Eqs. 2-25 – 2-28, the second order terms cancel out and the third order terms become less than 5% of the magnitude of the first order terms when the pressure difference is less than 75 MPa or when either $(c_s^o - c_s^i)/c_w^*$ or $(c_s^o - c_s^i)/\bar{c}_s$ is less than $\sqrt{0.3}$. When the magnitudes of the terms appearing in the exponential are large, the equations cannot be linearized.

2.4 Mass Transport across Cell Membranes: Case 2

The second example that was considered involves mass transport across a cell membrane with only an osmotic gradient. In this example, it is assumed that there is a biological cell that is treated as a two-component composite system as

illustrated in Figure 2-2. The cell is immersed in a hypertonic or hypotonic solution and undergoes osmotic shrinkage or swelling, respectively. It is assumed that the cell contains a thermodynamically dilute solution of water (w) and solute (s) and is immersed in a dilute solution of water and the same solute and that the cell is permeable to both the water and the solute. Also, an assumption is made that there is no tension in the membrane. It is assumed that the inside and outside of the cell are not at equilibrium with respect to water concentration or solute concentration. The entire system is surrounded by a thermal reservoir that keeps the cell and the surroundings at a constant temperature, *T*.

With the Onsager approach, the first step is again to write the entropy production during the process for the entire process. For the system shown in Figure 2-2, the differential change in entropy for the isolated system, dS_{sys} may be written as:

$$dS_{sys} = dS^{o} + dS^{i} + dS^{R} \qquad (2-62)$$

Again the differential entropies of each of the subsystems may be written in terms of the independent extensive variables of each of the subsystems by using the thermodynamic fundamental equation in the entropy form (Callen, 1985). For the fluid outside the cell and inside the cell the differential entropies are given by Eqs. 2-13 and 2-14.

If it is assumed that the reservoir is heated quasi-statically and that the internal energy of the isolated system is constant, them the differential energy of the reservoir may be written as:

$$dS^R = -\frac{1}{T}dU^\circ - \frac{1}{T}dU^i \qquad (2\text{-}63)$$

If it assumed that the total volume remains constant and that mass is conserved for both the water and solute, the constraints 2-17 through 2-19 may be applied.

Substituting Eqs. 2-13, 2-14 and 2-63 into Eq. 2-62 and applying constraints 2-17 through 2-19, the following expression is obtained:

$$dS_{sys} = \frac{(\mu_w^\circ - \mu_w^i)}{T}dN_w^i + \frac{(\mu_s^\circ - \mu_s^i)}{T}dN_s^i \qquad (2\text{-}64)$$

The rate of entropy production can be written in terms of the rate of change of the number of water and solute molecules inside the cell, $\dot{N}_w^i$ *and* $\dot{N}_s^i$, respectively. Thus, Eq. 2-64 may be re-written as:

$$\frac{dS_{sys}}{dt} = \frac{(\mu_w^\circ - \mu_w^i)}{T}\dot{N}_w^i + \frac{(\mu_s^\circ - \mu_s^i)}{T}\dot{N}_s^i \qquad (2\text{-}65)$$

If thermodynamically dilute solutions are assumed, then the differences in the chemical potentials of the water and solute are given by Eqs. 2-25 through 2-28 and substitution into 2-65 yields the following expression:

$$\frac{dS_{sys}}{dt} = \left[\frac{\dot{N}_s^i}{\tilde{c}_s} - \frac{\dot{N}_w^i}{c_w^*}\right]kT\left(c_s^\circ - c_s^i\right) \qquad (2\text{-}66)$$

The term in the square brackets is the differential volume flux between solute and water molecules. The driving force for this term is $kT\left(c_s^\circ - c_s^i\right)$, which is related to

the concentration gradient. By using the linearity assumptions of the Onsager approach and by identifying the term in the square brackets as the flux and the factor multiplying it as a thermodynamic force, the following relation is obtained:

$$\left[\frac{\dot{N}_s^i}{\bar{c}_s} - \frac{\dot{N}_w^i}{c_w^*}\right] = LkT\left(c_s^o - c_s^i\right) \qquad (2\text{-}67)$$

where the L is a phenomenological coefficient. In this example, Onsager's cross coefficients do not show up since there is only one flux and one force present.

Using the Statistical Rate Theory approach, the net rate of change of solute molecules inside the cell is given by Eq. 2-34.

The forward and backward entropy changes may be written as follows:

$$\Delta S_f = \Delta S^o + \Delta S^i + \Delta S^R \qquad (2\text{-}68)$$

$$\Delta S_b = -\left(\Delta S^o + \Delta S^i + \Delta S^R\right) \qquad (2\text{-}69)$$

Using the appropriate Euler relations (Callen, 1985), the changes in entropy for each phase are given in Eqs. 2-37 and 2-38. Again assuming that internal energy is constant and that the reservoir is heated quasi-statically, the change in entropy for the reservoir may be written as:

$$\Delta S^R = -\frac{1}{T}\Delta U^o - \frac{1}{T}\Delta U^i \qquad (2\text{-}70)$$

If it is assumed that the total volume of the system remains constant, that none of the water molecules cross the membrane, and that only one solute molecule

moves from the outside of the cell to the inside of the cell, then constraints 2-41 through 2-45 may be applied.

Next, substituting Eqs. 2-68 though 2-70, as well as Eqs. 2-37 and 2-38 into Eq. 2-34 as well as using constraints 2-41 through 2-45, the following expression is obtained:

$$\frac{dN_s^i}{dt} = K_*^s\left[\exp\left(\frac{\mu_s^o - \mu_s^i}{kT}\right) - \exp\left(\frac{\mu_s^i - \mu_s^o}{kT}\right)\right] \quad (2\text{-}71)$$

Again, using the Statistical Rate Theory approach, the net rate of change of water molecules inside the cell is given by Eq. 2-48.

The forward and backward entropy changes are again given by Eqs. 2-68 and 2-69 and the changes in entropy for each phase are given by Eqs. 2-37, 2-38 and 2-70.

If it is once again assumed that the total volume of the system remains constant (Eq. 2-41), that none of the solute molecules cross the membrane, and that only one water molecule moves from the outside of the cell to the inside of the cell, then constraints 2-49 through 2-52 may be applied:

Again substituting Eqs. 2-37, 2-38 and 2-68 through 2-70 into Eq. 2-48 and using the constraints from Eq. 2-41 and 2-49 through 2-52, the following expression is obtained:

$$\frac{dN_w^i}{dt} = K_o^w\left[\exp\left(\frac{\mu_w^o - \mu_w^i}{kT}\right) - \exp\left(\frac{\mu_w^i - \mu_w^o}{kT}\right)\right] \quad (2\text{-}72)$$

Equations 2-71 and 2-72 are complete nonequilibrium thermodynamic equations that describe the osmotic transport of solute and water across the membrane without any near equilibrium assumptions being made. In order to be able to compare these two equations to Onsager's linear near-equilibrium equations, we can linearize the exponentials. Thus making use of Eqs. 2-25 through 2-28 for dilute solutions, the following expressions are obtained for small values of the exponentials:

$$\frac{dN_s^i}{dt} = \frac{2K_o^s}{kT}\left[kT\left(\frac{\left(c_s^o - c_s^i\right)}{\tilde{c}_s}\right)\right] \quad (2\text{-}73)$$

$$\frac{dN_w^i}{dt} = \frac{2K_o^w}{kT}\left[kT\left(\frac{\left(c_s^i - c_s^o\right)}{c_w^*}\right)\right] \quad (2\text{-}74)$$

Adding and subtracting Eqs. 2-73 and 2-74 as required, results in an equation equivalent to Eq. 2-67 from the Onsager approach:

$$\left[\frac{\dot{N}_s^i}{\tilde{c}_s} - \frac{\dot{N}_w^i}{c_w^*}\right] = \frac{2}{kT}\left(\frac{K_o^s}{\tilde{c}_s^2} + \frac{K_o^w}{c_w^{*2}}\right)kT\left(c_s^o - c_s^i\right) \quad (2\text{-}75)$$

2.5 Discussion of Case 2

By comparing Eq. 2-67 obtained using the Onsager approach with Eq. 2-75 found using the Statistical Rate Theory approach, the following equation is obtained for the phenomenological coefficient, L:

$$L = \frac{2}{kT}\left(\frac{K_o^s}{\bar{c}_s^2} + \frac{K_o^w}{c_w^{\cdot 2}}\right) \qquad (2\text{-}76)$$

For this particular case of osmotic transport across cell membranes, since the tension in the membrane was neglected, there was only one flux and force present and as a result, only one phenomenological coefficient showed up in the equations. Once again the phenomenological coefficient was written entirely in terms of quantifiable parameters such as temperature, concentration and equilibrium exchange rates.

Kedem & Katchalsky developed an equation to describe water and solute permeability across a cell membrane (Kedem & Katchalsky, 1958). The equation they developed to describe the change in water and solute volume (V_{W+S}) with time (t) resulting from water and solute fluxes is given by:

$$\frac{dV_{W+S}}{dt} = -L_p ART\left\{\left(M_n^o - M_n^i\right) + \sigma\left(M_{ps}^o - M_{ps}^i\right)\right\} \qquad (2\text{-}77)$$

where L_p is the membrane hydraulic conductivity, A is the area of the cell, R is the universal gas constant, and T is absolute temperature. M is the osmolality with the superscripts denoting the internal cell solution (i) and the solution external to the cell (o) and the subscripts denoting the non-permeating solutes (n) and the permeating solutes (ps). Sigma (σ) is the reflection coefficient which

characterizes the degree of interaction between the water and solute. If we assume that water and solute completely interact and sigma is equal to zero, then the following expression is obtained:

$$\frac{dV_{w+s}}{dt} = -L_p ART\left(M_n^o - M_n^i\right) \qquad (2\text{-}78)$$

By adding Eqs. 2-73 and 2-74 from the Statistical Rate Theory approach and rearranging the equations to a similar form as Eq. 78, the following expression is obtained:

$$\frac{dV_{w+s}}{dt} = 2\left[\frac{\bar{v}_s K_e^s}{\tilde{c}_s} + \frac{\bar{v}_w K_e^w}{c_w^*}\right]\left(c_s^o - c_s^i\right) \qquad (2\text{-}79)$$

If a dilute solution assumption is made, directly comparing Eq. 2-78 and 2-79 results in the following:

$$L_p = -\frac{2}{ART}\left[\frac{\bar{v}_s K_e^s}{\tilde{c}_s} + \frac{\bar{v}_w K_e^w}{c_w^*}\right] \qquad (2\text{-}80)$$

2.6 Mass Transport across Cell Membranes: Case 3

The third example considered involves water transport only across a cell membrane with an osmotic gradient. In this example, it is assumed that there is a biological cell that may be treated as a two-component composite system as illustrated in Figure 2-3. The cell is immersed in a hypertonic or hypotonic solution and undergoes osmotic shrinkage or swelling, respectively. It is assumed that the cell contains a thermodynamically dilute solution of water (w) and solute (s) and is immersed in a dilute solution of water and the same solute

but that the cell is permeable only to the water. Also, an assumption is made that there is no tension in the membrane. It is assumed that the inside and outside of the cell are not at equilibrium with respect to water concentration or solute concentration. The entire system is surrounded by a thermal reservoir that keeps the cell and the surroundings at a constant temperature, T.

With the Onsager approach, the first step is again to write the entropy production for the entire process. For the system shown in Figure 2-3, the differential change in entropy for the isolated system, dS_{sys} is given by Eq. 2-62.

Again the differential entropies of each of the subsystems may be written in terms of the independent extensive variables of each of the subsystems by using the fundamental equation of thermodynamics in the entropy form (Callen, 1985).

For the fluid outside the cell and inside the cell the differential entropies are given by Eqs. 2-13 and 2-14 and the differential entropy of the reservoir is given by Eq. 2-63. It is assumed that the total volume remains constant (Eq. 2-17) and that mass is conserved for the water (Eq. 2-19). Since the membrane is not permeable to the solute, then the number of solute molecules on either side of the membrane is constant and $dN_s^i = dN_s^o = 0$. Substituting Eqs. 2-13, 2-14 & 2-63 into Eq. 2-62 and applying the above constraints results in the following equation:

$$dS_{sys} = \frac{(\mu_w^o - \mu_w^i)}{T} dN_w^i \qquad (2\text{-}81)$$

The rate of entropy production can be written in terms of the rate of change of the number of water molecules inside the cell, $\dot{N}_w^i$. Thus, Eq. 2-81 may be re-written as:

$$\frac{dS_{sys}}{dt} = \frac{(\mu_w^o - \mu_w^i)}{T} \dot{N}_w^i \qquad (2\text{-}82)$$

If thermodynamically dilute solutions are assumed, then the difference between the chemical potentials for the water may be written using Eq. 2-25 and Eq. 2-26 and substituting in Eq. 2-82 yields the following expression:

$$\frac{dS_{sys}}{dt} = \left[-\frac{\dot{N}_w^i}{c_w^*} \right] kT\left(c_s^o - c_s^i\right) \qquad (2\text{-}83)$$

The term in the square brackets is the flux and the driving force for this term is $kT\left(c_s^o - c_s^i\right)$, which is related to the concentration gradient. By using the linearity assumptions of the Onsager approach and by identifying the term in the square brackets as the flux and the factor multiplying it as a thermodynamic force, the following relation is obtained:

$$\left[-\frac{\dot{N}_w^i}{c_w^*} \right] = LkT\left(c_s^o - c_s^i\right) \qquad (2\text{-}84)$$

where the L is a phenomenological coefficient. Again, in this example, Onsager's cross coefficients do not show up since there is only one flux and force present.

Using the Statistical Rate Theory approach, since the membrane is not permeable to the solute, there will be no net rate of change of solute molecules.

The net rate of change of water molecules inside the cell may be written using Eq. 2-48.

The forward and backward entropy changes are again given by Eqs. 2-68 and 2-69 and the changes in entropy for each phase are given by Eqs. 2-37, 2-38 and 2-70.

If it is once again assumed that the total volume of the system remains constant (Eq. 2-41), that none of the solute molecules cross the membrane ($dN_s^i = dN_s^o = 0$), and that only one water molecule moves from the outside of the cell to the inside of the cell, then constraints 2-49 through 2-52 may be applied.

Again substituting Eqs. 2-37, 2-38 and 2-68 through 2-70 into Eq. 2-48 and using constraints 2-41 and 2-49 through 2-52, the following expression is obtained:

$$\frac{dN_w^i}{dt} = K_o^w \left[\exp\left(\frac{\left(\mu_w^o - \mu_w^i\right)}{kT} \right) - \exp\left(\frac{\left(\mu_w^i - \mu_w^o\right)}{kT} \right) \right] \qquad (2\text{-}72)$$

Equation 2-72 is the complete nonequilibrium thermodynamic equation that describes the osmotic transport of water across the membrane without any near equilibrium assumptions being made. In order to be able to compare this equation to Onsager's linear near-equilibrium equation, we can linearize the

exponentials. Thus making use of Eq. 2-25 and 2-26 for a dilute solution, the following expression is obtained for a small value of the exponential:

$$\frac{dN_w^i}{dt} = \frac{2K_o^w}{kt}\left[kT\left(\frac{\left(c_s^i - c_s^o\right)}{c_w^*}\right)\right] \qquad (2\text{-}74)$$

From the above equation, an equation equivalent to Eq. 2-84 from the Onsager approach can be written:

$$\left[-\frac{\dot{N}_w^i}{c_w^*}\right] = \frac{2}{kT}\left(\frac{K_o^w}{c_w^{*2}}\right)kT\left(c_s^o - c_s^i\right) \qquad (2\text{-}85)$$

2.7 Discussion of Case 3

By comparing Eq. 2-84 obtained using the Onsager approach with Eq. 2-85 found using the Statistical Rate Theory approach, the following equation is obtained for the phenomenological coefficient, L:

$$L = \frac{2}{kT}\left(\frac{K_o^w}{c_w^{*2}}\right) \qquad (2\text{-}86)$$

Again for this particular case of osmotic transport across cell membranes, since the tension in the membrane was neglected, there was only one flux and force present and as a result, only one phenomenological coefficient showed up in the equations. Once again the phenomenological coefficient was written entirely in terms of quantifiable parameters such as temperature, concentration and the equilibrium exchange rate.

The case three scenario is similar to the conditions presented by Jacobs & Stewart (1932) as well as by Kedem & Katchalsky (1958). They also neglected the hydrostatic pressure difference across the membrane. The rate of change of cell water volume (V_w) with time (t) was given by the following equation:

$$\frac{dV_w}{dt} = L_p ART\left(M^i - M^o\right) \qquad (2\text{-}87)$$

where dV_w/dt is the volume flux of water across the cell membrane, L_p is the membrane hydraulic conductivity, A is the area of the cell, R is the universal gas constant, and T is absolute temperature. M is the osmolality with the superscripts denoting the internal cell solution (i) and the solution external to the cell (o). The L_p in Eq. 2-87 is comparable to the phenomenological coefficient, L in the mass transport example of case 3.

In case three, Statistical Rate Theory allowed us to see how hydraulic conductivity depends on temperature, concentration and the equilibrium exchange rate K_e. The equilibrium exchange rate will also depend on temperature and concentration in a non-trivial way (Elliott & Ward, 1997a; Torri & Elliott, 1999). The effects of temperature on the membrane hydraulic conductivity will be examined in Chapter 4.

2.8 Conclusions

A corrected version of the osmotic transport equations derived by Kedem & Katchalsky from the Onsager approach to linear non-equilibrium thermodynamics

was presented. The linearity assumption that is made in the Onsager theory only holds true for systems near equilibrium and there is no way to know before hand from the theory under what conditions this assumption of linearity holds true. In addition, the phenomenological coefficients in the Onsager equations cannot be derived from the theory and must be evaluated empirically. This is relevant in cryobiology because currently values for the membrane hydraulic conductivity, L_p, must be determined empirically.

Several advances have been made by linearizing Statistical Rate Theory to find expressions for Onsager coefficients in terms of measurable parameters such as concentration, temperature, pressure and the equilibrium exchange rate.

Onsager's reciprocity relation is a very important hypothesis in transport phenomena and non-equilibrium thermodynamics. Its validity has been discussed in papers since the 1930's (Onsager, 1931a; Onsager, 1931b). Statistical Rate Theory was used to further verify Onsager's reciprocity hypothesis by showing the equality of the cross coefficients for the case in which both solute and water molecules may cross a cell membrane that has tension. In addition to verifying the reciprocity relation, the criteria for linearizing the equations (and thus the criteria for using Onsager equations) were derived.

For two other cases in which it was assumed there was no tension in the membrane, Statistical Rate Theory was used to directly compare with currently

used equations of osmotic transport across cell membranes to obtain expressions for hydraulic conductivity that show how it depends on temperature, concentration and the equilibrium exchange rate, K_e.

2.9 References

1. Callen, H. B. 1985. *Thermodynamics and an Introduction to Thermostatistics*, 2nd ed., (John Wiley & Sons, New York, 1985), 59-61.
2. Dejmek, M., & Ward, C. A. 1998. A Statistical Rate Theory study of interface concentration during crystal growth or dissolution. *J. Chem. Phys.* **108(20)**, 8698-8704.
3. Elliott, J. A. W., & Ward, C. A. 1997a. In: *Equilibria and Dynamics of Gas Adsorption on Heterogeneous Solid Surfaces, Studies in Surface Science and Catalysis*, **104**, edited by W. Rudzinski, W. A. Steel and G. Zgrablich, (Elsevier, New York, 1997), 285-333.
4. Elliott, J. A. W., & Ward, C. A. 1997b. Statistical Rate Theory description of beam-dosing adsorption kinetics. *J. Chem. Phys.* **106(13)**, 5667-5676.
5. Elliott, J. A. W., & Ward, C. A. 1997c. Temperature programmed desorption: A Statistical Rate Theory approach. *J. Chem. Phys.* **106(13)**, 5677-5684.
6. Fang, G., & Ward, C. A. 1998. Examination of the Statistical Rate Theory expression for liquid evaporation rates. *Phys. Rev. E.* **59**, 441-445.
7. Findlay, D., & Ward, C. A. 1982. Statistical Rate Theory of interface transport. IV. Predicted rate of dissociative adsorption. *J. Chem. Phys.* **76(11)**, 5624-5631.

8. Jacobs, M. H., & Stewart, D. R. 1932. A Simple Method for the Quantitative Measurement of Cell Permeability. *J. Cell. Comp. Physiol.* **1**, 71-82.

9. Kedem, O., & Katchalsky, A. 1958. Thermodynamic analysis of the permeability of biological membranes to non-electrolytes. *Biochimica et Biophys. Acta.* **27**, 229-246.

10. Kirkwood, J. G., & Fitts, D. D. 1960. Statistical mechanics of transport processes. XIV. Linear relations in multicomponent systems. *J. Chem. Phys.* **33(5)**, 1317-1324.

11. Miller, D. G. 1960. Thermodynamics of irreversible processes. The experimental verification of the Onsager reciprocal relations. *Chem. Rev.* **60**, 15-37.

12. Nerst, W., & Zeits, F. 1888. *Physik. Chem.* **2**, 613.

13. Onsager, L. 1931a. Reciprocal relations in irreversible processes. I. *Phys. Rev.* **37**, 405-426.

14. Onsager, L. 1931b. Reciprocal relations in irreversible processes. II. *Phys. Rev.* **38**, 2265-2279.

15. Skinner, F. K., Ward, C. A., and Bardakjian, B. L. 1993. Pump and exchange mechanism in a model of smooth muscle. *Biophysical Chem.* **45(3)**, 253-272.

16. Staverman, A. J. 1952. Apparent osmotic pressure calculations of solutions of heterodisperse polymers. *Rec. Trav. Chim.* **71**, 623-633.

17. Tikuisis, P., & Ward, C. A. 1992. In: *Transport Processes in Bubbles, Drops and Particles*, edited by R. Chhabra and D. Dekee, (Hemisphere Publishing Co., New York) 114-132

18. Torri, M., & Elliott, J. A. W. 1999. A Statistical Rate Theory description of CO diffusion on a stepped Pt(111) surface. *J. Chem. Phys.* **111(4)**, 1686-1698.

19. Ward, C. A. 1977. The rate of gas adsorption at a liquid interface. *J. Chem. Phys.* **67(1)**, 229-235.

20. Ward, C. A. 1983. Effect of concentration on the rate of Chemical Reactions. *J. Chem. Phys.* **79(11)**, 5605-5615.

21. Ward, C. A., & Elmoselhi, M. 1986. Molecular adsorption at a well defined gas-solid interphase: Statistical Rate Theory approach. *Surf. Sci.* **176**, 457-475.

22. Ward, C. A., & Fang, G. 1998. Expression for predicting liquid evaporation flux: Statistical Rate Theory approach. *Phys. Rev. E.* **59**, 429-440.

23. Ward, C. A., & Findlay, R. D. 1982. Statistical Rate Theory of interface transport. III. Predicted rate of nondissociative adsorption. *J. Chem. Phys.* **76(11)**, 5615-5623.

24. Ward, C. A., Findlay, R. D., and Rizk, M. 1982a. Statistical Rate Theory of interfacial transport. I. *J. Chem. Phys.* **76(11)**, 5599-5605.

25. Ward, C. A., Rizk, M., and Tucker, A. S. 1982b. Statistical Rate Theory of interface transport. II. Rate of isothermal bubble evolution in a liquid-gas solution. *J. Chem. Phys.* **76(11)**, 5606-5614.

26. Ward, C. A., Farabakhsh, B., and Venter, R. D. 1986b. Zeitscrift fur Physikalische Chemie Neue Folge, Bd. 147, S. 89-101, 727.

27. Ward, C. A., Tikuisis, P., and Tucker, A. S. 1986a. Bubble evolution in solutions with gas concentrations near the saturation value. *J. Colloid and Interface Sci.* **113(2)**, 388-398.

Figure 2-1 Case 1: A Two-component System of Water and Solute where Both May Permeate the Cell Membrane and where there is Tension in the Membrane

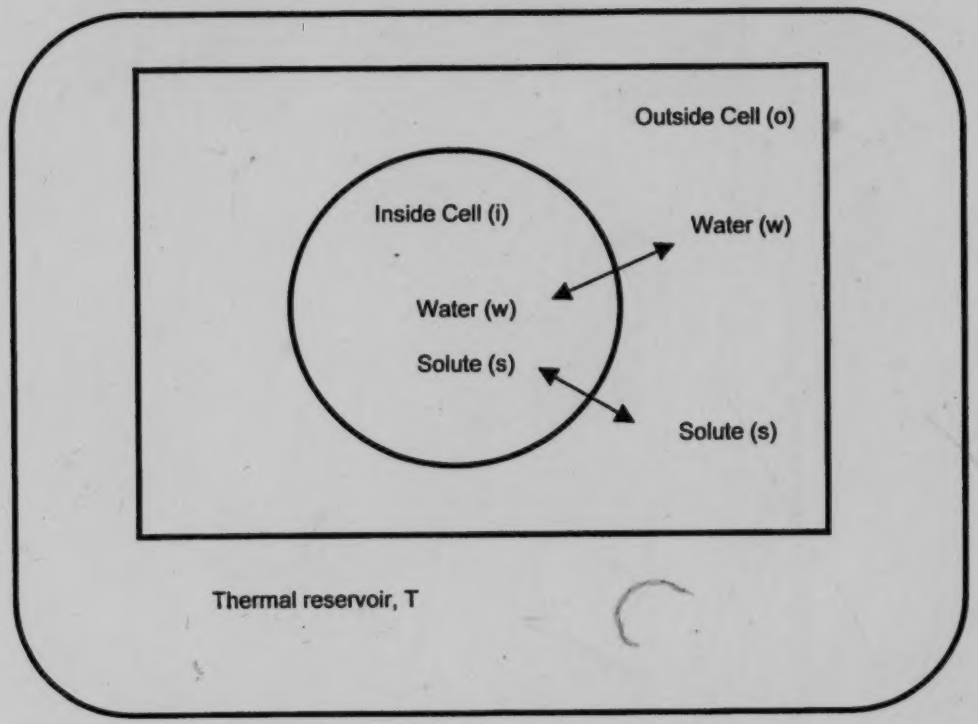

Figure 2-2 Case 2: A Two-component System of Water and Solute where Both May Permeate the Cell Membrane but where there is no Tension in the Membrane

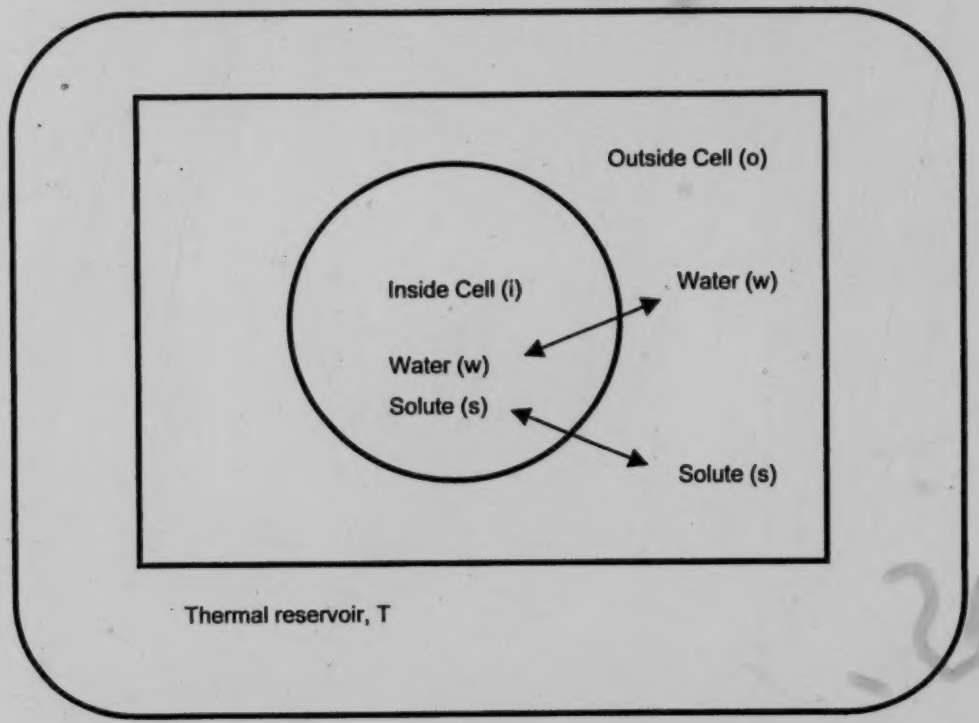

Figure 2-3 Case 3: A Two-component System of Water and Solute where Only the Water May Permeate the Cell Membrane and where there is no Tension in the Membrane

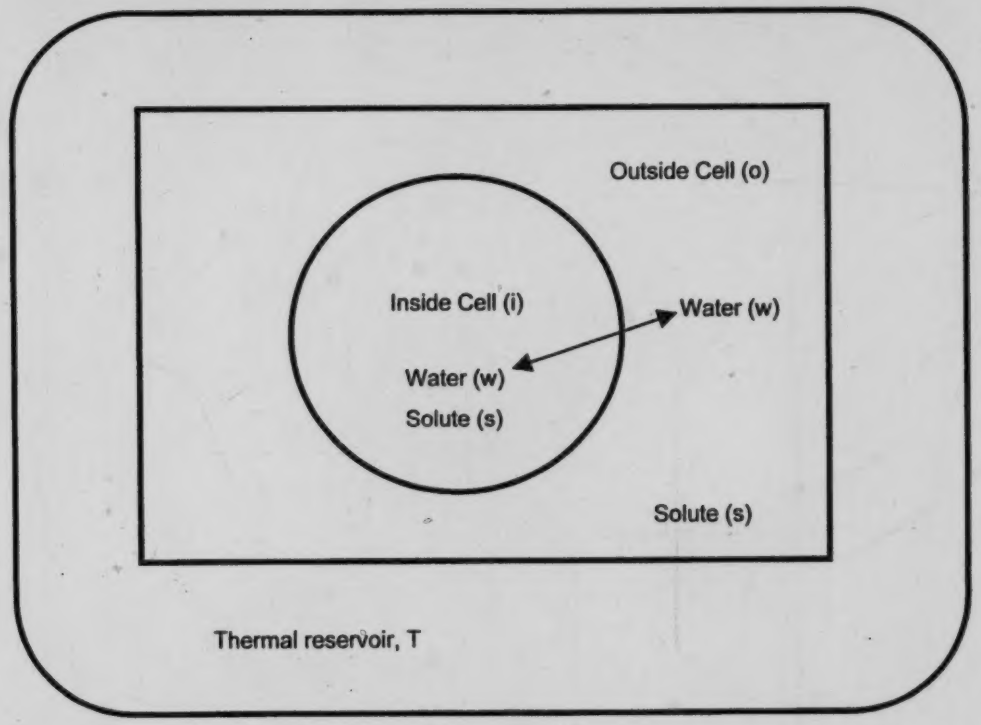

Chapter 3: The Effect of Cell Size Distribution on Predicted Osmotic Responses of Cells*

3.1 Introduction

Understanding the kinetics of cell osmotic response is a critical step in estimating water and solute fluxes across cell membranes. There is a need for easily applicable methods to determine permeability characteristics. Determination of the osmotic properties requires measurements of the equilibrium cell volume and the non-equilibrium cell volume as a function of time. Estimates of the membrane hydraulic conductivity of the cell plasma membrane to water and various solutes are obtained by fitting experimental data to theoretical predictions.

Since the 1950's, there have been a number of mathematical models developed to predict the osmotic parameters of cells (Davson & Danielli, 1952; Kedem & Katchalsky, 1958; Mazur, 1963). Changes in cell volume caused by differences in concentration across the cell membrane have been used extensively to determine the permeability characteristics of cell membranes to both water and permeating solutes (Jacobs & Stewart, 1932; Kedem & Katchalsky, 1958). Traditionally, a mathematical model of the osmotic response of cells is obtained by applying the membrane mass transport equation (Jacobs & Stewart, 1932) and the Boyle-van't Hoff equation (Luckè & McCutcheon, 1932) using numerical

* This chapter with minor modifications has been submitted to Biophysical Journal as: H. Y. Elmoazzen, C. C. V. Chan, J. P. Acker, J. A. W. Elliott, and L. E. McGann, "The Effect of Cell Size Distribution on Predicted Osmotic Responses of Cells"

methods. In applying these equations, it is normally assumed that all the cells are the same size, equal to the mean or mode of the population. However, biological cells with identical permeability characteristics have a distribution in cell size and will shrink at different rates when exposed to a hypertonic environment (Mazur, 1963). When there is a broad, non-guassian distribution of cell volumes, determining the 'average' volume that accurately represents the cell population is not trivial. Identifying the measure of central tendency for the cell population will affect the calculated osmotic parameters (Grover et al., 1969a; Grover et al., 1969b; Grover et al., 1972; Armitage & Juss, 1996). Armitage and Juss (1996) showed that cell size distributions for keratocytes were positively skewed, which is typical for mammalian cells. They concluded that the mean was not an appropriate measure of central tendency, and that the mode may be more applicable (Armitage & Juss, 1996). The size distribution of a population of cells will affect the average osmotic response, as larger spherical cells take longer to reach their final volume than smaller cells. In this chapter, an analytical model used to predict the change in the size distribution of a population of cells over time during cell shrinkage is examined.

Electronic particle counters are commonly used to study equilibrium size distributions of cells (Kubitschek, 1958; Gregg and Steidley, 1965; Adams et al., 1966; Anderson & Petersen, 1967; Grover et al., 1969a; Grover et al., 1969b; Grover et al., 1972; McGann et al., 1982; Armitage & Juss, 1996) as well as to measure changes in mean or mode cell volume that occur over time during

exposure to hypertonic and hypotonic solutions (Buckhold et al., 1965; McGann & Turc, 1980; Gilmore et al., 1995; Armitage & Juss, 1996; Gilmore et al., 1998; Acker et al., 1999). In kinetic studies, electronic particle counters are used to obtain rapid measurements of cell volumes that are then used to determine the cell permeability characteristics using theoretical models. This technique has been applied to many cell types such as mouse lymphoblasts (Buckhold et al., 1965), human lymphocytes (McGann & Turc, 1980), sperm cells from various species (Gilmore et al., 1998), and human keratinocytes (Acker et al., 1999). One of the benefits of using the electronic particle counter over optical methods is that it can rapidly and reproducibly collect data for the equilibrium and non-equilibrium volumes of the cell population (Acker et al., 1999). Electronic particle counters have been used in the past to study either the time evolution of a cell population as a whole (Buckhold et al., 1965) or to look at equilibrium size distributions (Armitage & Juss, 1996). Experiments have been conducted previously which have followed the time course of osmotic adaptation of a population distribution of cells; however, no discussion of the time dependence of the distributions was included (Buckhold et al., 1965). The cells used in this early experiment were slow responding mouse lymphoblasts.

In this study, the equipment and methods used allowed recording of both the volume of each cell, and the time at which it passed through the aperture of the electronic counter. This process allowed the time evolution of the cell size distribution to be followed. By solving mixing problems and obtaining high cell

counts, we have been able to gather volume distributions over short time intervals (1 sec) for rapidly responding cells. This is the first detailed study in which the effects of cell size distribution on osmotic parameters have been predicted, and includes the first experimental measurements for multiple types of fast responding cells. Experiments were conducted specifically for the purpose of analyzing the time dependence of cell size distributions.

Discrepancies between the behavior of a population of cells and a single cell will mean that the single-cell membrane mass transport model (or treating cells as though they had a single size) cannot be used to predict the osmotic response of the cells and that another model will be needed to obtain the membrane hydraulic conductivity.

3.2 Theory*

3.2a Osmotic Response of Cells of a Single Size

When a single cell is placed in an environment where the concentration of solute outside the cell is greater than the concentration of solute inside the cell, water will move out of the cell. The membrane mass transport model (Jacobs and Stewart, 1932) describes the rate of volume change:

* Equations 3-1 through 3-6 can be found in the standard literature. Simulations performed using these equations for cells with size distributions were conducted by C. C. V. Chan. Thus the calculations described in section 3.2 and used to create Figures 3-6 through 3-11 were done by C. C. V. Chan.

$$\frac{dV_w}{dt} = L_p ART(M^i - M^o) \qquad (3-1)$$

where L_p is the membrane hydraulic conductivity, A is the cell surface area, R is the universal gas constant, T is the absolute temperature, M^i is the intracellular osmolality and M^o is the external osmolality. The cell is assumed to be spherical in shape and its effective surface area for osmotic transport is assumed to be constant as the cell shrinks.

The Boyle van't Hoff equation is used to relate the intracellular osmolality, M^i, the isotonic osmolality, M_{iso}, and cell volume, V,

$$\frac{V}{V_{iso}} = \frac{M_{iso}}{M^i}(1 - v_b) + v_b \qquad (3-2)$$

where V_{iso} is the cell volume at the isotonic osmolality M_{iso}, and v_b is the osmotically inactive fraction of the isotonic cell volume.

An analytical solution that describes the volume of a single cell as a function of time is obtained by substituting Eq. 3-2 into Eq. 3-1 and integrating the differential equation (Dick, 1966). The final equation written as time as a function of volume is:

$$t = \left(\frac{a}{b} - \frac{c}{b^2}\right) \ln\left(\frac{c - bV}{c - bV_{iso}}\right) - \frac{V}{b} + \frac{V_{iso}}{b} \qquad (3-3)$$

where $a \equiv V_{iso}v_b$ (3-4)

$b \equiv L_pARTM^o$ (3-5)

$c \equiv L_pART(M_{iso}V_{iso}(1-v_b)+M^o v_b V_{iso})$ (3-6)

The effects on the osmotic response of varying the concentrations, (and therefore M^i and M^o), the membrane hydraulic conductivity, L_p, and the cell isotonic volume, can be examined using the above equations. The values for V_{iso}, M_{iso}, M^o, and temperature are all measured values. Values for L_p and v_b are found by fitting Eqs. 3-3 through 3-6 to experimental data using a least-squares error method. In the rest of this chapter, the L_p and v_b found by fitting the *mean* of the experimental volume distribution to the single-cell equation will be called L_{po} and v_{bo}, respectively.

From simulations performed by C. C. V. Chan using the equations, it has been found that for a fixed membrane hydraulic conductivity, increasing the extracellular concentration results in a faster osmotic response of the cell. Conversely, for a fixed extracellular concentration, a faster osmotic response corresponds to a higher membrane hydraulic conductivity. The calculations also show that the time it takes for a cell to reach its equilibrium volume in a hypertonic solution will increase as the isotonic volume of the cell increases.

3.2b Osmotic Response of Cells with Size Distributions

The purpose of obtaining a theoretical evolution of the size distribution of a population of cells is to compare the predicted evolution to the experimental evolution. As such, the initial size distribution of cells used for the experiment is chosen as the basis for the calculations. The membrane hydraulic conductivity, osmotically inactive fraction and temperature values obtained from the experiment are also used for the theoretical calculations.

To determine the theoretical osmotic response of cells with size distributions, the volumes at different times (1 second, 2 seconds etc.) for each of the cells in the initial size distribution are calculated using Eqs. 3-3 through 3-6. Two assumptions were made while performing the calculations:

1. The solutions that the cells were placed in were assumed to be dilute, such that the molarity of the solution was equal to the molality of the solution.

2. The cells were assumed to be spherical in shape. The effective surface areas of the cells were obtained from the isotonic volumes of the cells. It was also assumed that the surface area for osmotic transport remains constant as cells shrink. This is consistent with the way cell membranes are structured; during expansion or shrinkage, the membrane folds or unfolds, having no effect on the cell surface area.

3.3 Materials and Methods

3.3a Cell Culture

Two different cell lines were used to investigate the effects of cell size distribution on the osmotic response of the cells. The first cell line was the V-79W line of Chinese hamster fibroblasts. The fibroblasts were incubated at 37°C in an atmosphere of 95% (v/v) air + 5% (v/v) carbon dioxide in a supplemented medium consisting of minimum essential medium (MEM) with Hanks' salts, 16 mmol/L sodium bicarbonate, 2 mmol/L L-glutamine, 10% (v/v) fetal bovine serum and antibiotics (penicillin G (50 μg/mL), streptomycin (50 μg/mL)) (all components from GIBCO Laboratories, Grand Island, NY). Cells were maintained in tissue culture flasks (25 cm^2; Corning Glass Works, Corning, NY) and harvested by exposure to a 0.25% trypsin solution (GIBCO) for 10 min at 37°C. Single fibroblast cells were re-suspended in the supplemented MEM before being used experimentally.

The second cell line was the Madin-Darby Canine Kidney (MDCK; CCL 34) cell line obtained from the American Type Culture Collection (ATCC, Rockville, MD). These cells were cultured* at 37°C in an atmosphere of 95% (v/v) air + 5% (v/v) carbon dioxide in an antibiotic–free minimum essential medium (MEM) containing 10% (v/v) fetal bovine serum (all components from Gibco Laboratories). Cells were maintained in tissue culture flasks (25 cm^2, Corning Glass Works) before being dissociated into single cells by exposure to a 0.25% trypsin-EDTA solution

* The MDCK cells were cultured by J. P. Acker

(GIBCO) for 10 min at 37°C. The MDCK cells were re-suspended into the cell-specific tissue culture medium before being used experimentally.

3.3b Electronic Particle Counter

Electronic particle counters have been used previously to determine the membrane permeability characteristics of cells (Buckhold et al., 1965; McGann & Turc, 1980; Gilmore et al., 1998; Acker et al., 1999). Cells passing through the aperture in an electronic counter displace a volume of the conducting fluid resulting in a current pulse proportional to the volume of the cells. In kinetic studies, rapid measurement of the mean or mode cell volume allows for determination of the cell permeability characteristics using theoretical models. In this study, a Coulter counter (model ZB1, Coulter Inc, Hialeah, FL) was used to record the number and volume of cells in a hypertonic solution. The Coulter counter was connected to a personal computer via a pulse-height analyzer (The Great Canadian Computer Company, Spruce Grove, AB, Canada) as shown in Figure 3-1. This device, with the accompanying Cell Size Analyzer software, recorded the time and size of each cell passing through the Coulter aperture (McGann et al., 1982). The size range was divided into 256 "bins". Over each specified time interval, the cell count for each size bin was collected. Once a calibration factor is applied to the bin sizes, they then represent the actual volumes of the cells. The calibration was carried out with latex beads (Coulter Calibration Standards: 10 μm). This allowed size distributions to be created for each time interval.

3.3c Coulter Principle

A Coulter counter determines the number and size of the cells suspended in a conductive liquid by forcing the suspension to flow through a small aperture and by monitoring an electric current that flows through the aperture. Two electrodes are immersed in the conductive fluid on either side of the aperture tube as shown in Figure 3-2. As a result, when cells pass through the aperture, the resistance between the two electrodes changes. This produces a current that is proportional to the absolute volume of the cells. The number of current impulses that are counted as a specific amount of sample volume is drawn through the aperture represents the number of particles or cells within the suspension.

3.3d Osmotic Experiments

Experimental hypertonic solutions were prepared by diluting a 10X isotonic phosphate buffered saline solution (GIBCO). V-79W fibroblast or MDCK* cells in an isotonic solution (300 mOsmol/kg) were abruptly transferred into a well-mixed hypertonic salt solution of 1732 mOsmol/kg or 1533 mOsmol/kg respectively, and the kinetics of cell shrinkage were studied. It is very important that the solution be well-mixed in order to be able to visualize the cell kinetics taking place. The osmolalities of the salt solutions were measured with a freezing point depression osmometer (model 5004, Precision Systems, Inc.). The osmolalities and

* MDCK cell Coulter measurements were done by J. P. Acker.

densities* of the solutions were measured and the assumption of dilute solution was found to be reasonable.

3.3e Obtaining Size Distributions from Electronic Particle Counter Data

The Coulter counter, through the pulse height analyzer, was connected to a personal computer and the Cell Size Analyzer program was used to collect and store raw data generated by the Coulter counter. The Cell Size Analyzer program arranges the data into 256 size bins with each cell measurement time-stamped. In order to have a large enough number of cells in each size bin to generate smooth curves for the size distributions, time intervals of 1 second were selected over which to draw volume distributions and the size range of each bin was increased to 194.0 μm^3 giving a total of 22 bins for the MDCK cells and to 74.4 μm^3, giving a total of 25 bins for the V-79W cells.

3.4 Results

3.4a Experimental Cell Size Distributions as a Function of Time

The experimental cell size distributions as functions of time for the MDCK and V-79W cells are shown in Figures 3-3 and 3-4 respectively. As seen in the figures, the MDCK cells have a much broader cell size distribution than the V-79W cells. In Figure 3-3, the experimental cell size distribution in terms of the

* The densities of the solutions were measured by C. C. V. Chan

normalized cell count (the number of cells / total cell count) was plotted for the MDCK cells. The mean isotonic volume for these cells was 1715 μm^3. By fitting the mean of the experimental volume distribution to the single-cell equation, L_{po} was found to be 1.48 $\mu m^3/\mu m^2/atm/min$ and v_{bo} was found to be 0.40 in a 1533 mOsmol/kg solution at a temperature of 22°C. Similarly in Figure 3-4, the experimental cell size distribution in terms of the normalized cell count was plotted for the V-79W cells. The mean isotonic volume was 738 μm^3. L_{po} was 1.19 $\mu m^3/\mu m^2/atm/min$ and v_{bo} was 0.36 in a 1732 mOsmol/kg solution at a temperature of 22°C. Figure 3-5 shows the normalized cell volume vs. time for the V-79W cells and demonstrates the kinetics of cell shrinkage.

3.4b Theoretical Cell Size Distributions as a Function of Time

Starting with the experimental isotonic volume distributions, the time-varying theoretical distributions were created (by C. C. V. Chan) using values of temperature and osmotic pressure from the experimental conditions and using L_{po} and v_{bo} for L_p and v_b respectively. Figure 3-6 shows the theoretical size distribution for the MDCK cells as a function of time in a 1533 mOsmol/kg solution using an L_p of 1.48 $\mu m^3/\mu m^2/atm/min$ and an osmotically inactive fraction of 0.40 at a temperature of 22°C. Similarly, Figure 3-7 shows the theoretical size distribution for the V-79W cells as a function of time using an L_p of 1.19 $\mu m^3/\mu m^2/atm/min$ and an osmotically inactive fraction of 0.36 in a 1732 mOsmol/kg solution at a temperature of 22°C. From a comparison of Figures 3-3 and 3-6 or Figures 3-4 and 3-7, it is clear that the predicted osmotic response

is faster than the experimental osmotic response. Therefore L_{po} does not accurately characterize the osmotic response of a distribution of cells.

To find an estimate for L_p that describes the population better than L_{po}, theoretical distributions can be drawn using various L_p values in an attempt to match the predictions with experiments. In Figures 3-8 and 3-9, theoretical MDCK cell size distributions were created using chosen values for the membrane hydraulic conductivity, L_p, of 0.10 $\mu m^3/\mu m^2/atm/min$ and 0.30 $\mu m^3/\mu m^2/atm/min$, respectively. Similarly, in Figures 3-10 and 3-11, the theoretical V-79W cell size distributions were created using chosen values for L_p of 0.45 $\mu m^3/\mu m^2/atm/min$ and 0.75 $\mu m^3/\mu m^2/atm/min$, respectively. Once again, the values for the temperature, osmotic pressure, and isotonic volume were those used in the experiment, while the values of L_p were chosen to make Figures 3-8 and 3-9 agree with Figure 3-3 and to make Figures 3-10 and 3-11 agree with Figure 3-4.

3.5 Discussion

The size distributions for both the MDCK and the V-79W cells shown in Figures 3-3 to 3-4 and Figures 3-6 to 3-11 indicate that as time increases, the shapes of the distributions change as the curves shift to the left. This implies that a population of cells will have different cell shrinkage kinetics than a single cell (or cells with a uniform size), and that the single-cell membrane mass transport

equation applied to the *mean* volume distribution cannot be used to accurately obtain the membrane hydraulic conductivity for a population of cells.

When comparing the experimental size distribution as a function of time for the MDCK cells in Figure 3-3 with the theoretical size distribution as a function of time for the MDCK cells in Figure 3-6 (with the same membrane hydraulic conductivity for both), it appears that the predicted rate of cell shrinkage is higher than the experimental rate. For the MDCK cells, an L_{po} of 1.48 $\mu m^3/\mu m^2/atm/min$ was found for a 1533 mOsmol/kg solution. In order for the theoretically-obtained distribution changes to match the experimental distribution changes, an L_p of 0.30 $\mu m^3/\mu m^2/atm/min$ or smaller would be required, as seen in Figures 3-8 and 3-9. Assuming that the value of L_p obtained by fitting distribution data is closer to the real L_p for the plasma membrane, these numbers show that the L_p obtained by fitting experimental data with single-cell equations applied to the mean volume is in error by more than 390% for MDCK cells. Similar observations were made for the V-79W cells for which an L_{po} of 1.19 $\mu m^3/\mu m^2/atm/min$, based on the experimental mean volume changes at 1732 mOsmol/kg, was found. When comparing the experimental size distribution as a function of time for the V-79W cells in Figure 3-4, with the theoretical size distribution using the same membrane hydraulic conductivity in Figure 3-7, once again it appears that the predicted rate of cell shrinkage is higher than the experimental rate. In order for the theoretically-obtained distribution changes to match the experimental distribution changes, an L_p of approximately 0.75 $\mu m^3/\mu m^2/atm/min$ would be

required, as seen in Figures 3-10 and 3-11. In this case the error resulting from applying the single-cell equations to changes in the mean volume may be as much as 59%.

The MDCK cells have approximately twice the isotonic volume of the V-79W cells and thus require a longer time to reach equilibrium. However, for both of these cell types, the theoretical distributions during osmotic shrinkage calculated using L_{po} do not match the experimental measurements. The single-cell equation applied to the mean cell size does not accurately predict the osmotic response of a population of cells. A lower value for the membrane hydraulic conductivity than that obtained from the single-cell analysis was required to accurately describe the experimental data.

3.6 Conclusions

Analysis of the experimental data for both the MDCK and the V-79W cells, two cell types with different isotonic volumes and different cell size distributions, showed that the shapes of the cell size distributions do not stay constant over time when the cells are responding in a hypertonic environment. The membrane hydraulic conductivity obtained by averaging volume data tended to be too high. For the MDCK and V-79W cells, the values for L_p could be in error by as much as 390% and 59%, respectively. This implies that the single-cell membrane mass transport equation fit to the *mean* cell volume as a function of time does not

accurately model the osmotic response of cells with size distributions. Another model is needed to obtain the membrane hydraulic conductivity. As a minimum, as suggested by Armitage and Juss (1996), the *mode* of skewed distributions rather than the mean should be used for analysis. Ideally a method should be developed that takes the entire distribution into account.

3.7 References

1. Adams, R. B., Voelker, W. H., Gregg, E. C. 1967. Electric Counting and Sizing of Mammalian Cells in Suspension: An Experimental Evaluation. *Phys. Med. Biol.*, **12**, 79-92.
2. Acker, J. P., Pasch, J., Heschel, I., Rau, G., McGann, L. E. 1999. Comparison of Optical Measurement and Electrical Measurement Techniques For The Study Of Osmotic Responses Of Cell Suspensions. *Cryo-Letters,* **20**, 315-324.
3. Anderson, E. C., & Petersen, D. F. 1967. Cell Growth and Division. II. Experimental Studies of Cell Volume Distributions in Mammalian Suspension Cultures. *Biophys. J.*, **7**, 353-364.
4. Armitage, W. J., & Juss, B. K. 1996. Osmotic Response of Mammalian Cells: Effects of Permeating Cryoprotectants on Nonsolvent Volume. *J. Cell. Physiol.*, **168**, 532-538.
5. Buckhold, B., Adams, R. B., Gregg, E. C. 1965. Osmotic Adaptation of Mouse Lymphoblasts. *Biochimica et Biophys. Acta.*, **102**, 600-608.
6. Davson, H., & Danielli, J. F. 1952. In *The Permeability of Natural Membranes*, Cambridge, The University Press, 2nd edition.
7. Dick, D. A. T. 1966 In *Cell Water*, Butterworths, Washington.
8. Gilmore, J. A., McGann, L. E., Ashwood, E., Acker, J. P., Raath, C., Bush, M., Critser, J. K. 1998. Fundamental Cryobiology of Selected African

Mammalian Spermatozoa and its Role in Biodiversity through Development of Genome Resource Banking. *An. Rep. Sci.*, **53**, 277-297.

9. Gilmore, J. A., McGann, L. E., Liu, J., Gao, D. Y., Peter, A. T., Kleinhans, F. W., Critser, J. K. 1995. Effect of Cryoprotectant Solutes on Water Permeability of Human Spermatozoa. *Biol Reprod.*, **53**, 985-995.

10. Gregg, E. C., & Steidley, D. 1965. Electrical Counting and Sizing of Mammalian Cells in Suspension. *Biophys. J.*, **5**, 393-405.

11. Grover, N. B., Naaman, J., Ben-Sasson, S., Doljanski, F. 1969a. Electric Sizing of Particles in Suspensions. I. Theory. *Biophys. J.*, **9**, 1398-1414.

12. Grover, N. B., Naaman, J., Ben-Sasson, S., Doljanski, F., Nadav, E. 1969b. Electric Sizing of Particles in Suspensions. II. Experiments with Rigid Spheres. *Biophys. J.*, **9**,1415-1425.

13. Grover, N. B., Naaman, J., Ben-Sasson, S., Doljanski, F. 1972. Electric Sizing of Particles in Suspensions. III. Rigid Spheroids and Red Blood Cells. *Biophys. J.*, **12**, 1099-1117.

14. Jacobs, M. H., & Stewart, D. R. 1932. A Simple Method for the Quantitative Measurement of Cell Permeability. *J. Cell. Comp. Physiol.*, **1**, 71-82.

15. Kedem, O., & Katchalsky, A. 1958. Thermodynamic Analysis of the Permeability of Biological Cells Membranes to Non-electrolytes. *Biochimica et Biophys. Acta.*, **27**, 229-246.

16. Kubitschek, H. E. 1958. Electronic counting and Sizing of Bacteria. *Nature*, **182**, 234-235.

17. Luckè, B., & McCutcheon, M. 1932. *Physiol. Rev.*, **12**, 68-132.

18. Mazur, P. 1963. Kinetics of Water Loss from Cells at Subzero Temperatures and the Likelihood of Intracellular Freezing. *J. Gen. Physiol.*, **47**, 347-369.

19. McGann, L. E., & Turc, J. M. 1980. Determination of Water and Solute Permeability Coefficients. *Cryobiology*, **17**, 612-613.

20. McGann, L. E., Turner, A. R., Turc, J. M. 1982. Microcomputer Interface for Rapid Measurement of Average Volume Using an Electronic Particle Counter. *Med. & Biol. Eng. & Compute.*, **20**, 17-120.

Figure 3-1 Coulter Counter and Computer Set Up

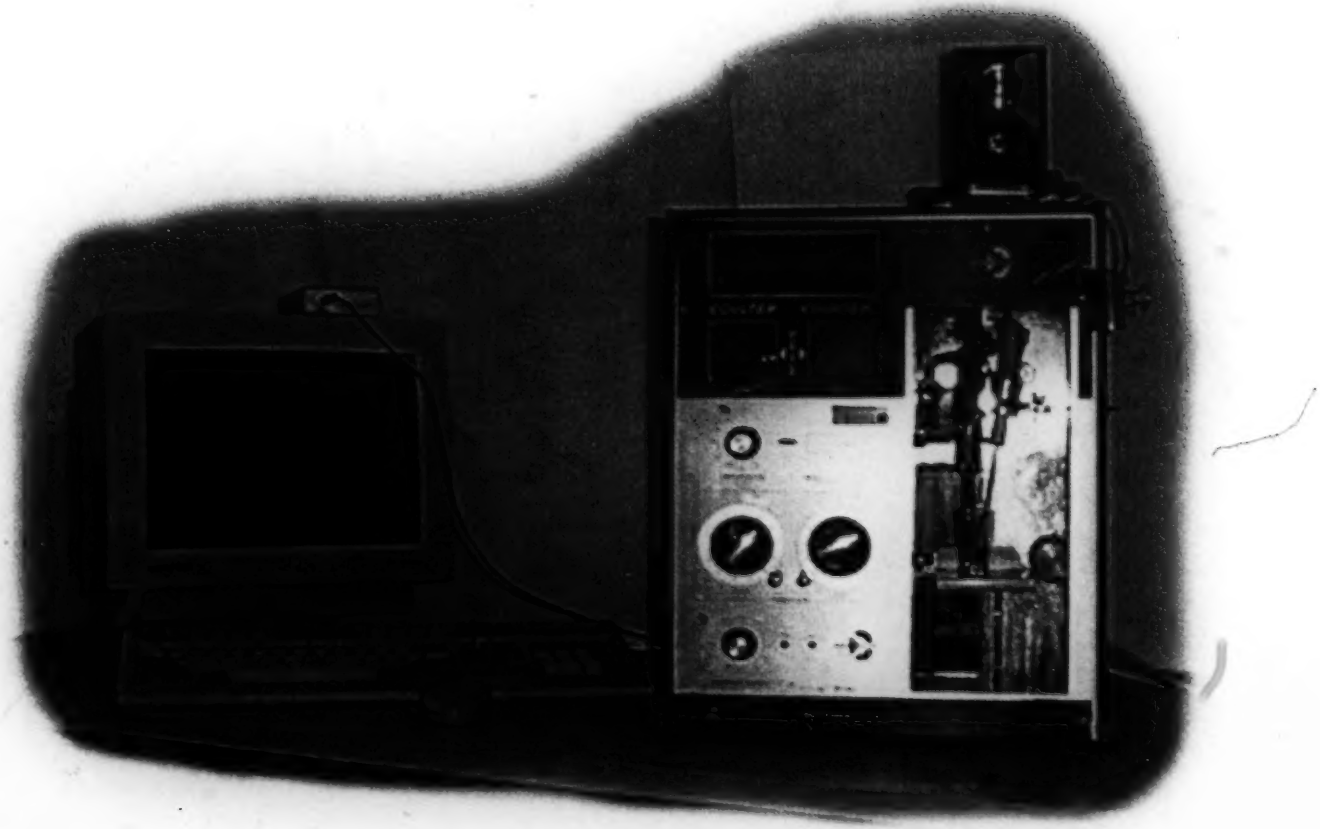

3-2 Coulter Counter Aperture and Electrode Set Up

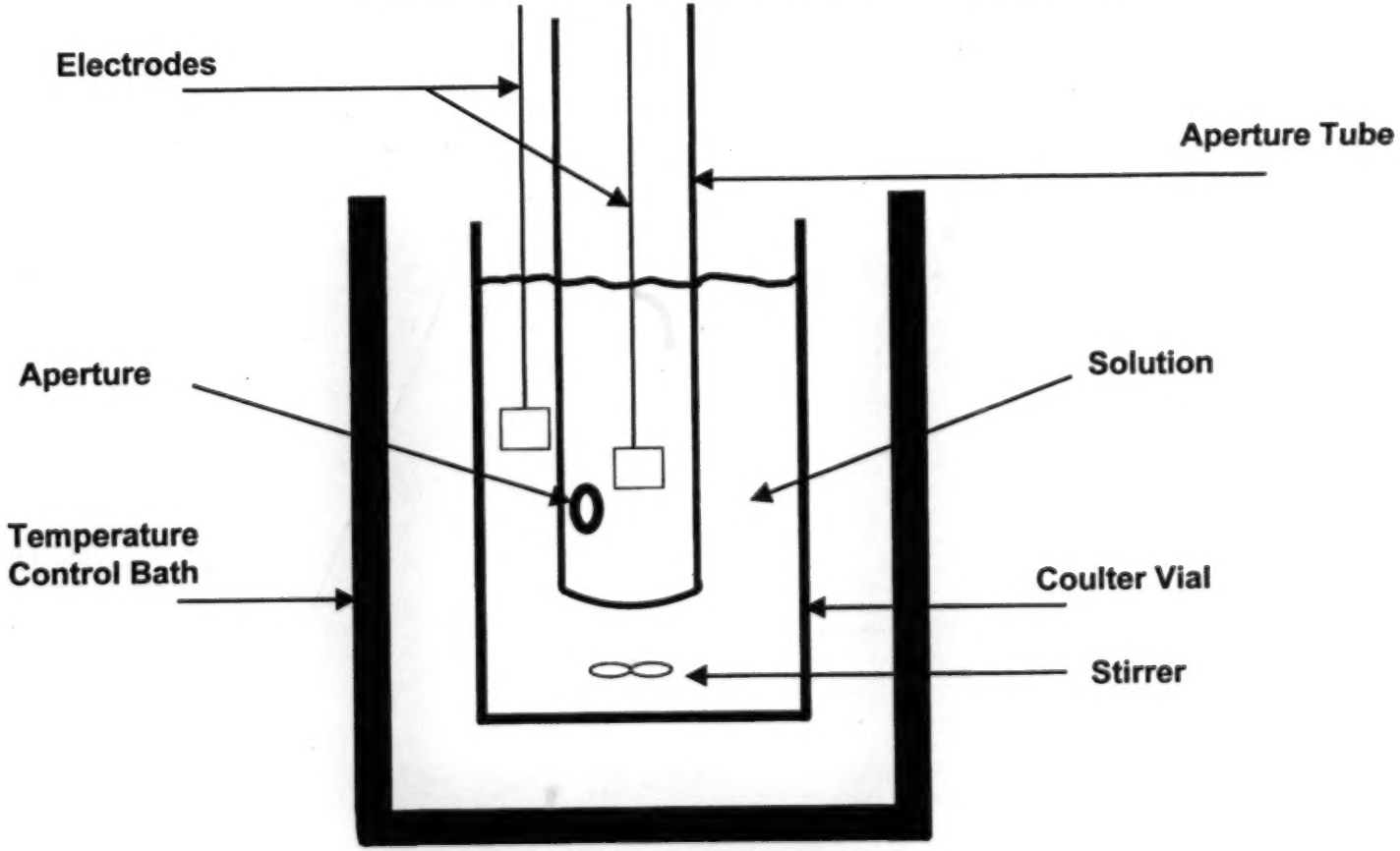

Figure 3-3 Experimental MDCK Cell Size Distributions as a Function of Time with an Lp_o of 1.48 (1533 mOsm/kg)

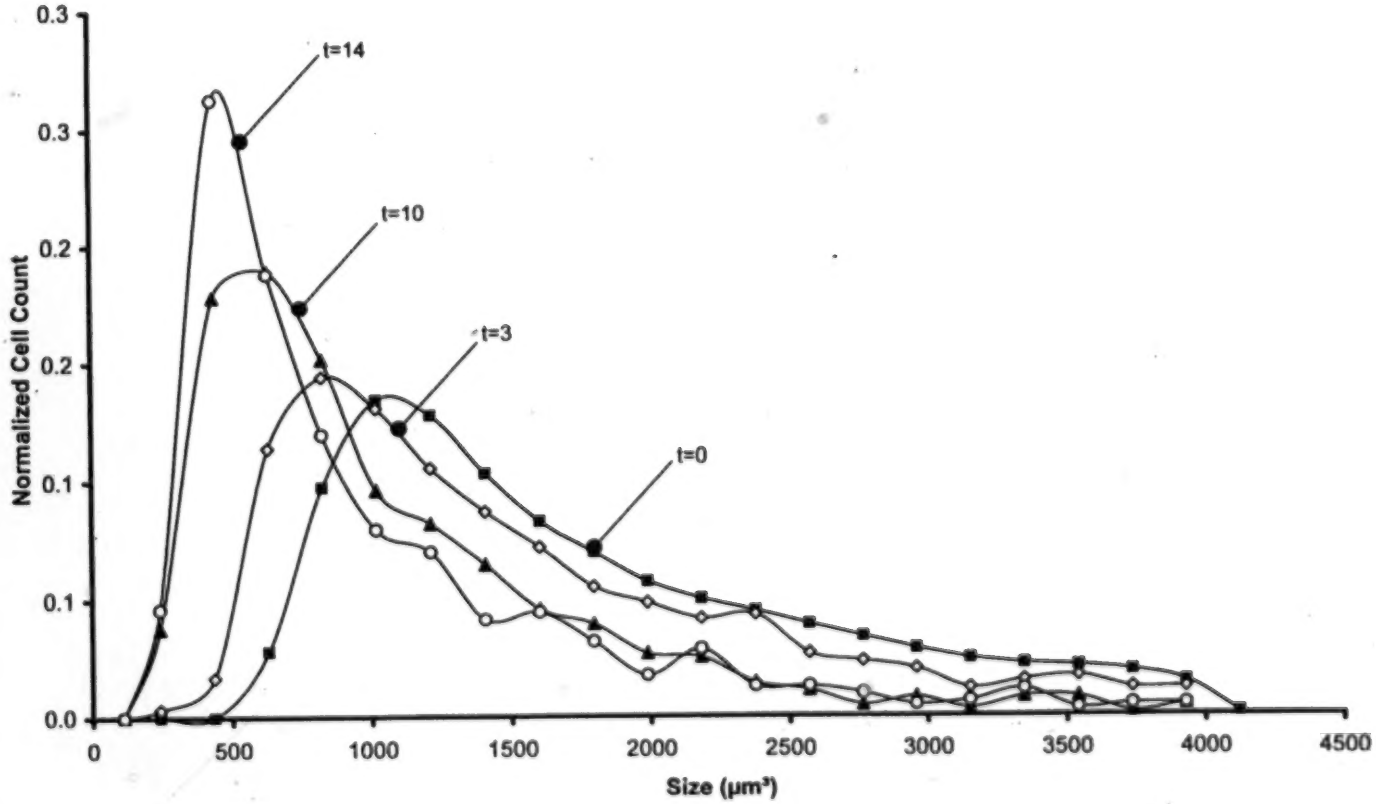

Figure 3-4 Experimental V-79W Cell Size Distributions as a Function of Time With an Lp_o of 1.19 (1732mOsm/kg)

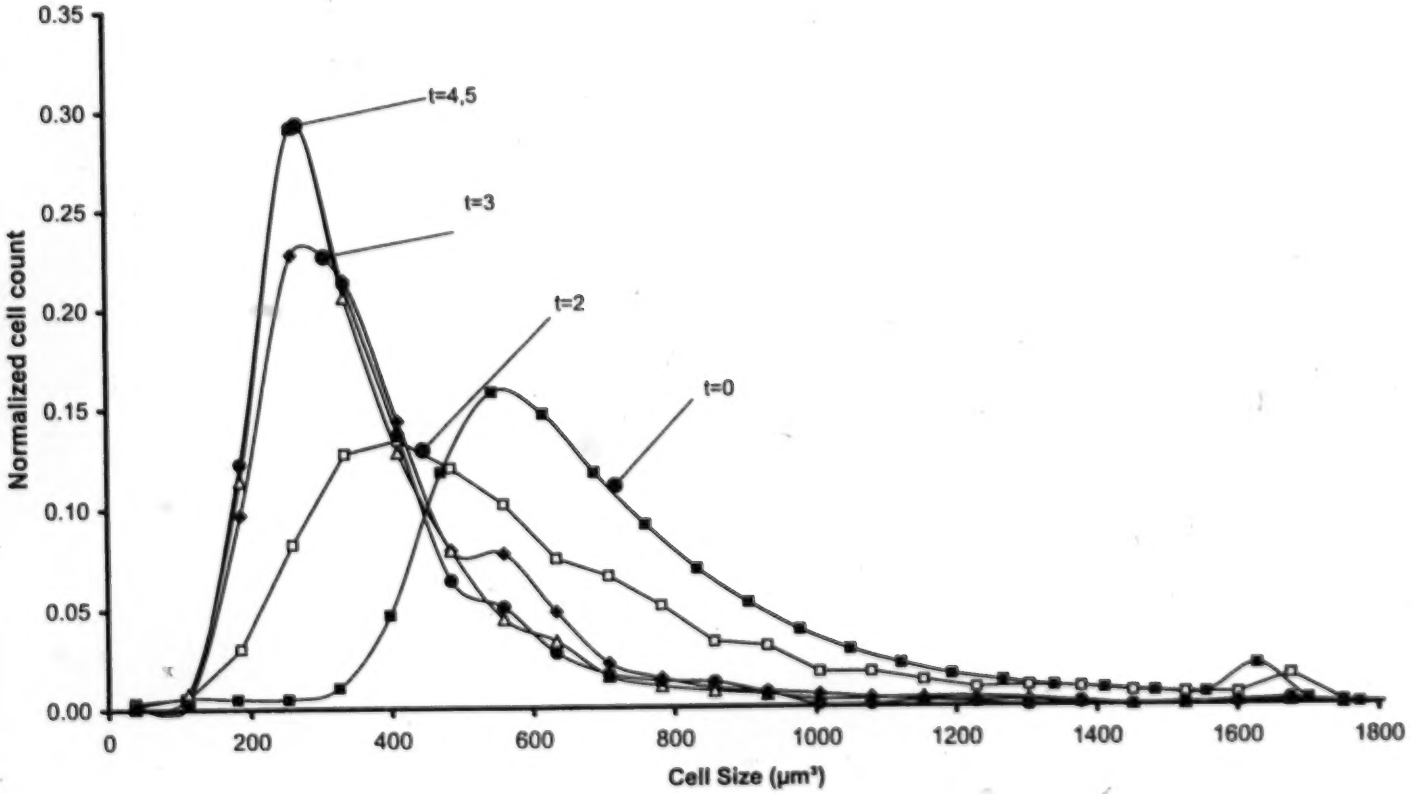

Figure 3-5 Normalized Cell Volume Vs Time for V-79W Cells with an Lp_o of 1.19 (1732 mOsm/kg)

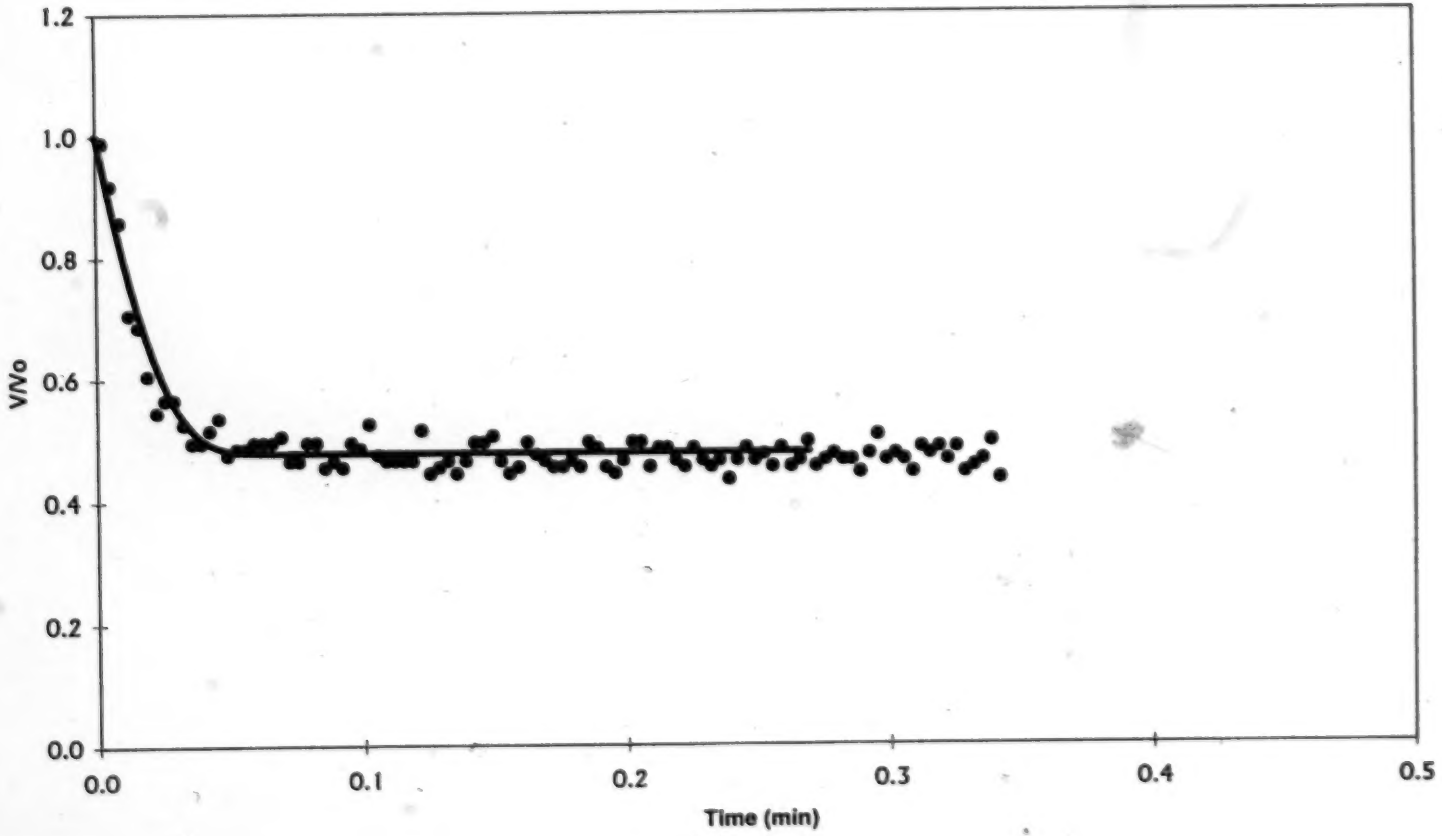

Figure 3-6 Theoretical MDCK Cell Size Distributions as a Function of Time Using an L_p of 1.48 (1533 mOsm/kg)*

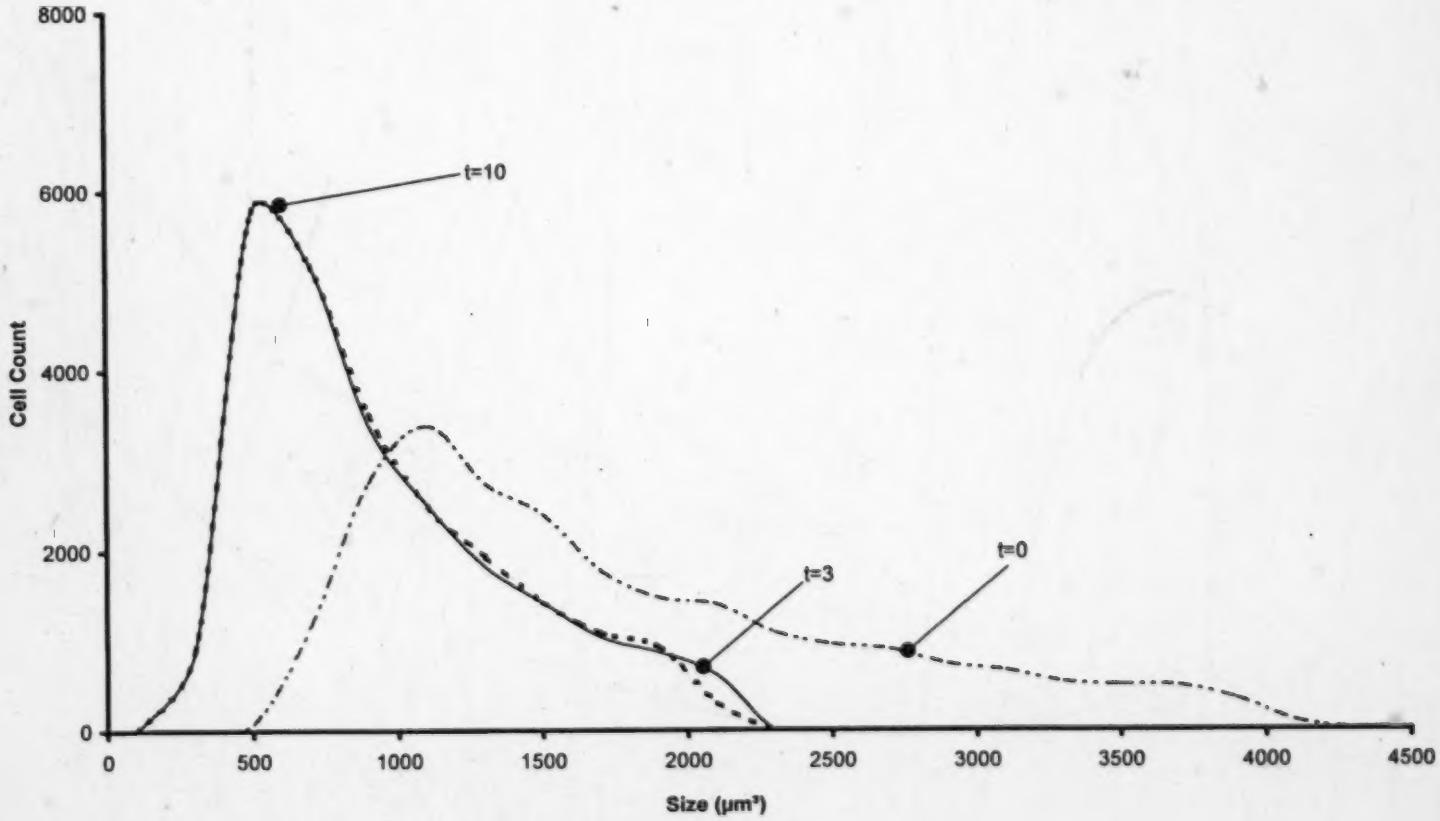

* The calculations for this figure were done by C. C. V. Chan

Figure 3-7 Theoretical V-79W Cell Size Distibution as a Function of Time Using an Lp of 1.19 (1732 mOsm/kg) *

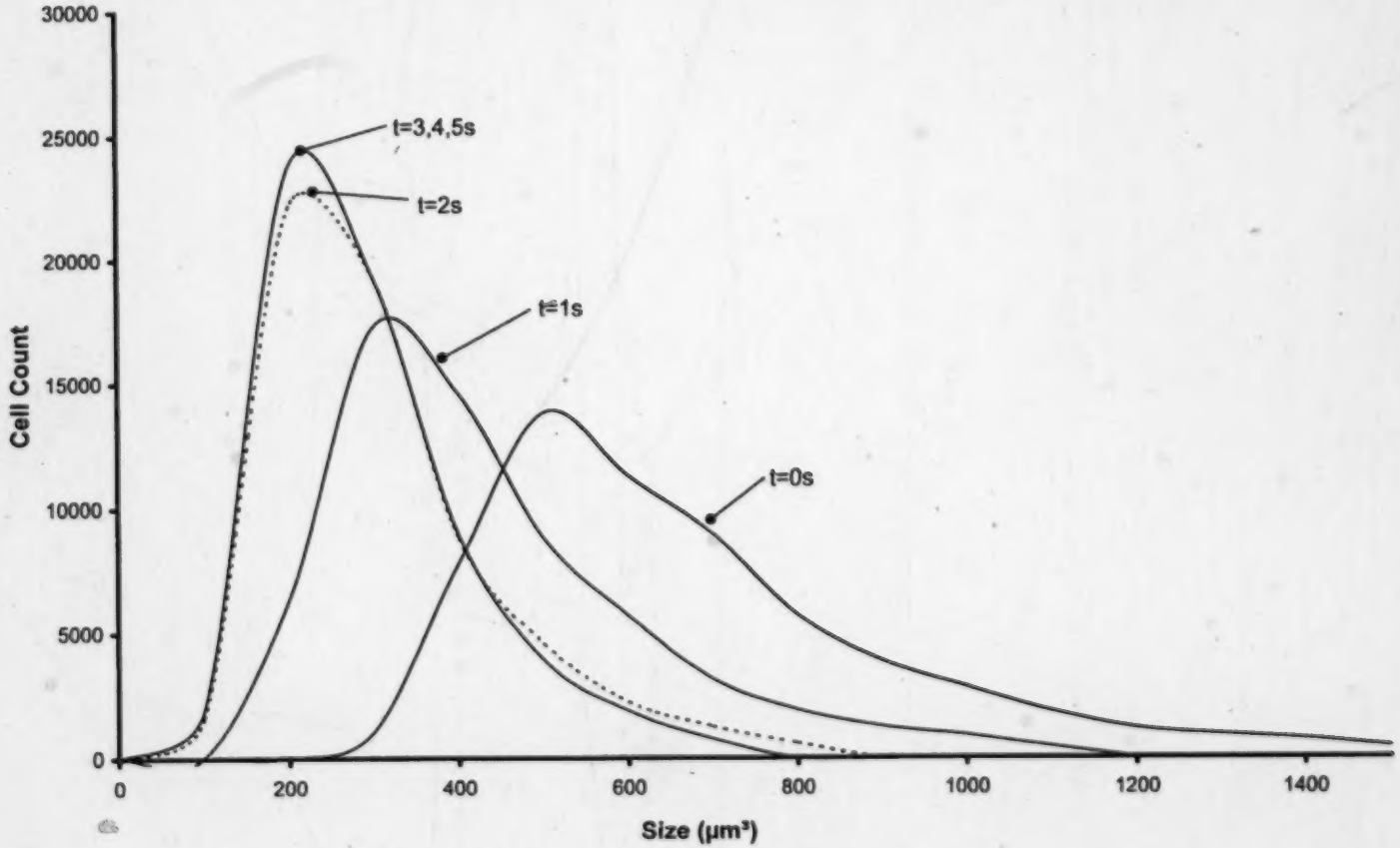

* The calculations for this figure were done by C. C. V. Chan

Figure 3-8 Theoretical MDCK Cell Size Distribution as a Function of Time Using an Lp of 0.10 (1533 mOsm/kg) *

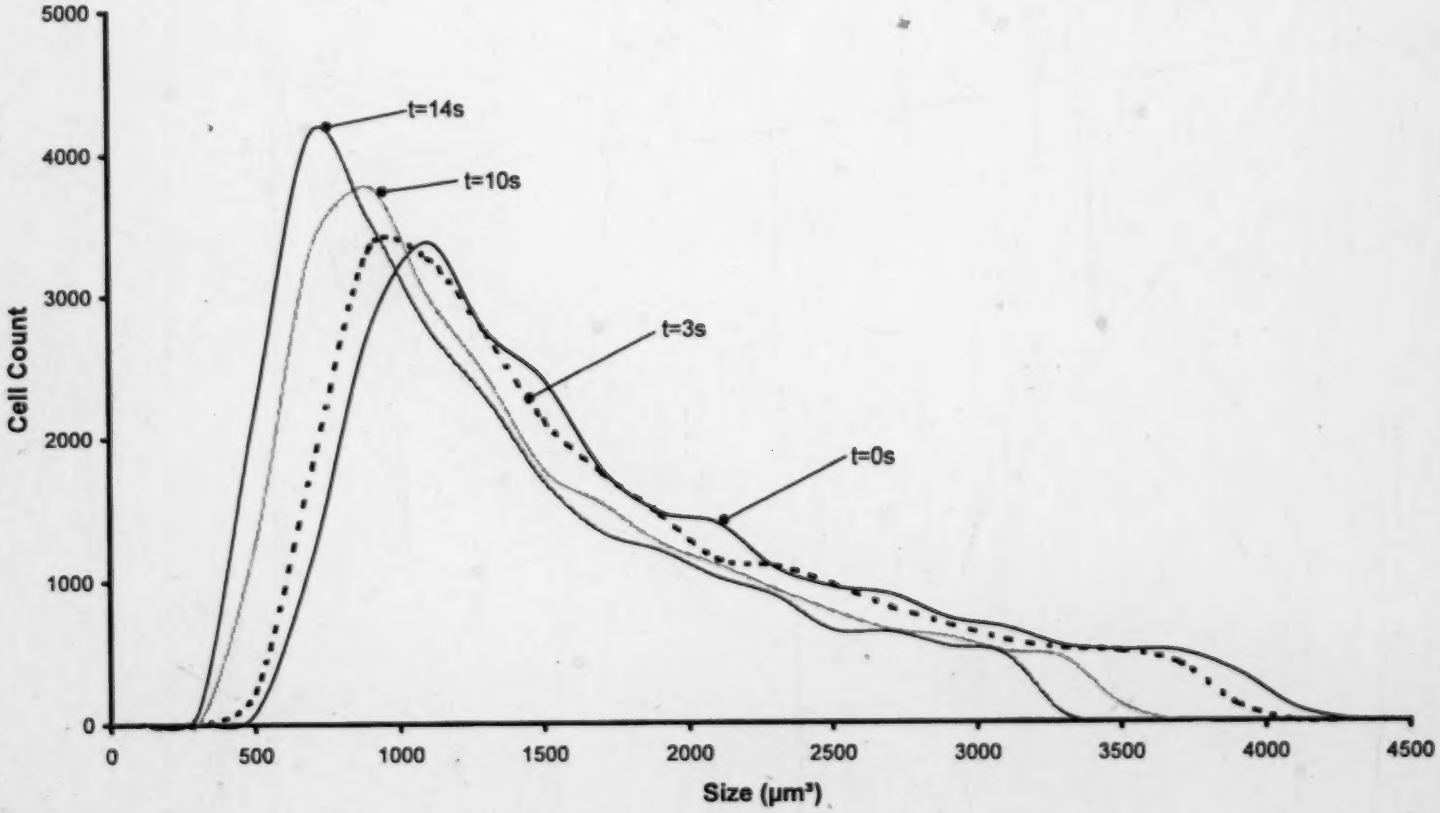

* The calculations for this figure were done by C. C. V. Chan

Figure 3-9 Theoretical MDCK Cell Size Distribution as a Function of Time Using an Lp of 0.30 (1533 mOsm/kg) *

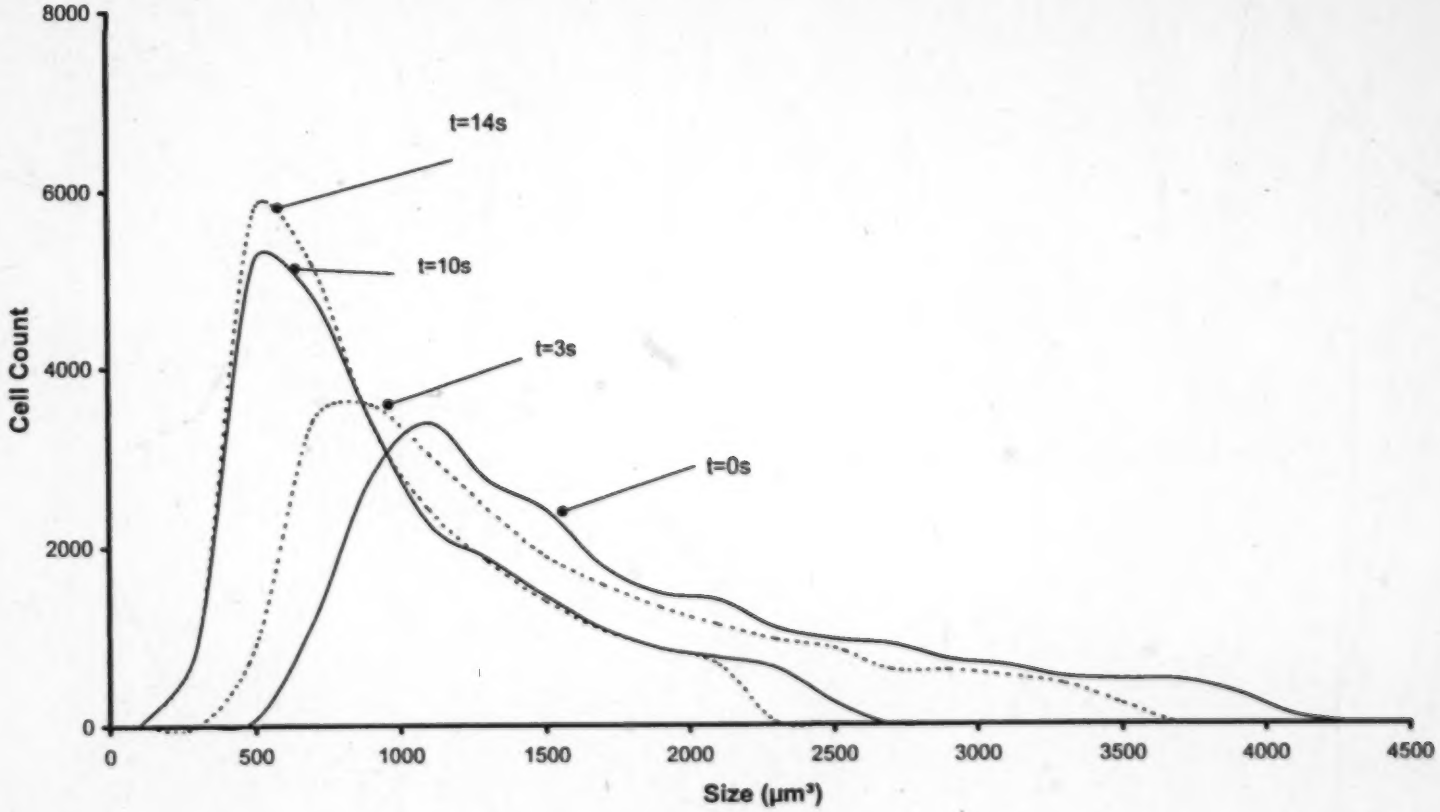

* The calculations for this figure were done by C. C. V. Chan

Figure 3-10 Theoretical V-79W Cell Size Distribution as a Function of Time Using an Lp of 0.45 (1732 mOsm/kg) *

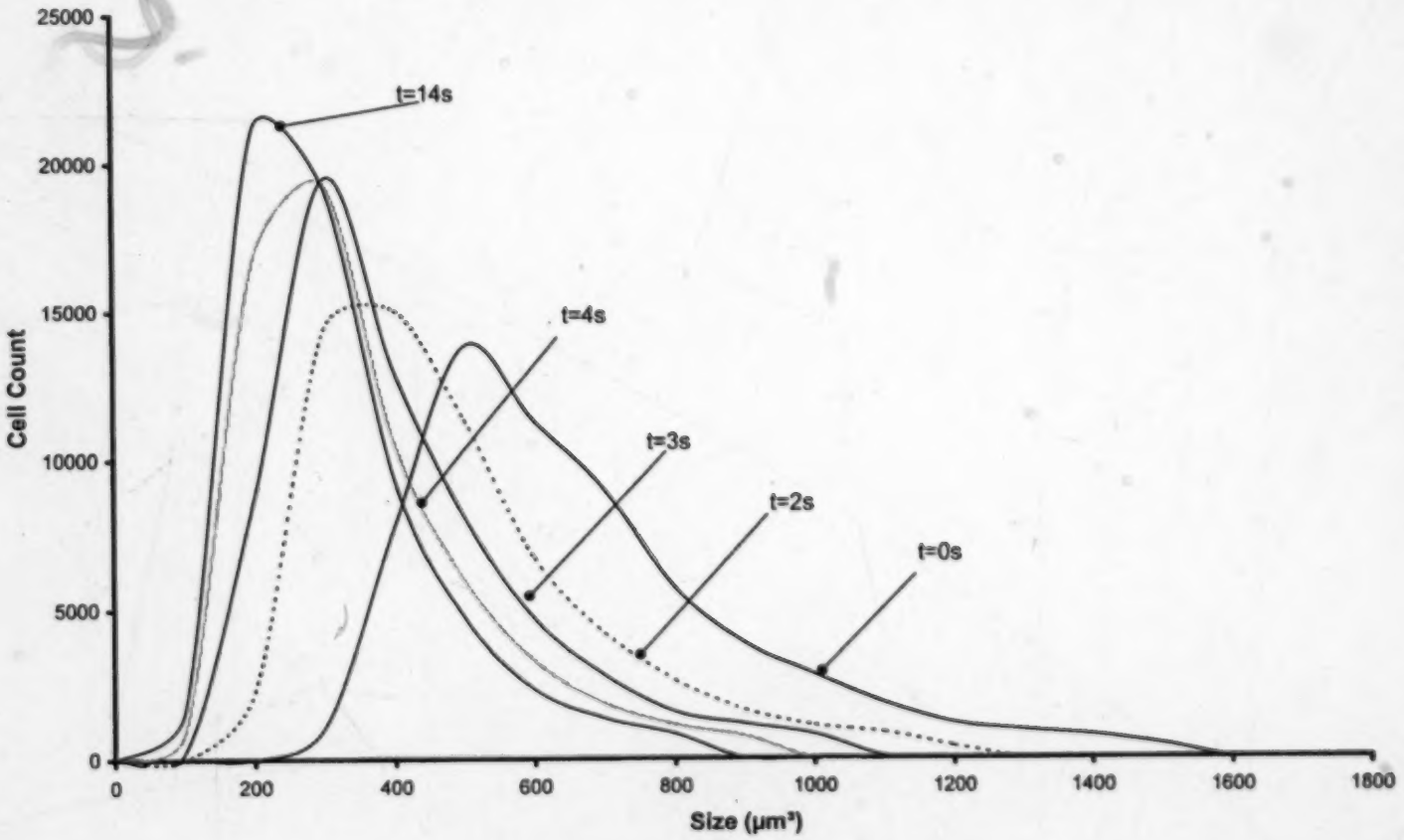

* The calculations for this figure were done by C. C. V. Chan

Figure 3-11 Theoretical V-79W Cell Size Distribution as a Function of Time Using an Lp of 0.75 (1732 mOsm/kg) *

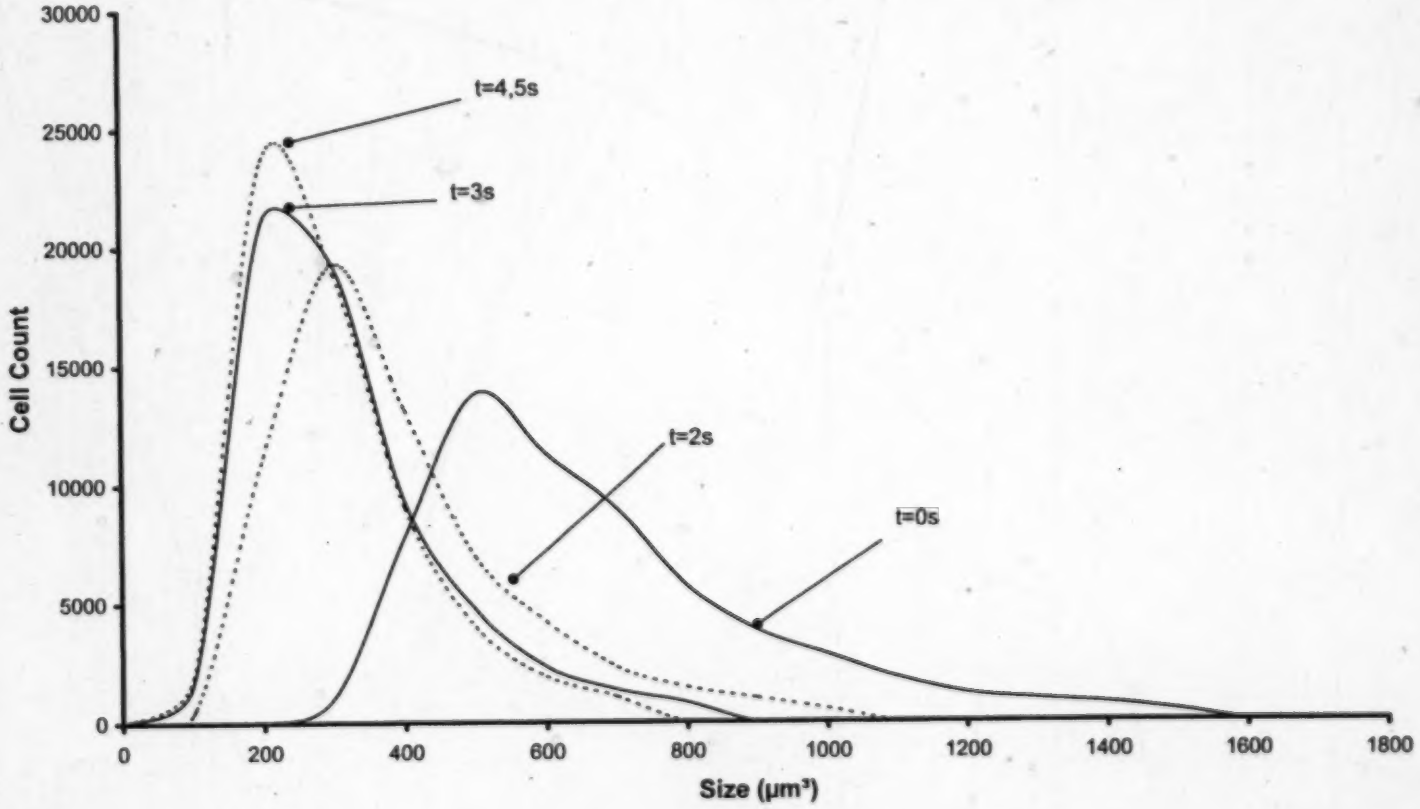

* The calculations for this figure were done by C. C. V. Chan

Chapter 4: The Effect of Temperature on Membrane Hydraulic Conductivity*

4.1 Introduction

4.1a Water Transport across Cell Membranes

Since the early 1930's, there have been numerous articles published on the subject of the mechanisms of water movement across cell membranes and the influence of temperature on water transport across cell membranes and tissues (Lucké & McCutcheon, 1932; Jacobs et al., 1935, Nevis, 1958; Hempling, 1961; Hays & Leaf, 1962; Farmer and Macey, 1970; Vieira et al., 1970; Sha'afi, 1977). The transport of ions and neutral solutes creates osmotic gradients and as a result, water moves passively across the cell membrane (Verkman et al., 1996). Verkman and his colleagues found that most cell membranes have adequate water permeability through membrane lipids to support volume regulation as well as other cell maintenance functions (1996). Despite the fact that water slowly crosses the cell membrane by diffusion through the lipid bilayer when a concentration gradient is present, some cells exhibit rapid trans-membrane water transport through specialized water channels (Macey, 1984; Preston et al., 1992; Verkman et al., 1996). For example, despite the fact that red blood cells have a very high water permeability via aqueous pores that accounts for 90% of the total water flux, bilayer diffusion still accounts for 10% of the total water flux across the

---

* This chapter with minor modifications has been submitted to Biophysical Journal as: H. Y. Elmoazzen, J. A. W. Elliott, and L. E. McGann, "The Effect of Temperature on Membrane Hydraulic Conductivity"

cell membrane (Finkelstein, 1987; Macey, 1984). Real cells have a background level of water transport via the lipid bilayer.

4.1b The Discovery of Aquaporins

It was suggested for some time from biophysical evidence that water channels existed in red blood cells, kidney tubule cells, and amphibian urinary bladder cells (Macey, 1984; Meyer & Verkman, 1987; Verkman, 1989; Verkman, 1992). Since this time, there have been remarkable advances in the identification, molecular cloning, and structure-function analysis of water transporting proteins. These "water-transporting" proteins or "water-selective" channels are known as aquaporins and have now been discovered in many animals and plants (Chrispeels & Agre, 1994; Verkman et al., 1996).

In 1992, Preston et al., identified the first water transporting protein, CHIP28 (channel-forming integral protein) in human red blood cells. It was the abundance of CHIP28 in the renal proximal tubule and red blood cells that suggested that CHIP28 might function as a water transporter (Preston & Agre, 1991). After the identification, characterization and cloning of the CHIP28 water-transporting protein family, it was demonstrated that there was an increased permeability on expression of CHIP28 in *Xenopus* oocytes (Preston et al., 1992). CHIP28 has been found to be widely distributed in other mammalian epithelia such as corneal endothelial cells and gall bladder epithelium, where it is thought to play a role in water permeability (Nielsen et al., 1993; Echevarría et al., 1993).

The anterior chamber of the eye also contains CHIP28 in several locations in addition to the corneal endothelium, including the non-pigmented epithelium of the ciliary body and the iris, and anterior epithelium of the lens (Echevarría et al., 1993; Nielsen et al., 1993; Kang et al., 1999).

The discovery of aquaporins has led to the increased identification of these channels and has changed our understanding of membrane water transport. The expression sites of the aquaporin family of proteins have been consistent with a role of water channels in fluid transport (Verkman et al., 1996). Other aquaporins have been identified in various tissues in the body such as the brain in ependymal cells and pia matter (Jung et al., 1994; Ma et al., 1994; Frigeri et al, 1995a; Frigeri et al., 1995b;), the epidermal layer of the skin (Frigeri et al., 1995a), and in various parts of the digestive system such as excretory ducts and in the gastric parietal cells of the stomach (Frigeri et al., 1995a). A complete list of the tissue distribution of aquaporins can be found in a review by Verkman et al. (1996).

4.1c Biophysical Properties used to Characterize Aquaporins

There are several biophysical properties that characterize water movement across cell membranes and serve as tools to test for water channels. The first test involves using the osmotic water permeability, P_f (cm/s). P_f is the net volume flow across the membrane in response to a hydrostatic or osmotic driving force.

P_f can be written in terms of an osmotic gradient where the change in cell volume with time is given as follows:

$$\frac{dV}{dt} = P_f A \bar{\upsilon}_w (M^i - M^o) \qquad (4\text{-}1)$$

where $\bar{\upsilon}_w$ is the partial molar volume of water, A is the cell area and M is the osmolality with the superscripts denoting the internal (i) and external (o) cell solution.

The osmotic water permeability coefficient has been found to vary in cell membranes of different compositions. A $P_f > 0.01$ cm/s for a single membrane has been considered suggestive of the presence of aquaporins (Verkman et al., 1996).

An accurate measure of osmotic permeability is essential in determining whether cells have water channels. Verkman et al., (1996) reviewed the current methods used to obtain water permeability measurements in vesicles, cells and tissues. To measure the water permeability in liposomes and vesicles, light-scattering and fluorescence-quenching are the two main techniques utilized. The light-scattering technique is based on the dependence of elastically scattered light on vesicle volume. Despite the fact that the technique is fairly simple to use, Verkman et al. (1996) point out that there are potential problems with quantitative data interpretation. The fluorescence-quenching technique is based on the concentration dependent self-quenching of fluorophores (Verkman et al., 1996). This technique has been used to determine the P_f values for plasma membrane

vesicles (Chen et al., 1988) and endosomes from toad urinary bladder and kidney (Verkman et al., 1988; Shi & Verkman, 1989; Ye et al., 1989, Harris et al., 1990).

To measure the P_f values in adherent cell monolayers, total internal reflection fluorescence is used (Verkman et al., 1996). A method has been developed to quantify the fluorescence concentration based on fluorescence excitation by total internal reflection fluorescence (Bicknese et al., 1993). The cells are loaded with a membrane-impermeant volume marker. A laser beam directed through a glass prism illuminates a thin layer of cytosol. As the cell shrinks in response to an osmotic gradient, the flourophore concentration in the illuminated region increases (Farinas et al., 1995).

The P_f values for oocytes have been measured based on the rate of swelling in response to dilution. The swelling of the oocytes is measured by estimating volume changes using a video monitor (Fishbarg et al., 1990). An improved method was developed using transmission light microscopy (Zhang et al., 1990; Zhang et al., 1991).

For water transport in epithelial cell layers such as those in kidney tubules and collecting ducts, P_f is measured by using an *in vitro* perfusion technique. The tubule is placed in an anisotonic solution while being perfused with an impermeable tracer. As a result the tracer concentration changes along the

length of the tubule and an osmotic gradient is created. The P_f value is determined from the tracer concentration, the solution osmolalities, the lumen flow, and the tubule length and surface area (Verkman, 1989).

The second test that is often used to determine the presence of water channels is the ratio of the osmotic-to-diffusional permeability. The diffusional permeability, P_d, is measured using labeled water in the absence of an osmotic gradient. A P_f / P_d ratio of unity is generally taken as an indication that water channels are absent, while a P_f / P_d ratio greater than 1 is taken as an indication that water moves through a channel (Finkelstein, 1987).

The osmotic water permeability, P_f can be directly related to the membrane hydraulic conductivity of the cell, L_p ($\mu m^3/\mu m^2/min/atm$) as follows:

$$P_f = \frac{RTL_p}{\bar{v}_w} \qquad (4-2)$$

The rate of change of cell volume with time, can be given by the following membrane mass transport model (Jacobs & Stewart, 1932):

$$\frac{dV_w}{dt} = L_p ART(M^i - M^o) \qquad (4-3)$$

where V_W is the water volume, t is time, A is the cell surface area, R is the universal gas constant, T is absolute temperature and M is once again the osmolality with the superscripts denoting the internal (i) and external (o) cell solution.

The third biophysical parameter that has been used to determine the absence or presence of aqueous pores is the Arrhenius activation energy (Verkman et al.,1996). The Arrhenius equation is given in the following form:

$$L_p = L_p^{\circ} \exp\left(-\frac{E_a}{RT}\right) \qquad (4-4)$$

where once again L_p is the membrane hydraulic conductivity, L_p° is a constant, and E_a is the activation energy. This equation describes the temperature dependence of a rate of reaction and is based on the probability of a molecule overcoming an energy barrier. The membrane permeability is measured as a function of temperature and the temperature dependence is generally expressed in terms of the activation energy. The activation energy is found by making an Arrhenius plot of the data (ln (L_p) vs 1/RT) and least squares fitting for the slope, which equals minus E_a. Both L_p° and E_a are determined from the data and thus are the two fitting parameters. The activation energy can generally yield insight as to the mode of water transport across the cell membrane (via diffusion through the lipid bilayer or via water channels).

Based on limited empirical data, it's been found that lipid bilayer solubility-diffusion is characterized by a high Arrhenius activation energy (E_a>10kcal/mol) (Fettiplace and Haydon, 1980; Finkelstein, 1987). This implies that water molecules encounter a hydrophobic environment when crossing the membrane (Sha'afi, 1977) and that there is reduced water movement at lower temperatures

where lipid packing is tighter (Chrispeels and Agre, 1994). Conversely, channel-mediated water transport appears to be characterized by an Arrhenius activation energy of less than 7 kcal/mol (Verkman et al., 1996). This implies that as a water molecule crosses the membrane, it encounters polar groups similar to the polar environment of the bulk solution outside the membrane (Macey, 1984). When certain mercurial compounds inhibit water transport through aquaporins in red blood cells, the apparent activation energy for osmotic transport increases from 4.8 to 11.5 kcal/mol (Macey et al., 1973). This is in agreement with calculations that assume water dissolves in the membrane as discrete molecules and moves across the membrane by diffusion (Price and Thompson, 1969).

Verkman et al. (1996) point out that conclusions about channel-mediated water transport should be viewed cautiously and that complex lipid phase transitions in membranes and the presence of multiple pathways for water transport often yield non-linear Arrhenius plots that are not easily interpreted.

4.2 Objective

The objective of this study was to use the temperature dependence of water permeability to characterize the fundamental physical mechanisms of water transport across real cell membranes and to demonstrate that insight into water transport mechanisms may be gained using easily performed experiments using an electrical particle counter.

The osmotic response of V-79W Chinese hamster fibroblast cells was measured in a hypertonic solution at various temperatures and the membrane hydraulic conductivity was determined. The results were fit with the general Arrhenius equation with 2 free parameters and then fit with two specific membrane models that each had only 1 free parameter. Data from the literature including that for human bone marrow stem cells (McGann et al., 1987), hamster pancreatic islets (Liu et al., 1995) and articular cartilage chondrocytes (McGann et al., 1988) was also examined. Using fairly simple experiments with an electronic particle counter, we are able to get an idea of the likelihood of water transport through aqueous pores.

4.3 Theory

The water movement across cell membranes was analyzed using two different single-parameter diffusion models and compared with the general 2-parameter Arrhenius equation. The two diffusion models used were diffusion through aqueous pores and solubility-diffusion through a lipid bilayer modeled as liquid hexadecane.

4.3a Diffusion through Aqueous Pores

In the first model, water is assumed to move across the membrane via pores as illustrated in Figure 4-1. This model was used by Price & Thompson (Price & Thompson, 1969), assuming that the pores are of sufficient size that the water

moving across the membrane essentially has bulk properties. Pagnelli & Solomon (1957) used this idea of bulk properties and obtained calculations for pores as small as 3 Å. Using this proposed model, the only energy barriers are due to diffusive or viscous resistance. Thus, the activation energy for the self-diffusion of water, 4.6 kcal/mol (Wang et al., 1953), was assumed to be the effective energy barrier for permeation. In this model, the water movement across the membrane may be described using Fick's Law of Diffusion

$$J = -D\frac{\partial c}{\partial x} \qquad (4-5)$$

where J is the flux of water across the cell membrane, D is the diffusion coefficient and $\partial c/\partial x$ is the concentration gradient of water across the cell membrane. The diffusion coefficient can be written using the following expression (Hiemenz & Rajagopalan, 1997):

$$D = \frac{kT}{f} \qquad (4-6)$$

where k is the Boltzman constant, T is absolute temperature and f is the friction factor. The friction factor is assumed to be proportional to the viscosity. As a result, we obtain the following expression for the diffusion coefficient:

$$D \propto \frac{kT}{\eta} \qquad (4-7)$$

For water between –40 and 0°C, the values for the self-diffusion coefficient of water were obtained from the literature (Franks, 1985). For water between 0 and 20°C and for water between 20 and 100°C, the viscosity η is given by Eqs. 4-8 and 4-9 respectively, (CRC Handbook of Chemistry and Physics 1987).

$$\log_{10}\eta_T = \frac{1301}{998.33 + 8.1855\,(T-20) + 0.00585\,(T-20)^2} - 1.30233 \qquad (4\text{-}8)$$

$$\log_{10}\frac{\eta_T}{\eta_{20}} = \frac{1.3272\,(20-T) - 0.001053\,(T-20)^2}{T+105} \qquad (4\text{-}9)$$

These expressions for viscosity as a function of temperature describe the temperature dependence of diffusion. The membrane hydraulic conductivity, L_p is directly proportional to the diffusion coefficient. As a result, we obtained the temperature dependence of the membrane hydraulic conductivity. Using a best-fit least square error method, a curve can then be fit to actual cell data.

Eq. 4-5 can be rewritten as follows:

$$J = \frac{1}{A_p M_m \bar{v}_w^*}\frac{dV}{dt} = -D\frac{\partial c}{\partial x} \qquad (4\text{-}10)$$

where J is the flux of water molecules across a cell membrane, A_p is the pore area M_m is the molar mass of water and $\bar{v}_w^*$ is the specific volume of water. Assuming a dilute solution and equating Eqs. 4-3 and 4-10, we obtain an expression that gives us the relationship between membrane hydraulic conductivity, the thickness of the pore Δx and the ratio of the pore area to the membrane area.

$$L_p = \frac{DM_m\bar{v}_w^*}{(\Delta x)RT}\frac{A_p}{A} \qquad (4\text{-}11)$$

However, some of these parameters are not easily obtained.

4.3b Solubility-Diffusion through a Lipid Bilayer Modeled as Liquid Hexadecane

In the second model, water is assumed to move across the membrane via a solubility-diffusion mechanism through the lipid bilayer as illustrated in Figure 4-2. The membrane is assumed to be a homogeneous layer through which water dissolves as discrete molecules and moves across the membrane. Hanai & Haydon (1966) suggested this as a possible mechanism for water transport across the lipid bilayer. The theory assumes that the diffusion process consists of a series of molecular jumps of length λ. There is a rate of solubilization across the solution-membrane interface, k_{sm}, a rate for the diffusion across the membrane, k_m, and a rate of transport across the membrane-solution interface, k_{ms}. The solubility-diffusion model given by Hanai & Haydon (1966) is:

$$\frac{1}{P_f} = \frac{2}{k_{sm}\lambda} + \frac{m}{k_m \lambda \frac{k_{sm}}{k_{ms}}} \qquad (4\text{-}12)$$

where m is the number of jumps required for a molecule to move across the membrane. Each rate constant, k_α, is assumed to have the following temperature dependence:

$$k_\alpha = B_\alpha \exp\left(\frac{-E_{a\alpha}}{RT}\right) \qquad (4\text{-}13)$$

where the B_α's are constants.

If the membrane interior is hydrophobic, then the partition coefficient of water between the solution and the membrane, k_{sm}/ k_{ms} is small, and $k_{sm} << k_{ms}$. Price and Thompson (1969) point out that if a reasonably small value of λ is assumed,

around 4-5 Å (Zwolinski et al., 1949), then when $k_{ms} \geq k_m$, the first term on the right-hand side of Eq. 4-12 is negligible with respect to the second term on the right-hand side of Eq. 4-12. The equation then reduces to:

$$P_t = \frac{k_m \lambda}{m} \frac{k_{sm}}{k_{ms}} \qquad (4\text{-}14)$$

The diffusion coefficient for water in the membrane, D, can be written as:

$$D = k_m \lambda^2 \qquad (4\text{-}15)$$

The membrane thickness, δ can be written as:

$$\delta = m\lambda \qquad (4\text{-}16)$$

Eq. 4-14 can then be written as:

$$P_t = \frac{D}{\delta} \frac{k_{sm}}{k_{ms}} \qquad (4\text{-}17)$$

Equating Eqs. 4-2 and 4-17 results in the following expression:

$$L_p = \frac{D\bar{\upsilon}_w}{\delta RT} \frac{k_{sm}}{k_{ms}} \qquad (4\text{-}18)$$

By substituting the conditions from Eq. 4-13, the expression for L_p can be written as follows:

$$L_p = D_o \exp\left(\frac{-E_{am}}{RT}\right) \frac{B_{sm} \exp(-E_{asm}/RT)}{B_{ms} \exp(-E_{ams}/RT)} \frac{\bar{\upsilon}_w}{\delta RT} \qquad (4\text{-}19)$$

$$L_p = \frac{D_o \bar{\upsilon}_w}{\delta RT} \frac{B_{sm}}{B_{ms}} \exp\left(\frac{-(E_{am} + E_{asm} - E_{ams})}{RT}\right) \qquad (4\text{-}20)$$

where D_o is a constant. Let G be defined as follows:

$$G \equiv \frac{D_o \bar{\upsilon}_w}{\delta R} \frac{B_{sm}}{B_{ms}} \qquad (4\text{-}21)$$

As a result, Eq. 4-20 can be written as:

$$L_p = \frac{G}{T}\exp\left(\frac{-(E_{am} + E_{asm} - E_{ams})}{RT}\right) \qquad (4-22)$$

The net value for the activation energy is that of the sum for the diffusion process and for the two partitioning processes. These quantities are unknown for the bilayer. It was assumed that the permeability barrier was effectively due to the hydrocarbon region of the bilayer and could be approximated by values of bulk hydrocarbons (Hanai and Hydon, 1966). In this model, liquid hexadecane was used to model the membrane. Of the hydrocarbons studied by Price and Thompson (1969), hexadecane was found to be nearest in size to lecithin, the major phospholipid of the cell membrane, and had an overall activation energy of 11.3 kcal/mol for the water permeation process (Schatzberg, 1965). Thus the temperature dependence of water diffusion in liquid hexadecane was obtained from the literature (Schatzberg, 1965).

$$L_p = \frac{G}{T}\exp\left(\frac{-11.3}{RT}\right) \qquad (4-23)$$

Thus once again we have the temperature dependence of the membrane hydraulic conductivity. Using a least square error method, a best-fit curve was fit to the actual cell data.

4.4 Methods and Materials

4.4a Cell Culture

The cell line used to study the temperature dependence of osmotic response was the V-79W line of Chinese hamster fibroblasts. The cell culture was described earlier in section 3.3a.

4.4b Osmotic experiments

Experimental hypertonic solutions were prepared by diluting a 10X isotonic phosphate buffered saline solution (Gibco). 200 μl of V-79W fibroblasts cells in an isotonic solution (~300 mOsmol/kg) were abruptly transferred into a 10 ml well-mixed hypertonic salt solution of approximately 900 mOsmol/kg and the kinetics of cell shrinkage were studied. The osmolalities of the salt solutions were measured with a freezing point depression osmometer (model 5004, Precision Systems, Inc.). The equilibrium volumes of the cells were measured using the electronic particle counter. Experiments were conducted at 4, 11, 22 and 33°C with the number of repetitions being between 14 and 22 at any given temperature. The temperature of the sample was recorded at the end of each run using a thermocouple.

4.4c Calculation of Osmotic Parameters

The isotonic cell volume was determined by measuring the mean volume of the V-79W fibroblasts in isotonic saline. Using the electronic particle counter, the hydraulic conductivity (L_p) for the V-79W fibroblast cells was determined by

measuring the kinetic changes of the mean cell volume while cells were experiencing an anisotonic environment. The rate of water movement across the plasma membrane during exposure to the hypertonic or hypotonic osmotic solutions is proportional to the hydraulic conductivity of the membrane, as well as the difference in osmotic pressure. L_p was calculated using the membrane mass transport model given in Eq. 4-3.

Armitage and Juss (1996) observed that cell size distributions for keratocytes were positively skewed, which is typical for mammalian cells; they concluded that the mean was an inappropriate measure of central tendency, and that the mode may be more applicable (Armitage & Juss, 1996). To quantify cell size distribution effects (see chapter 3 of this thesis, Elmoazzen et al., 1999), a subset of the data was analyzed using the mode volume changes to calculate the membrane hydraulic conductivity for the V-79W hamster fibroblast cells for a comparison. For the rest of the analysis, the mean volume change was used in order to compare with the Coulter mean data in the literature.

The temperature dependence of the hydraulic conductivity was fit with the general 2-parameter Arrhenius equation as well as with the two membrane diffusion models. Coulter data for the mean volume change for determining the permeability characteristics from the literature was also examined including data for human bone marrow stem cells (McGann et al., 1987), hamster pancreatic

islets (Liu et al., 1995) and articular cartilage chondrocytes (McGann et al., 1988).

4.5 Results

A summary of the experimental values of the membrane hydraulic conductivity calculated from the mean cell volumes for the V-79W hamster fibroblast cells at different temperatures is shown in Table 4-1.

Table 4-1- L_p's for V-79W Hamster Fibroblast Cells at Various Temperatures (calculated using the mean cell volume, E_a = 4.7 kcal/mol)

Temperature (°C)	Membrane Hydraulic Conductivity, L_p ($\mu m^3/\mu m^2/min/atm$)
3.6 ± 0.5	1.02 ± 0.14
11.9 ± 0.7	1.13 ± 0.22
22 ± 0.3	1.82 ± 0.14
33.2 ± 0.4	2.20 ± 0.40

Figure 4-3 shows a plot of temperature versus membrane hydraulic conductivity for the V-79W hamster fibroblast cells obtained using the *mean* cell volume when exposed to a hypertonic solution of approximately 900 mOsmol/Kg. Experimental results were obtained at temperatures of 4, 12, 22 and 33°C. The fibroblasts had a mean isotonic volume of 724 μm^3 and an osmotically inactive fraction between 0.28 and 0.38. At each temperature, there were between 14

and 22 experiments conducted. The experimental data was then fit with the Arrhenius equation, from which the activation energy of 4.7 kcal/mol was obtained, as well as with the two different diffusion models.

A summary of the experimental values of the membrane hydraulic conductivity calculated from the subset of data calculated using the *mode* cell volumes for the V-79W hamster fibroblast cells at different temperatures is shown in Table 4-2.

Table 4-2- L_p's for V-79W Hamster Fibroblast Cells at Various Temperatures (calculated using the mode cell volume, E_a = 5.1 kcal/mol)

Temperature (°C)	Membrane Hydraulic Conductivity, L_p ($\mu m^3/\mu m^2$/min/atm)
3.9	1.17
10.4	1.29
22.0	1.73
34.3	2.59

Figure 4-4 shows a plot of temperature versus membrane hydraulic conductivity for the V-79W hamster fibroblast cells using the *mode* cell volume. A sample run was analyzed at each temperature simply to examine the effects of cell size distributions. At 4, 11, 22, and 33°C, the membrane hydraulic conductivity values were 1.17, 1.29, 1.73 and 2.59 $\mu m^3/\mu m^2$/min/atm, respectively when the mode

was used in the calculations, compared with 1.02 ± 0.14, 1.13 ± 0.22, 1.82 ± 0.14 and 2.20 ±40 $\mu m^3/\mu m^2/min/atm$ when the mean was used.

A summary of the experimental values of the membrane hydraulic conductivity calculated for the human bone marrow stem cells at different temperatures is shown in Table 4-3.

Table 3- L_p's for Human Bone Marrow Stem Cells at Various Temperatures (calculated using the mean cell volumes, E_a = 6.4 kcal/mol, McGann et al., (1987))

Temperature (°C)	Membrane Hydraulic Conductivity, L_p ($\mu m^3/\mu m^2/min/atm$)
3.0 ± 2	0.144 ± 0.011
20±1	0.283 ± 0.012

Figure 4-5 shows a plot of temperature versus membrane hydraulic conductivity for the human bone marrow stem cells calculated using the mean. Experimental results are shown for different progenitor cells when exposed to a 30 mOsm/kg solution. At 3 ± 2°C and 20 ± 1°C, the hydraulic conductivities were 0.144 ± 0.011 $\mu m^3/\mu m^2/min/atm$ and 0.283 ± 0.012 $\mu m^3/\mu m^2/min/atm$, respectively (McGann et al., 1987). The cells had an average isotonic volume of 440 μm^3. The experimental data was then fit with the Arrhenius equation, from which an activation energy of 6.4 kcal/mol was obtained, as well as with the two different diffusion models.

A summary of the experimental values of the membrane hydraulic conductivity calculated for the hamster pancreatic islets at different temperatures is shown in Table 4-4.

Table 4-4- L_p's for Hamster Pancreatic Islet Cells at Various Temperatures (calculated using the mean cell volume, E_a = 11.4 kcal/mol, Liu et al., (1995))

Temperature (°C)	Membrane Hydraulic Conductivity, L_p ($\mu m^3/\mu m^2/min/atm$)
0	0.01 ± 0.001
8	0.06 ± 0.01
22	0.25 ± 0.03
37	0.54 ± 0.07

Figure 4-6 shows a plot of temperature versus membrane hydraulic conductivity for hamster pancreatic islets. Experimental results are shown for the cells when exposed to a 600 mOsm/kg PBS solution. Values for L_p were determined for individual pancreatic islet cells to be 0.01 ± 0.001, 0.06 ± 0.01, 0.25 ± 0.03, and 0.54 ± 0.07 at 0, 8, 22, and 37°C, respectively (Liu et al., 1995). The experimental data was then fit with the Arrhenius equation, from which an activation energy of 11.4 kcal/mol was obtained, as well as with the two different diffusion models.

A summary of the experimental values of the membrane hydraulic conductivity calculated for the articular cartilage chondrocytes at different temperatures is shown in Table 4-5.

Table 4-5- L_p's for Articular Cartilage Chondrocytes at Various Temperatures (calculated using the mean cell volume, E_a = 15.4 kcal/mol, McGann et al., (1995))

Temperature (°C)	Membrane Hydraulic Conductivity, L_p ($\mu m^3/\mu m^2/min/atm$)
3	0.039 ± 0.004
8	0.181 ± 0.010
24	0.305 ± 0.025

Figure 4-7 shows a plot of temperature versus membrane hydraulic conductivity for articular cartilage chondrocytes when exposed to a hypertonic solution of 900 mOsmol/kg. The average value of L_p was found to be 0.039 ± 0.004, 0.181 ± 0.010, and 0.305 ± 0.025 $\mu m^3/\mu m^2/min/atm$ at 3, 18 and 24°C, respectively (McGann et al., 1988). The experimental data was then fit with the Arrhenius equation, from which an activation energy of 15.4 kcal/mol* was obtained, as well as with the two different diffusion models.

* The permeability data from the original paper by McGann et al., 1988 was re-analyzed for this thesis and the reported activation energy of 8.06 kcal/mol was found to be incorrect. The activation energy was re-calculated and found to be 15.4 kcal/mol.

4.6 Discussion

For the V-79W hamster fibroblast cell data, the aqueous pore model and the Arrhenius equation both fit the data equally well for the temperature range over which the experiments were conducted (Figure 4-3). The solubility-diffusion model was a poor fit for the data. These results indicate the possible presence of aqueous pores in V-79W hamster fibroblast cells and suggest that it is very unlikely that water moves across the membrane primarily by a solubility-diffusion mechanism through the lipid bilayer.

The plot of temperature versus hydraulic conductivity calculated with the *mode* volume for the V-79W cells is shown in Figure 4-4. Similar results to those using the mean cell volume were obtained. Once again, it appeared as if water movement was via pores. Although individual L_p values are different according to whether found with the mean or the mode, conclusions based on trends of L_p with temperature are not affected.

The aqueous pore model and the Arrhenius curve both fit the data for the human bone marrow stem cells (Figure 4-5). Although the Arrhenius curve appears to fit the data somewhat better, the aqueous curve is still within the error bars of the actual results, thus implying that once again aqueous pores may be present in these stem cells. The solubility-diffusion model provided a very poor fit to the data, indicating that water movement most likely does not primarily occur by the solubility-diffusion mechanism.

The graph of temperature versus hydraulic conductivity for the pancreatic islets (Figure 4-6) indicates that the Arrhenius curve and the solubility-diffusion model both fit the data equally well whereas the aqueous pore model is a poor fit. This implies that water movement in islets may take place via the solubility-diffusion mechanism. Pancreatic islets are complex in structure and are made up of several different cell types thus the assumption that all the cells are shrinking and swelling at the same rate is likely invalid. A single water permeability for the multicellular islets was measured, representing an average over all the cells. Kleinhans (1999) indicates that when measuring multicellular embryos, permeability parameters are often determined by assuming a simple spherical cell for fitting purposes and thus the values obtained are phenomenological averages. This may account for the observation that neither of the two diffusion models nor the 2-parameter Arrhenius equation accurately fit through all the data points for pancreatic islets.

The data for the chondrocytes (Figure 4-7) indicates that neither the aqueous pore model nor the solubility-diffusion model fit the data very well. The chondrocytes appear to be more strongly dependent on temperature and therefore neither one of the 2 diffusion models could explain the water movement across the lipid bilayer. This may be an indication that other factors contribute to water movement in chondrocytes. Active water transport may be responsible for the strong dependence on temperature.

In the literature, it has been noted that there is no *a priori* reason that the activation energy should be low for water movement through aqueous pores (Verkman et al., 1996). Verkman and his colleagues note that the activation energy will depend on the nature of the rate-limiting barrier for water movement and the energetics of water-pore interaction. As indicated in the theory section of this chapter, section 4.3, for the diffusion through aqueous pores model, the water moving across the membrane was assumed to have bulk properties and the only energy barriers were due to diffusive and viscous resistance. This then gives reason to the observed outcomes of low activation energy for water movement through aqueous pores.

The value for the membrane hydraulic conductivity for each cell type was converted to a P_f value using Eq. 4-3. It was found that for the V-79 W hamster fibroblast cells P_f was 0.0041 and 0.0039 cm/s using the mean and mode values for volume at 22°C, respectively. From the analysis, the V-79W cells appeared to have aqueous pores. However, as mentioned earlier, a P_f of 0.01 cm/s has been taken to be indicative of aquaporins (Verkman et al., 1996). Thus from the P_f value only, it would appear that these cells do not have pores. This may be an indication that the P_f value may not be an accurate indication of the presence of aqueous pores. Similarly, from the analysis, it appeared as if the human bone marrow stem cells appeared to contain aqueous pores. However, once again when the P_f value was calculated, it was again less than the 0.01 cm/s value which is used as an indication of aqueous pores. At 20°C, the P_f value for the

bone marrow stem cells was found to be 0.0006 cm/s. The P_f values for the pancreatic islets at 22°C and for the bovine chondrocytes at 24°C were found to be 0.0056 cm/s and 0.00068 cm/s, respectively. These cells did not appear to contain aquaporins and the P_f values obtained agreed with these conclusions.

Using Eq. 4-3, the minimum value of L_p for a cell that contains aquaporins at 22°C was calculated to be 4.46 $\mu m^3/\mu m^2/min/atm$, which was higher than any value for the hydraulic conductivity. Verkman et al., (1986) stated that a P_f value >0.01 was indicative of aqueous pores, but state that these biophysical parameters lack theoretical justification. As a result, the utilization of P_f to determine the presence of aqueous pores may not be accurate.

4.7 Conclusions

Analysis of the experimental data suggests that the method of water movement across cell membranes may be examined using two diffusion models in conjunction with measured permeability data at different temperatures from an electronic particle counter. The temperature dependence of the membrane hydraulic conductivity could be used as a tool to identify the possible presence of aqueous pores in cell membranes. Using this approach, osmotic transport in V-79W hamster fibroblast cells and bone marrow stem cells both appeared to be through aqueous pores. However, water transport across the cell membranes of the hamster pancreatic islets appeared to be through lipid diffusion, since the

solubility-diffusion curve best explained the data. Bovine chondrocytes showed a much stronger temperature dependent mechanism for water movement than either of the two proposed diffusion models. Therefore water movement may occur by a more complicated mechanism than simple diffusion. Using simple electronic counter experiments in conjunction with the diffusion models we are able to obtain a description that may be able to indicate possible mechanisms of water movement across cell membranes. Also, the criteria that $P_f > 0.01$ cm/s used to indicate the presence of aquaporins lacks theoretical justification and may not be an accurate biophysical criteria.

4.8 References

1. Acker, J. P., Pasch, J., Heschel, I., Rau, G., McGann, L. E. 1999. Comparison of Optical Measurement and Electrical Measurement Techniques for the Study of Osmotic Responses of Cell Suspensions. *Cryo. Lett.*, **20**, 315-324.

2. Armitage, W. J., & B. K. Juss. 1996. Osmotic Response of Mammalian Cells: Effects of Permeating Cryoprotectants on Nonsolvent Volume. *J. Cell. Physiol.* **168**, 532-538.

3. Bicknese, S., Periasamy, N., Shohet, S. B., Verkman, A. S. 1993. Cytoplasmic viscosity near the cell plasma membrane: measurements by evanescent field frequency-domain microfluorimetry. *Biophys. J.* **65**, 1272-1282.

4. Buckhold, B., Adams, R. B., Gregg, E. C. 1965. Osmotic Adaptation of Mouse Lymphoblasts. *Biochimica et Biophys. Acta*. **102**, 600-608.

5. Chen, P. Y., Pearce, D., Verkman, A. S. 1988. Membrane water and solute permeability determined quantitatively by self-quenching of an entrapped fluorophore. *Biochemistry*. **27**, 5713-5719.

6. Chrispeels, M. J., Agre, P. 1994. Aquaporins: water channel proteins of plants and animal cells. *Trends in Biochemical Sciences*. **19**, 421-425.

7. Echevarría, M., Kuang, K., Iserovich, P., Li, J., Preston, G. M., Agre, P., Fischbarg, J. 1993. Cultured bovine corneal endothelial cells express CHIP28 water channels. *Am. J. Physiol.* **265**, C1349-C1355.

8. Elmoazzen, H. Y., Chan, C. C. V., Acker, J. P., Elliott, J. A. W., McGann, L. E. 1999. The effect of cell size distribution on predicted osmotic responses of cells. Submitted to: *Biophys. J.*

9. Farinas, J., Simenak, V., Verkman, A.S. 1995. Cell volume measured in adherent cells by total internal reflection microfluorimetry: application to permeability in cells transfused with water channel homologs. *Biophys. J.* **68**, 1613-1620.

10. Farmer, R. E. L & Macey, R. I. 1970. Perturbation of red blood cell volume: Rectification of osmotic flow. *Biochim. Biophys. Acta*, **196**, 53-65.

11. Fettiplace, R., & Haydon, D. A. 1980. Water permeability of lipid membranes. *Physiol. Rev.*, **60**, 510-550.

12. Finkelstein, A. 1987. "Water movement through lipid bilayers, pores and plasma membranes: theory and reality" Wiley, New York.

13. Fischbarg, J., Kunyan, K., Vera, J. C., Arant, S., Silverstein, S., Loike, J., Rosen, O. M. 1990. Glucose channels serve as water channels. *Proc. Natl. Acad. Sci. USA*, **87**, 3244-3247.

14. Franks, F. 1985. In "Biophysics and biochemistry at low temperatures" New York: Cambridge University Press.

15. Frigeri, A., Gropper, M., Brown, D., Verkman, A. S. 1995a. Localization of MIWC and GLIP water channel homologs in neuromuscular epithelial and glandular tissues. *J. Cell Sci.* **108**, 2993-3002.

16. Frigeri, A., Gropper, M., Turck, C. W., Verkman, A. S. 1995b. Immunolocalization of the mercurial-insensitive water channel and glycerol

intrinsic protein in epithelial cell plasma membranes. *Proc. Natl. Acad. Sci. USA.* **92**, 4328-4331.

17. Gilmore, J. A., McGann, L. E., Ashwood, E., Acker, J. P., Raath, C., Bush, M., Critser, J. K. 1998. Fundamental Cryobiology of a Selected African Mammalian Spermatozoa and its Role in Biodiversity through Development of Genome Resource Banking. *An. Rep. Sci.* **53**, 277-297.

18. Gilmore, J. A., McGann, L. E., Liu, J., Gao, D. Y., Peter, A. T., Kleinhans, F. W., Critser, J. K. 1995. Effect of Cryoprotectant Solutes on Water Permeability of Human Spermatozoa. *Biol. Reprod.* **53**, 985-995.

19. Hanai, T., & Haydon, D. A. 1966. The permeability to water of bimolecular lipid membranes. *J. Theoret. Biol.*, **11**, 370-382.

20. Harris, H. W., Handler, J. S., Blumenthal, R. 1990. Apical membrane vesicles of ADH-stimulated toad bladder are highly water permeable. *Am. J. Physiol.* **258**, F237-F243.

21. Hays, R. M., Leaf, A. 1962. The state of water in the isolated toad bladder and its modification by vasopressin. *J. Gen. Physiol.*, **45**, 933-948

22. Hempling, H. G. 1961. Permeability of the Ehrlich ascites tumor cell to water. *J. Gen. Physiol.*, **44**, 365-379

23. Hiemenz, P. C., & Rajagopalan, R. 1997. *Principles of Colloid and Surface Chemistry*, (Marcel Dekker, Inc., New York) 78-82.

24. Jacobs, M. H., Glassman, H. N., Parpart, A. K. 1935. Osmotic properties of erythrocyte, temperature coefficients of certain hemolytic processes. *J. Cell. Comp. Physiol.*, **7**, 197-225.

25. Jacobs, M. H., & D. R. Stewart. 1932. A Simple Method for the Quantitative Measurement of Cell Permeability. *J. Cell. Comp. Physiol.* **1**, 71-82.

26. Jung, J. S., Bhat, R. V., Prston, G. M., Guggino, W. B., Baraban, J. M., Agre, P. 1994. Molecular characterization of an aquaporin cDNA from brain: candidate osmoreceptor and regulation of water balance. *Proc. Natl. Acad. Sci. USA*, **91**, 13052-13056.

27. Kang, F., Kuang, K., Li, J., Fischbarg, J. 1999. Cultured bovine corneal epithelial cells express a functional aquaporin water channel. *Invest. Opthalmol. Vis. Sci.*, **40**, 253-257.

28. Kleinhans, F. W. 1999. Membrane permeability modeling: Kedem-Katchalsky vs a two-parameter formalism. *Cryobiology*, **37**, 271-289.

29. Liu, C., Benson, C. T., Gao, D., Haag, B. W., McGann, L. E., Critser, J. K. 1995. Water permeability and its activation energy for individual hamster pancreatic islet cells. *Cryobiology*, **32**, 493-502.

30. Lucké, B & McCutcheon, M. 1932. The living cell as an osmotic system and its permeability to water. *Physiol. Rev.*, **12**, 68-138.

31. Ma, T., Frigeri, A., Hasegawa, H., Verkman, A. S. 1994. Cloning of a water channel homolog expressed in brain meningeal cells and kidney collecting duct that functions as a stilbene-sensitive glycerol transporter. *J. Biol. Chem.*, **269**, 21845-21849.

32. Macey, R. I. 1984. Transport of water and urea in red blood cells. *Am. J. Physiol.*, **246**, C195-C203.

33. Macey, R. I., Karen, D. M., and Farmer, R. E. L. 1973. In *"Passive Permeability of Cell Membranes"* (F. Kreuzer and T. F. G. Slegers, eds) vol 3, 331

34. McGann, L. E., Janowska-Wieczorek, A., Turner, A. R., Hogg, L., Muldrew, K. B., Turc, J. M. 1987. Water permeability of human hematopoetic stem cells. *Cryobiology*, **24**, 112-119.

35. McGann, L. E., Stevenson, M., Schachar, N. 1988. Kinetics of osmotic water movement in chondrocytes isolated from articular cartilage and applications to cryopreservation. *J. Orthop. Res.*, **6**, 109-115.

36. McGann, L. E., & J. M. Turc. 1980. Determination of Water and Solute Permeability Coefficients. *Cryobiology* **17**, 612-613.

37. McGann, L. E., A. R. Turner, J. M. Turc. 1982. Microcomputer Interface for Rapid Measurement of Average Volume Using an Electronic Particle Counter. *Med. & Biol. Eng. & Compute.* **20**, 17-120.

38. Meyer, M. M & Verkman, A. S. 1987. Evidence for water channels in proximal tubule cell membranes. *J. Membr. Biol.*, **96**, 107-119.

39. Nevis, A. H. 1958. Water transport in invertebrate peripheral nerve. *J. Gen. Physiol.*, **41**, 927-958.

40. Nielsen, S., Smith, B. L., Christensen, E. I., Agre, P. 1993. Distribution of the aquaporin CHIP in secretory and resorptive epithelia and capillary endothelia. *Proc. Natl. Acad. Sci. USA*, **90**, 7275-7279.

41. Pagnelli, C. V., & Solomon, A. K. 1957. The rate of exchange of tritiated water across the human red blood cell membrane. *J. Gen. Physiol.*, **41**, 259-277.

42. Preston, G. M., & Agre, P. 1991. Isolation of the cDNA for erythrocyte integral membrane protein of 28 kilodaltons: member of an ancient channel family. *Proc. Natl. Acad. Sci. USA*, **88**, 11110-11114.

43. Preston, G. M., Carroll, T. P., Guggino, W. B., Agre, P. 1992. Appearance of water channels in *Xenopus* oocytes expressing red cell CHIP28 protein. *Science Wash. DC*, **256**, 385-387.

44. Price, H. D., & Thompson, T. E. 1969. Properties of liquid bilayer membranes separating two aqueous phases: temperature dependence of water permeability. *J. Mol. Bio*, **41**, 443-457

45. Schatzberg, P. 1965. Diffusion of water through hydrocarbon liquids. *J. Polymer Sci. Pt C*, **10**, 87-92.

46. Sha'afi, R. I. 1977. Water and small nonelectrolyte permeation in red cells. In: *Membrane Transport in Red Cells*, edited by J. C. Ellory and V. L. Lew. London: Academic, 221-256.

47. Shi, L. B., & Verkman, A. S. 1989. Very high water permeability in vasopressin-dependent endocytic vesicles in toad urinary bladder. *J. Gen Pysiol.* **94**, 1101-1115.

48. Verkman, A. S. 1989. Mechanisms and regulation of water permeability in renal epithelia. *Am. J. Physiol.* **257**, C837-C85

49. Verkman, A. S. 1992. Water channels in cell membranes. *Annu. Ev. Physiol.*, **54**, 97-108.

50. Verkman, A. S., Lencer, W., Brown, D., Ausiello, D. A. 1988. Endosomes from kidney collecting tubule contain the vasopressin-sensitive water channel. *Nature Lond.* **333**, 268-269.

51. Verkman, A. S., VanHoek, A. N., Ma, T., Frigeri, A., Skach, W. R., Mitra, A., Tamarappoo, B. K., Farinas, J. 1996. Water transport across mammalian cell membranes. *Am. J. Physiol*, **270**, C12-C30.

52. Vieiera, F. L., Sha'afi, R. I., Solomon, A. K. 1970. The state of water in human and dog red cell membranes. *J. Gen. Pysiol.*, **55**, 451-466.

53. Wang, J. H., Robinson, C. V., Edelman, I. S. 1953. Self-diffusion and structure of liquid water. III. Measurement of the self-diffusion of liquid water with H^2, H^3, and O^{18} as tracers. *J. Amer. Chem. Soc.*, **75**, 466-470.

54. Weast, R. C. 1987. *CRC Handbook of Chemistry and Physics, 68th Edition.* CRC Press Inc. Boca Raton: Florida.

55. Ye, R., Shi, L. B., Lencer, W., Verkman, A. S. 1989. Functional colocalization of water channels and proton pumps on endocytic vesicles from proximal tubule. *J. Gen. Physiol.* **93**, 885-902.

56. Zhang, R., Logee, K., Verkman, A. S. 1990. Expression of mRNA coding for kidney and red cell water channels in *Xenopus* oocytes. *J. Biol. Chem.* **265**, 15375-15378.

57. Zhang, R., and Verkman, A. S. 1991. Water and urea transport in *Xenopus* oocytes: expression of mRNA from toad urinary bladder. *Am. J. Physiol.* **260**, C26-C34.

58. Zwolinski, B. J., Eyring, H., Reese, C. E. 1949. Diffusion and membrane permeability. *J. Phys. & Colloid Chem.*, **53**, 1426-1453.

Figure 4-1 Diffusion through Aqueous Pores

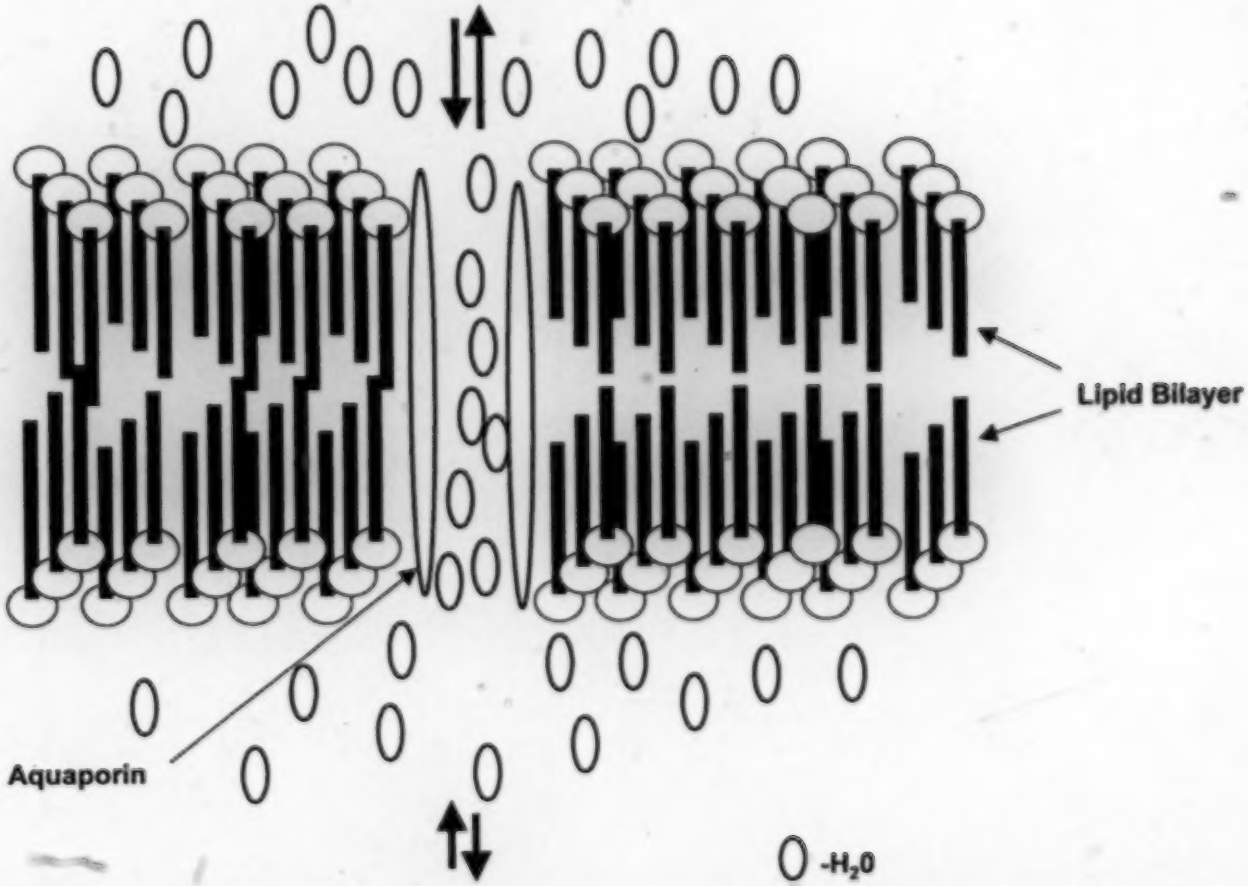

Figure 4-2 Solubility-Diffusion Through a Lipid Bilayer Membrane

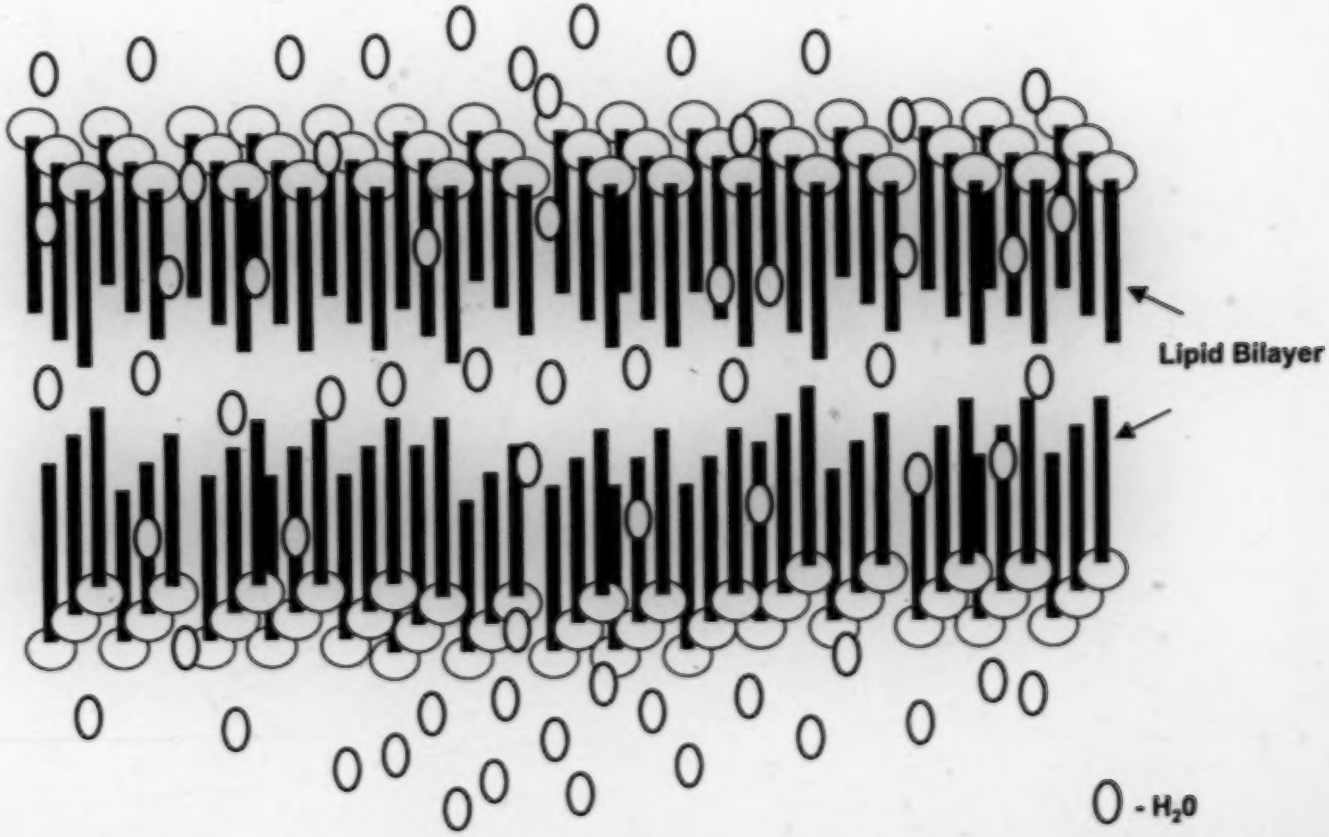

Figure 4-3 Temperature Vs L_p for V-79W Hamster Fibroblasts (using mean cell volumes)

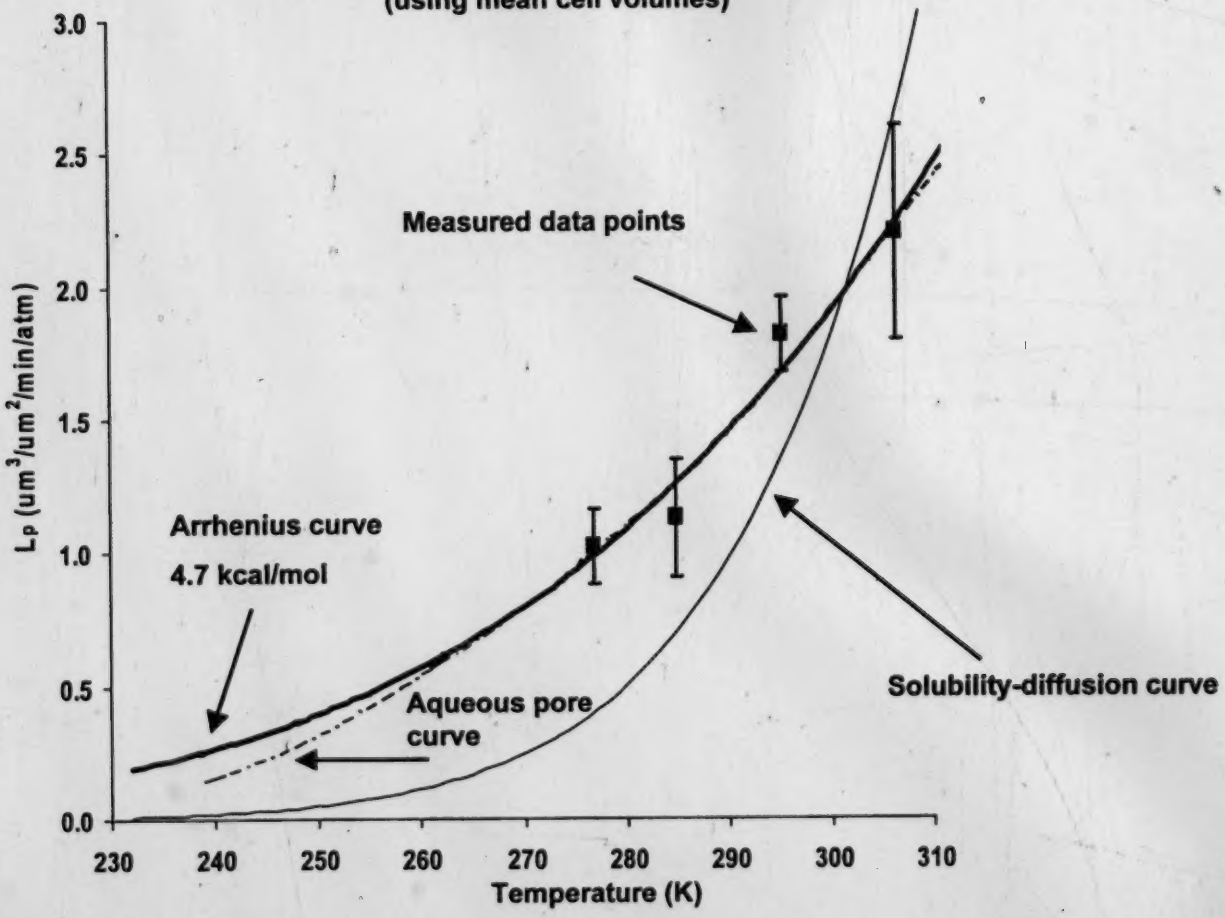

Figure 4-4 Temperature Vs Lp for V-79W Hamster Fibroblasts
(using mode cell volumes)

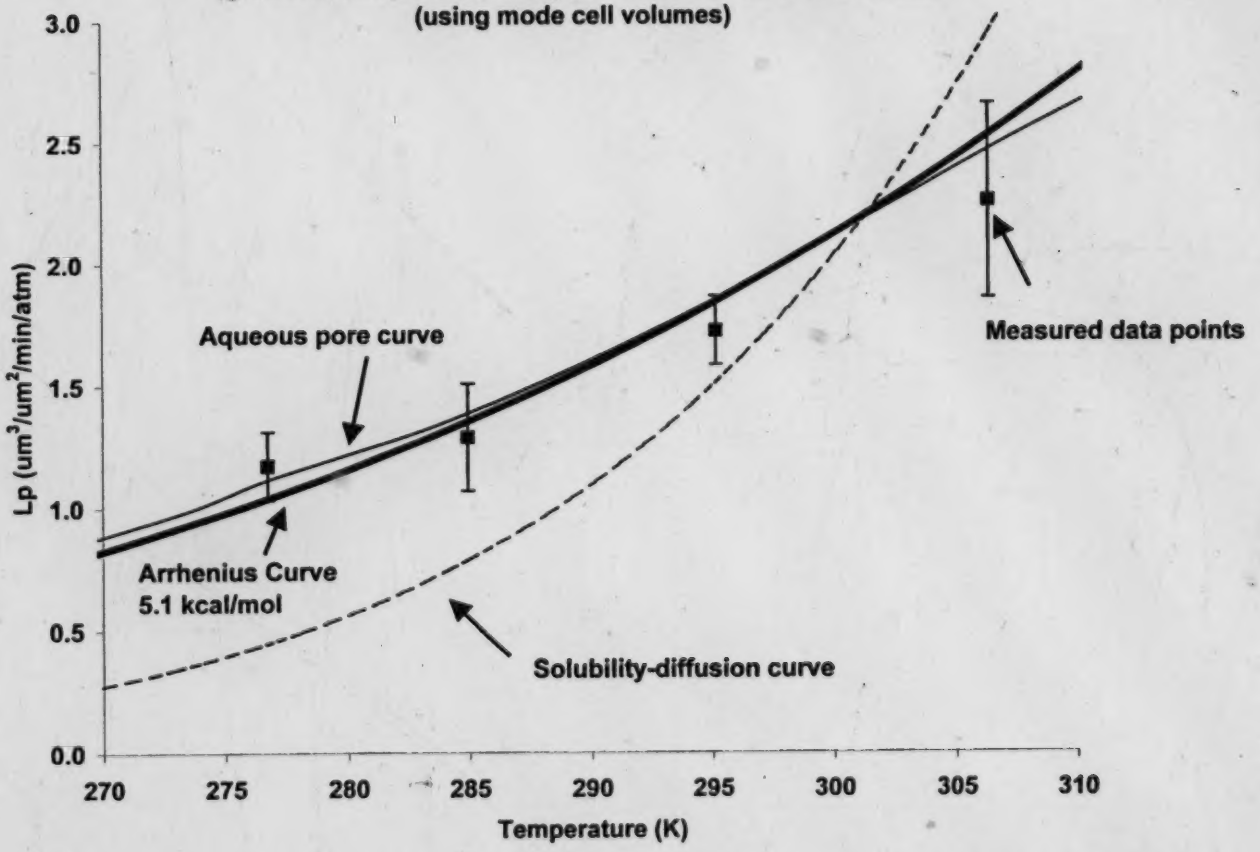

Figure 4-5 Temperature Vs L_p for Human Bone Marrow Stem Cells

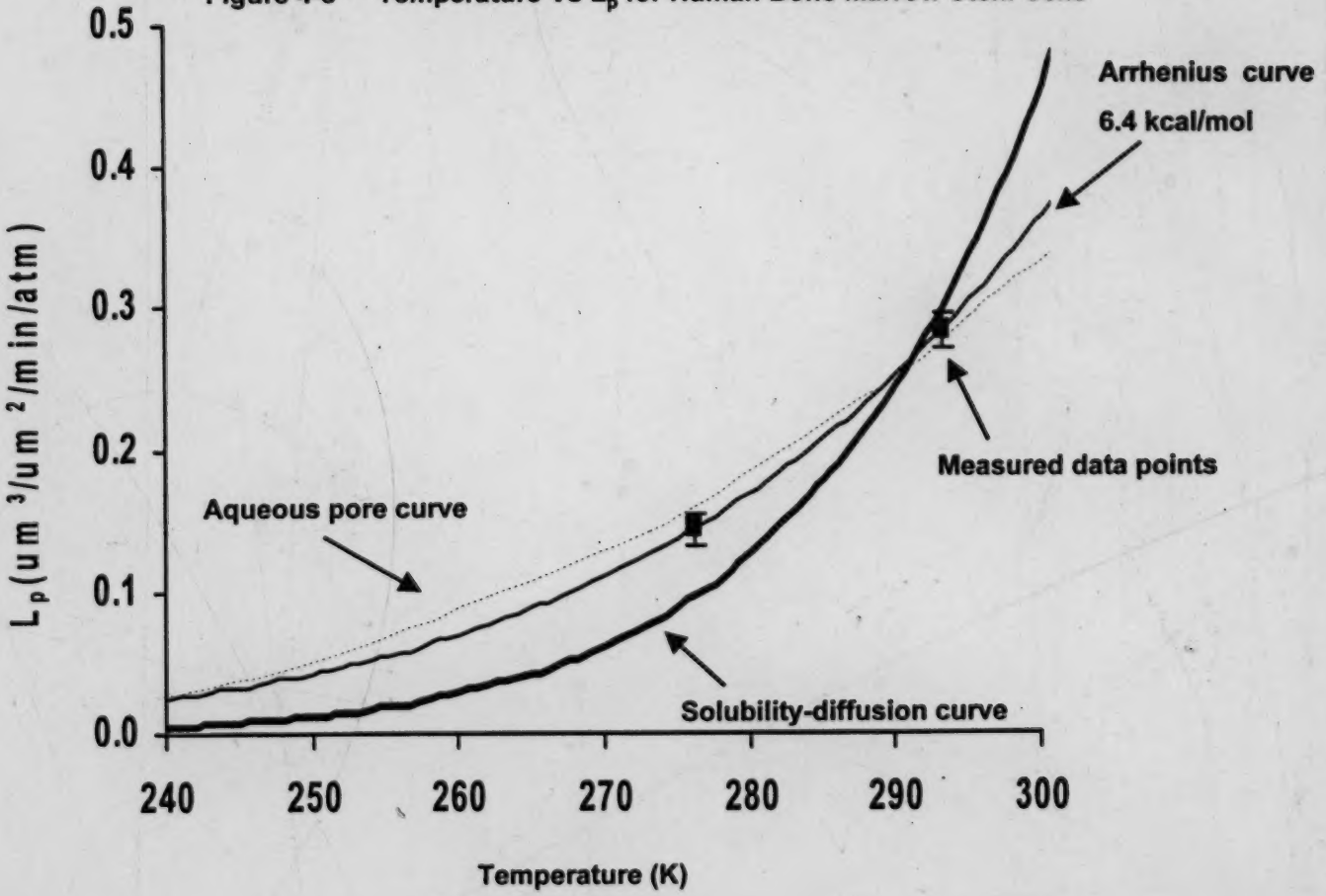

Figure 4-6 Temperature Vs L_p for Hamster Pancreatic Islets

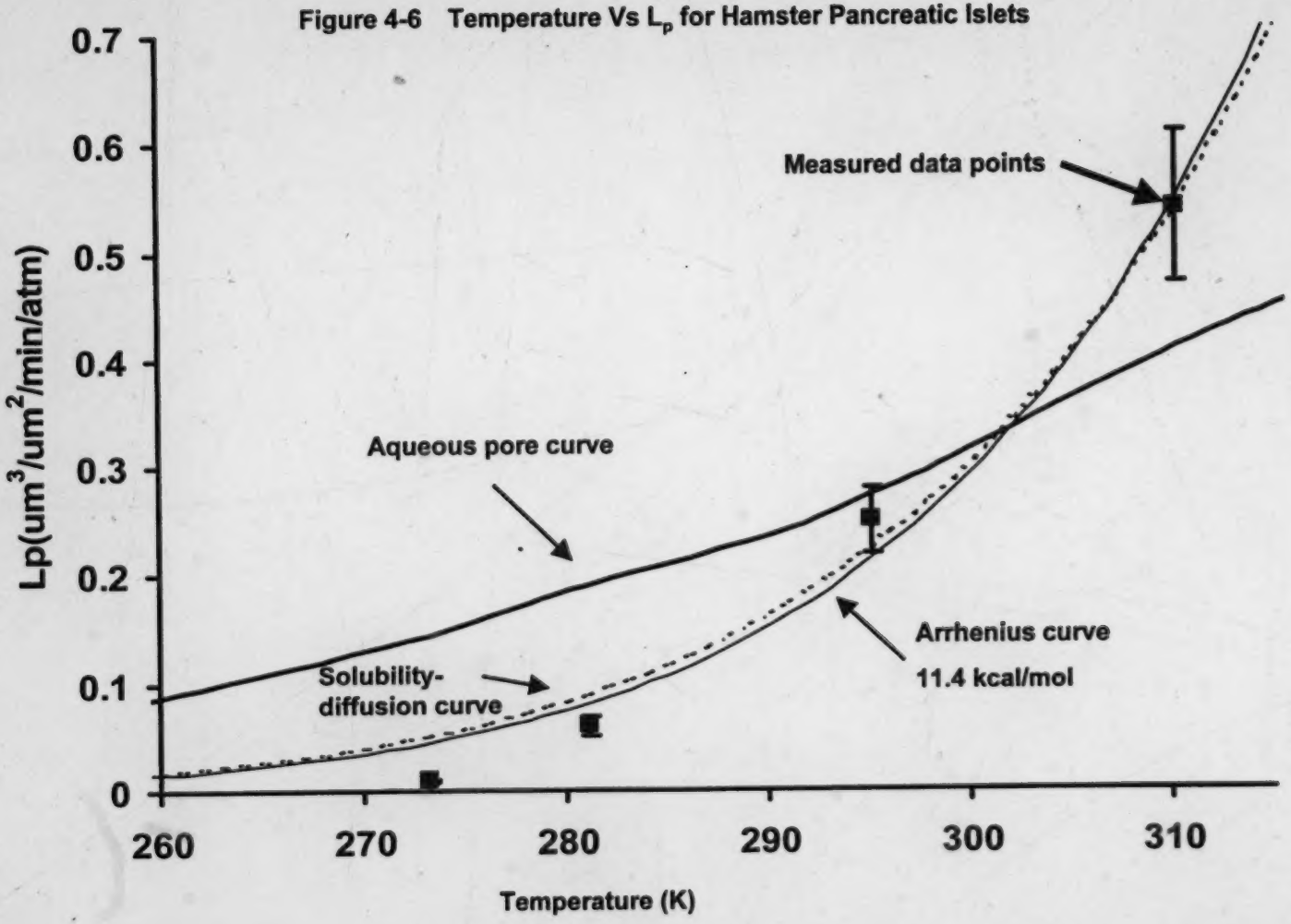

Figure 4-7 Temperature Vs L_p for Articular Cartilage Chondrocytes

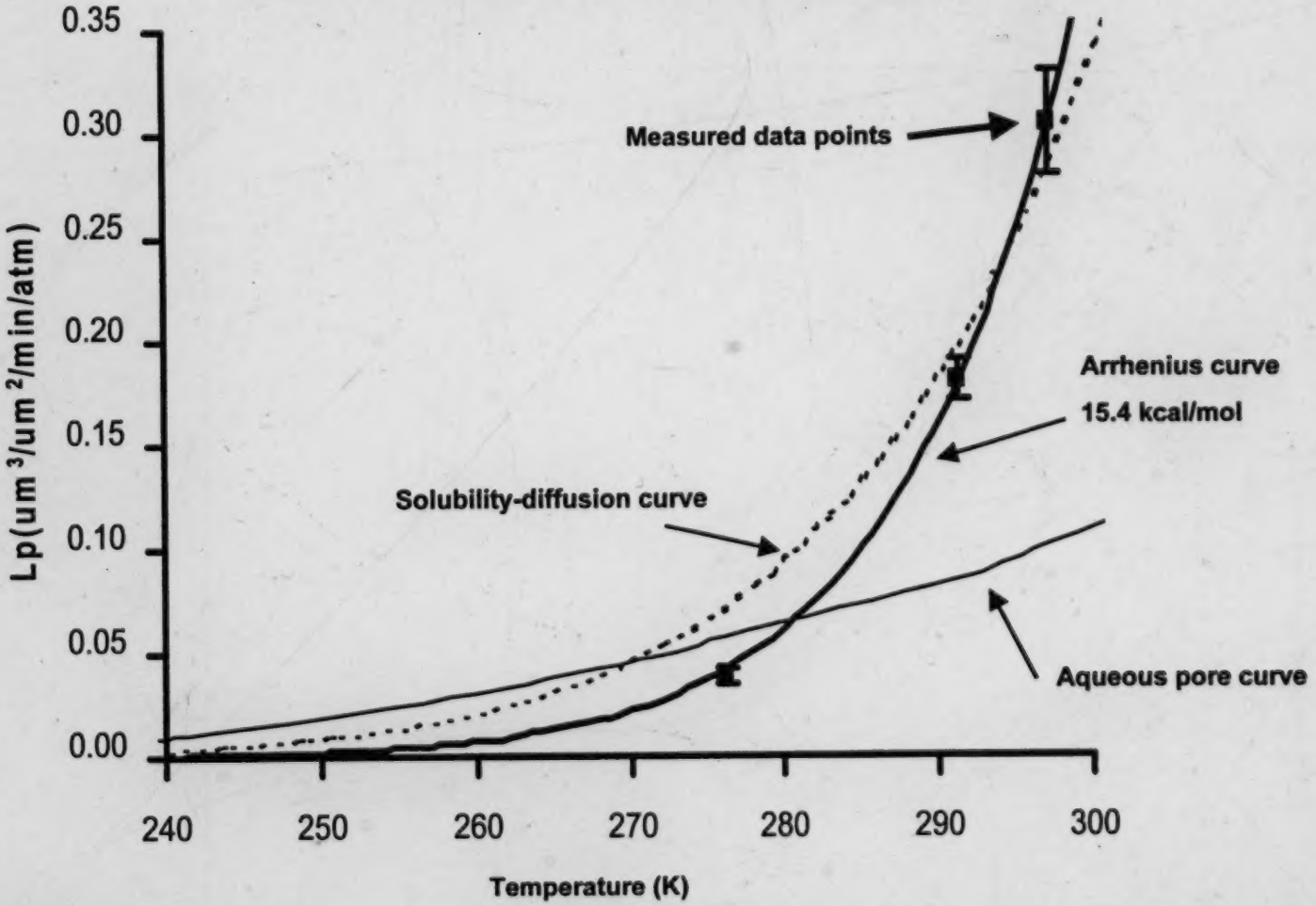

Chapter 5: Overall Discussion and Conclusions

The objective of this thesis was to gain an insight into the movement of water across cell membranes and the parameters that affect cell permeability, in particular cell size distribution and temperature.

The current theoretical descriptions of osmotic transport across cell membranes are based on the work of Kedem and Katchalsky, which was based on Onsager's linear theory of non-equilibrium thermodynamics. A corrected version of the osmotic transport equations derived by Kedem and Katchalsky from the Onsager approach to linear non-equilibrium thermodynamics was presented in this thesis. Statistical Rate Theory, a relatively new complete theory of non-equilibrium thermodynamics, was explored and used to develop new osmotic transport equations. The two approaches were compared. By linearizing Statistical Rate Theory, a non-linear theory of non-equilibrium thermodynamics, several advances in the theoretical description of osmotic transport were made.

The phenomenological coefficients in the Onsager approach cannot be derived from theory and must be evaluated empirically. Using Statistical Rate Theory, explicit equations for the Onsager coefficients were developed for three separate cases: 1) a two-component system of water and solute where both may permeate the cell membrane and where there is tension in the membrane, 2) a two-component system of water and solute where both may permeate the membrane but where there is no tension in the membrane, 3) a two-component

system of water and solute where only the water may permeate the cell membrane and where there is no tension in the membrane. The equations for the Onsager coefficients in the three cases were written in terms of measurable or otherwise obtainable, physical parameters such as temperature, concentration and the equilibrium exchange rate, which also depend on concentration and temperature in a non-trivial way.

Using the Statistical Rate Theory Approach, explicit conditions under which the assumption of linearity holds were developed. Such conditions cannot be derived from within the Onsager approach.

The Onsager reciprocity hypothesis in transport phenomena is a very important hypothesis that has been discussed since the 1930's. Statistical Rate Theory was used to verify the hypothesis for case 1 by showing the equality of the cross coefficients.

Statistical Rate Theory reveled to us that hydraulic conductivity is dependent on temperature, concentration and the equilibrium exchange rate, which also depends on temperature and concentration in a non-trivial way.

Cell size distribution was the first parameter for which the effect on membrane hydraulic conductivity was examined. It was demonstrated for both the MDCK cells and the V-79W cells, two cell types with different isotonic volumes and

different cell size distributions, that the shapes of the cell size distributions did not stay constant over time when the cells were responding in a hypertonic environment. The membrane hydraulic conductivity obtained by using the *mean* volume data tended to be too high. This implied that the single-cell membrane mass transport equation fit to the *mean* cell volume as a function of time did not accurately model the osmotic response of cells with size distributions. Another model is needed to obtain the membrane hydraulic conductivity. As a minimum, the *mode* of skewed distributions rather than the mean should be used for analysis. Ideally a method should be developed that takes the entire distribution into account.

Temperature was the second parameter for which the effect on membrane permeability was examined. Analysis of the experimental data suggested that the method of water movement across cell membranes may be examined using two different diffusion models in conjunction with measured permeability data at different temperatures from an electronic particle counter. The temperature dependence of the membrane hydraulic conductivity could be used as a tool to identify the possible presence of aqueous pores in cell membranes. Using this approach, osmotic transport in V-79W hamster fibroblast cells and bone marrow stem cells both appeared to be through aqueous pores. However, water transport across cell membranes of hamster pancreatic islets appeared to be through lipid diffusion. Water transport across cell membranes of bovine chondrocytes appeared to occur by a more complicated mechanism than simple

diffusion. As well, it was demonstrated the criteria of $P_f > 0.01$ cm/s used to indicate the presence of aqueous pores lacks theoretical justification and may not be an accurate biophysical criteria.

There is, in cryobiology, a definite need to understand the parameters that affect cell membrane permeability. As cryobiologists continue studying cells and tissues of increasing complexity, there is an even greater need to understand water movement across cell membranes. A realization that came to me while creating this thesis is that water transport across biological cell membranes is a complex process that depends on many parameters, which affect the determined value for the hydraulic conductivity. With a greater understanding of these parameters, values for the hydraulic conductivity may be obtained with a smaller degree of error. Ideally, the osmotic transport equations presented in this thesis would be used to obtain values for membrane permeability so that it would be possible to model the optimal conditions for the addition and removal of cryoprotectants and the optimal cooling rate for cryopreservation. This thesis has provided a clearer understanding of the parameters that effect cell membrane permeability and the importance of these parameters to water movement across cell membranes. With this information, more accurate mathematical models can now be developed and this may lead us on a path to improving cryopreservation protocols.